

**A PROPOSED ENERGY MANAGEMENT STRATEGY FOR A HYBRID PV-WIND-
BATTERY STORAGE SYSTEM**

By

SAMEER CAMROODIEN

212294644

Dissertation submitted in partial fulfilment of the requirements for the degree

**Master of Technology: Electrical, Electronics, and Computer Engineering
in the Faculty of Engineering
at the Cape Peninsula University of Technology**

Supervisor: Dr. E F Orumwense.

External Co-Supervisor - Prof. K Abo-Al-Ez

Bellville

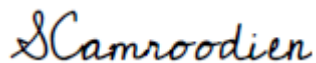
August 2024

CPUT copyright information

The dissertation/thesis may not be published either in part (in scholarly, scientific, or technical journals), or as a whole (as a monograph), unless permission has been obtained from the University

DECLARATION

I, Sameer Camroodien, declare that the contents of this dissertation/thesis represent my own unaided work, and that the dissertation/thesis has not previously been submitted for academic examination towards any qualification. Furthermore, it represents my own opinions and not necessarily those of the Cape Peninsula University of Technology.

**03 January 2023**

Signed**Date**

ABSTRACT

This thesis presents a comprehensive study on the development and implementation of an energy management strategy for a Hybrid Power System (HPS) that integrates photovoltaic (PV) panels, wind turbines, and battery storage. The primary goal is to ensure a continuous and reliable supply of electricity to the load by efficiently utilizing the available renewable energy resources.

The study begins with the modelling and simulation of the HPS components using MATLAB Simulink. The PV, wind, and battery models are developed and tested individually to ensure their accuracy and performance under various operating conditions. A controller is designed to manage the energy flow within the HPS, making real-time decisions based on the availability of resources and load demands.

Simulations are conducted to evaluate the performance of the HPS under different scenarios, including varying weather conditions and resource availability. The results demonstrate that the PV model operates effectively within the HPS, providing a stable power output when solar irradiance is sufficient. The Doubly-Fed Induction Generator (DFIG) model shows robust performance, seamlessly integrating into the HPS and compensating for the PV system's limitations during low solar irradiance periods. The battery storage unit proves to be a crucial component, ensuring power supply continuity when both PV and wind resources are unavailable.

The controller's ability to accurately determine the availability of each energy source and manage the energy flow is validated through various test cases. The results indicate that the controller effectively optimizes the use of available resources, maintaining a steady power supply to the load plus maximizing system efficiency.

In conclusion, this research successfully develops an energy management strategy for a hybrid power system consisting of PV, wind, and battery, demonstrating its potential to enhance the reliability and efficiency of renewable energy systems. The findings provide positive insights for the design and implementation of HPS, contributing to the advancement of green energy solutions.

ACKNOWLEDGEMENTS

I wish to thank:

- My Wife, Tabassum Zalganir: For your endless patience, love, and understanding throughout this journey. Your support has been the cornerstone of my perseverance.
- My Son, Mohamed Saabir: For bringing joy and inspiration into my life, reminding me daily of the importance of dedication and hard work.
- Dr.Orumwense: For his invaluable guidance, encouragement, and support throughout the research and writing process. Your insights and expertise were instrumental in shaping this thesis.
- Cape Peninsula University of Technology: For providing the resources and facilities that were essential for completing this research.

DEDICATION

This thesis is dedicated to my loved ones, family, and friends, whose solid support, encouragement, and belief in my abilities have been the foundation of my journey. To my parents, for their endless sacrifices and unconditional love, and to my siblings, for their relentless motivation and understanding.

I also dedicate this work to my professors and mentors, whose guidance and wisdom have shaped my academic path and instilled in me a passion for learning and discovery.

Lastly, to all those who have believed in me and supported me throughout this journey, this thesis is a testament to your faith and encouragement. Thank you for being my pillars of strength and for inspiring me to strive for excellence.

Contents

DECLARATION.....	ii
ABSTRACT	iii
ACKNOWLEDGEMENTS	iv
DEDICATION	v
LIST OF FIGURES	viii
LIST OF TABLES	xi
LIST OF APPENDICES.....	xii
GLOSSARY	xiii
CHAPTER ONE: INTRODUCTION	1
1.1 Background	1
1.2 Objectives of the study	2
1.3 Scope and Limitations.....	3
1.4 Dissertation Outline.....	4
CHAPTER TWO: LITERATURE REVIEW	6
2.1 An Overview of Renewable Energy.....	6
2.2 Environmental Impact of Renewable Energy	8
2.3 Hybrid Power Systems – HPS	9
2.4 Solar Power Renewable Energy System	11
2.5 Wind Energy.....	23
2.6 Battery Storage	30
2.7 Energy Management Systems in Hybrid Power Systems	36
2.8 Comparison and Evaluation of EMS Approaches for Hybrid Power Systems.....	40
CHAPTER THREE: MATHEMATICAL MODELLING OF PROPOSED ENERGY MANAGEMENT STRATEGY .	43
3.1 Introduction	43
3.2 Development of the HPS model	43
3.3 System Model	44
3.4 PV Model Design.....	44
3.4.1 Assumptions for the PV model:.....	45
3.4.2 Model Selection for PV model.....	45
3.4.3 Design of the PV Model	45
3.4.4 Results and Its Significance.....	46
3.4.5 Mathematical models for PV design	47
3.4.6 Purpose of the Mathematical Models.....	48
3.4.7 Maximum Power Point Tracking (MPPT) Controller Design for the PV Model.....	49
3.5 Development of the Wind Energy System.....	51

3.6	Development of the battery storage unit.....	54
3.6.1	Battery Selection	54
3.6.2	Adjustments for the Lithium-Ion Battery Model.....	55
3.6.3	Mathematical Equations for the Battery Model	55
3.6.4	State of Charge (SOC) and Battery Protection	56
3.7	Development Of Event-Based Availability Controller.....	57
CHAPTER FOUR: MODEL AND ANALYSIS OF THE HPS		63
4.1	Modelling the PV System	63
4.2	Testing PV Model Methodology	65
4.3	Modelling the Wind System.....	69
4.4	Wind System testing methodology.....	71
4.5	Battery Storage Unit Modelling	74
4.6	Battery Model Testing Methodology.....	76
4.7	Modelling the Event-Based Controller for the Hybrid Power System (HPS)	78
4.8	Modelling the Entire Hybrid Power System (HPS).....	80
CHAPTER FIVE: DISCUSSION OF RESULTS.....		82
5.1	Introduction	82
5.2	PV Model Results in the HPS.....	82
5.3	Results of the Battery Storage Unit in the HPS.....	86
5.4	Results of Controller Monitoring the Availability of Each Source Supply.....	87
5.5	Battery Status Results	95
5.6	Load Results	96
5.7	AC/DC/AC PWM Converter Results When the Load Demand is Met	98
5.8	AC/DC/AC PWM Converter Results for the Source Available but Not Selected to Supply the Load	98
5.9	Discussion on the Results of the PV Performance in the HPS	99
5.10	Discussion of the Battery Status Results.....	100
5.11	Discussion on the Controller Results	100
5.12	Simulation Analysis	100
5.13	Drawbacks Associated with the Models Simulated.....	101
CHAPTER SIX: CONCLUSION AND RECOMMENDATIONS		102
REFERENCES		105
APPENDIX A: PV Model Specifications		112
APPENDIX B: Code		114
APPENDIX C: AC/DC/AC PWM/ Converter		117
APPENDIX D: HPS Results Under Various Scenarios.....		118

LIST OF FIGURES

Figure 2-1 Solar PV system basic principle.....	12
Figure 2-2 components of a PV module.....	13
Figure 2-3: Ideal model of solar cell	15
Figure 2-4: PV Cell Single Diode Model with Series Resistor Only.....	16
Figure 2-5: PV Cell Single Diode Model with Both Shunt and Series Resistor	16
Figure 2-6: Double Exponential Model of a PV Cell	17
Figure 2-7: Two-Diode Model with Shunt and Series Resistor	17
Figure 2-8: Block diagram illustration of the general MPPT process/algorithm	18
Figure 2-9: current-voltage characteristic for a PV array	19
Figure 2-10: Flow chart illustrating the operation of the P&O method/algorithm.	20
Figure 2-11: Flow chart of the algorithm for the incremental inductance method.....	21
Figure 2-12: A feedback control system of a PV battery charging	22
Figure 2-13: An equivalent circuit of a DC-AC inverter connected to a PV array	22
Figure 2-14: Overview of a wind turbine.....	24
Figure 2-15: Block diagram of a PMSG wind energy design	25
Figure 2-16: Schematic of a DFIG incorporated in a wind energy conversion system	26
Figure 2-17: Wind Turbine power flow diagram.....	27
Figure 2-18: An offshore wind farm with three bladed horizontal axis wind turbines	28
Figure 2-19: Vertical-axis wind turbine	28
Figure 2-20: Variable Speed Pitch-Regulated Wind Turbine Schematic.....	29
Figure 2-21: Block diagram of a battery charging control system	31
Figure 2-22: Comparison of The Voltage Profiles of Various BESS's.....	34
Figure 3-1: Schematic of the HPS System Model	44
Figure 3-2: PV solar cell with single-diode and series resistance	45
Figure 3-3 MATLAB Simulink PV Model.....	46
Figure 3-4 MPPT controller algorithm for the PV system.....	50
Figure 3-5: Doubly-fed induction generator and wind turbine schematic	52
Figure 3-6: The pitch control system implemented with the DFIG	53
Figure 3-7: Boolean expression depicting the relationship among the expected inputs and outputs of the HPS controller	60
Figure 3-8 The MATLAB Simulink flowchart for controller operation	61
Figure 4-1: AC/DC/AC PWM converter as an equivalent PV model and DC/AC converter...	64
Figure 4-2: Integration of the equivalent PV model with the DC/AC converter and load	64
Figure 4-3: Voltage vs power trend for the designed PV model with varying irradiance.....	65
Figure 4-4: Voltage versus current trend for the designed PV model with varying irradiance	66

Figure 4-5: Voltage versus power trend of the designed PV model with varying temperature	67
Figure 4-6: Voltage versus current trend for the designed PV model with varying temperature	68
Figure 4-7 The three-phase voltage source connected to the doubly-fed induction generator wind turbine.	70
Figure 4-8: The wind equivalent block internal system captures and processes the wind energy data received from the workspace.....	71
Figure 4-9 Simulated outputs of the DFIG wind turbine, showing DC link voltage (V _{dc}), rotor speed, wind speed, and pitch angle in response to a step input, where wind speed increases from 8 m/s to 14 m/s over 10 seconds.	72
Figure 4-10 Grid data acquisition results, showing reactive power, positive sequence voltage and current of the plant, and motor speed of the DFIG wind turbine, highlighting its interaction with the grid.	73
Figure 4-11 Model of the Lithium-Ion battery used in Simulink	74
Figure 4-12 Integration of the Lead-Acid battery model with the AC/DC/AC PWM converter	75
Figure 4-13 Battery model Integration with DC/AC PWM converter and load	75
Figure 4-14 Battery model output when connected to AC/DC/AC PWM converter with load	76
Figure 4-15 Modified SOC levels for a 10-second simulation in the equivalent battery model integrated into the HPS.....	77
Figure 4-16 Modified armature current output for the 10-second simulation in the equivalent battery model integrated into the HPS	78
Figure 4-17 Simulink schematic of the event-based controller	79
Figure 4-18: Hybrid Power System (HPS) Simulink design showing the PV system, wind system, battery storage, controller, and load interconnected.....	81
Figure 5-1: Voltage vs. Power for PV model integrated with DC/AC converter	82
Figure 5-2: Voltage vs. Current for PV model integrated with DC/AC converter	83
Figure 5-3: Voltage vs. Power output for PV model integrated with DC/AC converter	83
Figure 5-4: Voltage vs. Current output for PV model integrated with DC/AC converter	84
Figure 5-5: Ideal tracking of MPPT points for Voltage vs. Current output for the PV model resulting in optimal performance with maximum output.....	84
Figure 5-6: Ideal tracking of MPPT points for the Voltage vs. Power output of the PV model resulting in optimal performance and maximum power output.....	85
Figure 5-7: Display on the AC/DC/AC PWM converter with the PV model equivalent when the PV model is not available for supply	85
Figure 5-8: The PWM converter's operation during discharging of the Lithium-Ion battery model equivalent.....	86

Figure 5-9: The PWM converter's operation during the charging of the Lithium-Ion battery model equivalent.....	87
Figure 5-10: Output of controller for CASE 1 illustrating that no source is available to supply the load.....	88
Figure 5-11: The output of the controller for CASE 2 illustrating the battery is discharged to supply the load.....	89
Figure 5-12: The output of the controller for CASE 3 illustrating that the wind energy system supplies the load.....	90
Figure 5-13: The output of the controller for CASE 4 illustrating that the wind energy system supplies the load.....	91
Figure 5-14: The output of the controller for CASE 5 illustrating that the PV system supplies the load.....	92
Figure 5-15: The output of the controller for CASE 6 illustrating that the PV system supplies the load.....	93
Figure 5-16: The output of the controller for CASE 7 illustrating that the battery will charge via the wind energy system while the PV system supplies the load.	94
Figure 5-17: The output of the controller for CASE 8 illustrating that the PV system will supply the load.....	95
Figure 5-18: The output of the controller display when the battery exceeds the maximum limit of SOC.....	95
Figure 5-19: Battery status output from the controller for CASE 2, showing the battery supplying the load.....	96
Figure 5-20: The battery status output from the controller for CASE 7, showing the load being supplied by PV while wind energy charges the battery.....	96
Figure 5-21: The load result when supplied by one of the HPS sources.....	97
Figure 5-22: The load result when no source is available to supply the load	97
Figure 5-23: AC/DC/AC PWM converter result connected to energy source the controller has selected to supply the load	98
Figure 5-24: The result on the AC/DC/AC PWM converter connected to the available source that was not selected to supply the load	99

LIST OF TABLES

Table 2-1: Comparison of Various Battery Types 33

Table 2-2: Comparison of EMS Approaches 40

Table 3-1: Battery selection weighting 55

Table 3-2 Battery parameters implemented in the NiMH battery model..... 56

Table 3-3: HPS controller possible inputs and corresponding outputs..... 58

LIST OF APPENDICES

APPENDIX A: PV Model Specifications	112
APPENDIX B: Code	114
APPENDIX C: AC/DC/AC PWM/ Converter	117
APPENDIX D: HPS Results Under Various Scenarios	118

GLOSSARY

AC/DC/AC Converter: A power converter that transforms alternating current (AC) into direct current (DC) and then back to AC, used for efficient power management in hybrid systems.

Battery Energy Storage System (BESS): A technology that stores energy to be used at a later stage, typically using chemical batteries, and facilitates in balancing supply and demand in energy systems.

Boost Inverter: A type of inverter that increases (boosts) the voltage from a lower input voltage to a higher output voltage.

Controller: A device or software that manages the operation of a system, ensuring optimal performance and efficiency. In this context, it refers to the energy management controller for the Hybrid Power System (HPS).

Doubly-Fed Induction Generator (DFIG): A type of generator commonly used in wind turbines, allowing for variable speed operation and improved efficiency by using both rotor and stator windings.

Fill Factor Technique: A method used in photovoltaic systems to determine the maximum power point (MPP) by analysing the ratio of the maximum attainable power to the product of open-circuit voltage and short-circuit current.

Hybrid Power System (HPS): A system that integrates multiple renewable energy sources, such as wind and solar, with battery storage to offer a consistent and efficient electricity supply.

Maximum Power Point Tracking (MPPT): A method used in photovoltaic systems to continuously adjust the operating point to ensure maximum power generation despite changing environmental conditions.

Photovoltaic (PV) System: A renewable energy technology that converts sunlight directly into electricity using solar cells.

Permanent Magnet Synchronous Generator (PMSG): A type of generator that uses permanent magnets to create a magnetic field, eliminating the need for separate excitation and improving efficiency, particularly in variable-speed wind turbines.

State of Charge (SOC): A measure of the current charge level of a battery relative to its capacity, expressed as a percentage.

Tip Speed Ratio (TSR): The ratio of the speed of the tip of a wind turbine blade to the speed of the wind, used to optimize the efficiency of wind energy capture.

Wind Turbine Induction Generator (WTIG): A type of generator which converts mechanical energy from wind turbines into electrical energy, typically using the principle of electromagnetic induction.

Zinc Bromine Battery: A type of flow battery which utilizes zinc and bromine as electrolytes, known for high energy density and the ability to discharge completely without damage.

CHAPTER ONE: INTRODUCTION

1.1 Background

Renewable energy is classified as a clean source of energy for electricity generation (International Energy Agency, 2021). As greenhouse gas (GHG) emissions continue to rise on a global level, renewable energy sources become a logical and viable option to mitigate climate change and global warming. Although renewable energy is unpredictable in nature, it is worth implementing due to its promising results when installed in an appropriate environment. The integration of multiple sources of renewable energy sources, such as wind and Photovoltaic, increases the systems reliability as a hybrid solution while incorporating a battery energy storage system.

Investigating alternatives to generating electricity is crucial for any country or region, as it can provide remote areas with access to electricity efficiently and cost-effectively. Among these alternatives, renewable energy sources stand out as viable solutions, offering promising results despite their inherent unpredictability. With GHG emissions on the rise, the reliance on fossil fuels for electricity generation poses a significant threat to global warming and climate change. In this context, renewable energy emerges as a clean and sustainable form of energy, presenting one of the most promising solutions to combat the global warming crisis.

Photovoltaic (PV) and wind systems have played integral roles in energy systems over the years. PV systems harness sunlight to generate electricity, while wind systems convert wind energy into electrical power. Their impact lies in their ability to provide renewable energy in abundance, mitigating the dependency on finite fossil fuel resources and reducing (GHG) emissions. Research has shown that integrating PV and wind systems into energy mix or electrical power grid can enhance system reliability, increase energy independence, and contribute to environmental sustainability.

Several studies have highlighted the potential benefits of PV and wind systems in electricity generation. For instance, (Sawle, et al., 2016) demonstrated the effectiveness of PV systems in remote area electrification, while (Ullah, et al., 2024) emphasized the importance of wind energy integration for grid stability. These works underscored the importance of exploring renewable energy solutions, particularly the synergistic integration of PV and wind systems, in addressing global energy challenges.

However, relying exclusively on a single renewable energy source may not be sufficient to meet the demands of modern energy systems. Therefore, an integrated approach that combines numerous renewable energy sources, including PV and wind systems, is essential

to ensure energy security and sustainability. Developing innovative control systems to optimize the utilization of renewable energy sources and decrease reliance on the main grid is critical for achieving this goal.

Investigating alternative energy sources to generating electricity is crucial for any country or region as it can offer remote areas with access to electricity in a cost-effective and efficient manner. Renewable energy sources are a viable solution worth pursuing due to its promising results when implemented in the correct situation even though renewable energy is unpredictable in nature. Globally, with greenhouse gas emissions increasing, the burning of fossil fuels to generate electricity is a great threat to global warming, which results in climate change. Renewable energy is classified as a clean form of energy and offers one of the best solutions to combat the global warming crisis. Renewable energy sources demonstrate great potential hence it is worth investigating. However, one renewable energy source won't be feasible enough on its own. Therefore, a combination of renewable energy sources working together will provide a better solution. A revolutionary control system to determine which renewable energy source is best to supply power is critical to ensure demand is always met and system efficiency is at its highest, while reliance on the main grid is minimised as much as possible.

1.2 Objectives of the study

1.2.1 Problem statement

Modern hybrid power systems are composed of a cluster of renewable energy and storage systems. These systems can operate both on-grid and off-grid to meet the energy demands of local loads. Due to the irregular nature of renewable energy sources such as solar and wind, integrating storage systems like batteries is essential to ensure the high reliability and stability of the power supply, especially in off-grid mode, where there is no backup from the main utility grid. This necessitates the design of an effective energy management system.

The research questions addressed in this study are:

- How is energy balance achieved in a hybrid PV-wind-battery power system when a reliable energy management system is implemented?
- What is the effect of the proposed energy management system on the overall system's performance, efficiency, and its ability to adapt under different operating scenarios and conditions?
- How accurate is the proposed energy management system in predicting and managing energy flows?

1.2.2 Aim of the research

This thesis seeks to develop an Energy Management System (EMS) for a hybrid PV-wind-battery power system that efficiently manages energy generation and storage. The system will integrate photovoltaic (PV) solar and wind energy as primary sources, with a storage battery serving as a backup to ensure consistent energy supply. The EMS will dynamically assess and optimize energy dispatch decisions based on real-time conditions, ensuring the load is continuously met even when renewable energy production is insufficient. The performance of the proposed energy management strategy will be simulated and evaluated using MATLAB to validate its effectiveness in different operational scenarios.

1.2.3 Objectives of the research

- Develop an energy management strategy that optimally integrates renewable energy sources (PV and wind) with battery storage to meet fluctuating energy demands.
- Design and implement a system to coordinate the operations of the PV, wind, and battery storage to ensure system stability and reliability.
- Create a hybrid power system (HPS) that efficiently adapts to varying environmental conditions and energy load demands.
- Design a control algorithm that dynamically adjusts energy generation and storage based on fluctuations in renewable energy availability and load requirements.
- Implement and simulate the proposed energy management system in MATLAB Simulink to analyse system dynamics and optimize energy distribution across the hybrid system.
- Evaluate the performance of the proposed energy management strategy under different operational scenarios, including varying renewable energy availability and load conditions.

1.3 Scope and Limitations

In this study, only wind and solar PV energy are considered as the renewable energy sources. Chemical batteries are the only type of energy storage devices examined for integration into the HPS. The area in which the HPS is intended to be implemented is generalized based on the cases deduced from weather conditions. Specific areas are not considered for the cases. In general, the HPS is designed to be implemented in relatively sunny and windy areas that are not prone to severe stormy weather conditions. No software other than MATLAB Simulink is used for the models and simulations in this dissertation.

1.4 Dissertation Outline

The layout of this dissertation report is as follows:

- Chapter 1: Introduction

This section provides an overview of the dissertation topic, scope of the project, as well as the aims and objectives. It sets the foundation for the study and outlines the key research questions and hypotheses to be addressed.

- Chapter 2: Literature review

This section presents the literature review encompassing the research performed on each important facet of this thesis topic and the research plan for this thesis based on the findings from the literature review.

- Chapter 3: Mathematical Modelling of Proposed Energy Management Strategy

This chapter delves into the fundamental methodology employed in the development of the Hybrid Power System (HPS) and its associated controller. It begins with a detailed exploration of the modelling process for the individual components of the HPS, namely the photovoltaic (PV) system, wind turbine system, and battery storage system. The intricacies of modelling each component are examined, encompassing factors such as system specifications, environmental conditions, and component characteristics.

Furthermore, this chapter explains the development of the energy management controller tailored for the HPS. Through a systematic approach, the design and implementation of the controller are thoroughly outlined, focusing on the integration of control algorithms, feedback mechanisms, and optimization techniques. The rationale behind the controller's architecture and functionality is explained, underscoring its pivotal role in orchestrating the seamless operation of the HPS.

- Chapter 4: Model and Analysis of the HPS

Building upon the groundwork laid in Chapter 3, this chapter delves deeper into the mathematical modelling of the energy system model for the Hybrid Power System (HPS) using MATLAB Simulink. Specifically, it focuses on the integration of the previously developed models of the PV, wind, and battery systems into a comprehensive HPS model.

Through a systematic approach, the chapter explains the process of integrating the energy management controller with the HPS model in MATLAB Simulink. This integration enables the simulation of the HPS's dynamic behaviour under various operating conditions and load

demands. The chapter also discusses the validation of the HPS model, highlighting the fidelity of the simulations to real-world performance.

Together, Chapters 3 and 4 provide a comprehensive overview of the methodology employed in the development and modelling of the Hybrid Power System, laying the foundation for subsequent analyses and evaluations in the dissertation.

- Chapter 5: Discussion of Results

This chapter presents the simulations results obtained from the developed HPS model performed on the HPS model developed in Chapter 4 using MATLAB Simulink. The simulations analyse the performance of the HPS under various operating conditions, considering factors such as resource availability and system efficiency. The results obtained from these simulations provide insights into the performance of the HPS under different scenarios, highlighting the efficiency and effectiveness of the system in managing resource availability and meeting load demands.

- Chapter 6: Conclusions and Recommendations

The conclusions drawn from the findings of this thesis are stated in this chapter. Additionally, recommendations for future research directions and improvements to the proposed energy management strategy for hybrid PV-wind-battery storage systems will be presented. The chapter concludes the dissertation by summarizing the key insights and contributions to the field.

CHAPTER TWO: LITERATURE REVIEW

2.1 An Overview of Renewable Energy

Renewable energy has gained increasing attention globally as governments and organizations recognize the environmental impact of conventional energy sources. Based on a report by the Energy Information Administration (Nair & Garimella, 2010), coal accounted for 41% of global electricity generation in 2006. Remarkably, recent data from 2020 (carbonbrief.org, 2020) indicates that coal still meets approximately 40% of global electricity demand. This persistence underscores the urgent need for transitioning to sources of renewable energy to mitigate CO₂ emissions and reduce environmental pollution.

From (Odoi-Yorke, et al., 2022), it was well noted that the global energy sector has significantly become dependent on fossil fuel usage for electricity generation. In (Ritchie, et al., 2024), it is shown that fossil fuels are a significant contributor to the emissions of greenhouse gasses which results in drastic climate change effects. Furthermore, studies indicate that fossil fuels are finite and will deplete at some point in time. Even though the effects that fossil fuels are causing to the environment are known, it is still the primary energy source of electricity generation in developed and developing countries globally (Statista Research Department, 2024).

In South Africa, 88.8% of electricity production comes from coal (Ayamolowo, et al., 2022). Despite this heavy reliance on coal, the current power production is still insufficient to meet the country's demand, leading to scheduled outages to prevent a nationwide blackout. Eskom, the main power utility, depends on diesel generators to minimize load-shedding, burning approximately 9 million litres of diesel daily to maintain power supply (Labuschagne, 2022). Eskom is also recognized as the world's largest emitter of health-damaging sulphur dioxide (SO₂) (Centre Environmental Rights, 2021), a significant air pollutant that poses severe health risks, including respiratory and cardiovascular diseases. The high levels of SO₂ emissions highlight the urgent need for transitioning to cleaner energy sources. Moreover, with the ongoing Russian-Ukrainian war, the rising cost of crude oil makes it increasingly expensive for Eskom to continue its current rate of diesel consumption. Therefore, developing a greener and more independent energy source is crucial for improving public health, reducing environmental impact, and ensuring energy security.

To catalyse the implementation of renewable energy systems, such as photovoltaic (PV) and wind systems, micro systems could be utilised to supply electricity to remote areas.

These micro systems can serve as the cornerstone for extending access to renewable energy. As advancements in micro hybrid systems progress, multiple micro systems can be interconnected to form larger-scale hybrid power systems, allowing for broader coverage and increased energy generation capacity (Zebra, et al., 2021). This approach aims to provide electricity to communities currently lacking access, ultimately raising their standard of living and enhancing overall quality of life. However, it's critical to note that the benefits of renewable energy extend beyond just underprivileged communities, impacting society. There are numerous facets of renewable energy technologies (RETs) to analyse.

RETs encompass a diverse array of technologies designed to harness renewable energy sources such as biomass, geothermal, solar, wind, and hydro. These technologies are pivotal in diversifying and decentralizing energy generation, thus lowering reliance on finite fossil fuel resources and reducing the environmental impacts coupled with conventional energy generation (Zhang, 2024).

- **Solar Energy:** Solar technologies, including concentrated solar power (CSP) and photovoltaic (PV) panels systems, harness solar energy and convert it into heat or electricity. PV panels are commonly installed in solar farms or on rooftops to generate electricity, while CSP systems concentrate sunlight to produce high-temperature heat for power generation (Lange, 2013).
- **Wind Energy:** Wind turbines harness kinetic energy from the wind which is then converted into electrical power. Wind farms, onshore and offshore, are implemented in areas with consistent wind patterns to harness this renewable resource efficiently.
- **Hydroelectric Energy:** Hydroelectric power plants generate electricity by employing the gravitational force of flowing water. Dams and reservoirs are used to collect water, which is released through turbines to generate electricity as it flows downstream.
- **Geothermal Energy:** Geothermal power plants harness the Earth's heat stored deep underground to generate electricity or provide heating and cooling. Geothermal energy is exploited via geothermal heat pumps or geothermal power plants.
- **Biomass Energy:** Biomass technologies utilize organic materials such as wood, agricultural residues, and solid waste from municipalities to generate heat, electricity, and/or biofuels. Biomass combustion, gasification, and anaerobic digestion are common processes employed in biomass energy production.

In this work, the focus will be on harnessing solar and wind energy, two of the most ample and viable sources of renewable energy, particularly within the context of South Africa's energy landscape. The study will concentrate on integrating photovoltaic (PV) systems and wind turbines into a hybrid power system (HPS) that also incorporates battery storage to ensure a stable and continuous energy supply. These sources of renewable energy are chosen due to their complementary nature; while solar energy is most effective during the day, wind energy can be harnessed at various times, including during night hours or periods of low sunlight. By concentrating on these two renewable energy sources, this research aims to develop an efficient energy management strategy that optimizes the use of solar and wind resources to meet energy needs, thereby reducing dependence on fossil fuels and lessening impacts on the environment.

2.2 Environmental Impact of Renewable Energy

Given the focus of this work on renewable energy technologies (RETs), particularly photovoltaic (PV) systems and wind turbines, it is essential to understand their prospective environmental impact and benefits. The shift from conventional fossil fuel-based energy sources to renewable energy is not only necessary to mitigate the detrimental effects of greenhouse gas emissions but also to ensure sustainable and cost-effective electricity generation. The utilization of renewable energy in hybrid power systems (HPS) offers numerous advantages, including enhanced energy security, reduced environmental footprint, and lower operating costs (Paska, et al., 2009).

In this section, the environmental impact and benefits of renewable energy, specifically solar and wind energy, will be discussed in detail. The subsections will focus on the clean energy attributes of renewables, the challenges and alternatives to grid extension, the growing viability of renewable energy as a sustainable generation scheme, and the overall benefits that renewable energy integration brings to HPS. This discussion will highlight why solar and wind energy are the focal points of this research and how their integration into a hybrid system can address both environmental and energy access challenges.

2.2.1 Renewable energy as a clean energy form

There is a great need for an alternative resource of electricity generation since the burning of fossil fuels produces extreme amounts of greenhouse gases (Wang & Azam, 2024). It has negative impacts on the economy to continue to depend on fossil fuels as the costs are increasing. It seems that renewable energy is the future of electricity generation mainly due to it being clean and highly accessible globally. It will also decrease the dependency on fossil fuels by switching over to renewable technologies.

2.2.2 Grid extension impacts

Extending the grid to remote areas is often cost-prohibitive, particularly in developing countries. For example, in Malawi, 90% of rural areas lack access to electricity, while in South Africa, 15% of the population remains unelectrified (data.worldbank.org, 2019) (tradeingeconomics.com, 2019). Renewable energy solutions, such as small-scale wind turbines and solar microgrids, provide economical and sustainable alternatives to grid extension, enabling remote communities to access reliable electricity (Mtshali, et al., 2011).

2.2.3 Renewable energy as an alternative energy generation scheme

Renewable energy is increasingly viable as fossil fuel resources dwindle and prices rise. Renewable technologies offer lower operating costs and reduced maintenance, making them attractive for sustainable energy generation (Mtshali, et al., 2011). By combining renewable energy sources such as photovoltaic (PV) systems and wind turbines, we can improve energy security and lower environmental impacts.

2.2.4 Renewable Energy Benefits

Beyond providing electricity to various areas, the shift from fossil-fuel centred electricity generation to renewable energy within an HPS framework offers significant environmental and health benefits (Ouerghi, et al., 2024). The reduction in greenhouse gas emissions associated with fossil fuels is a key advantage, as these emissions are detrimental to human health and the environment. Mitigating the usage of fossil fuels is essential to prevent irreversible environmental damage.

Additionally, the simplicity and efficiency of network infrastructure in HPS are enhanced by reducing the need to convert DC to AC. This results in fewer harmonics introduced into the system (Mtshali, et al., 2011).

HPSs also offer cost benefits by minimizing the need for extensive distribution and transmission lines, further reducing overall system costs.

2.3 Hybrid Power Systems – HPS

Hybrid Power Systems (HPS) combine multiple sources of renewable energy, such as solar, wind, hydroelectric, and biomass, along with energy storage technologies, to provide a more reliable and efficient electricity generation solution. Unlike standalone renewable energy systems, which may suffer from intermittency and variability due to weather

conditions, HPS leverages the balancing nature of different energy sources to enhance overall system performance and reliability.

Hybrid Power Systems (HPS) combine various sources of renewable energy with energy storage systems to consistently meet energy demand. By integrating multiple renewable energy technologies, HPS mitigate the limitations of individual sources, such as intermittency and variability, ensuring a more reliable and stable energy supply (Olabode, et al., 2021).

2.3.1 Integration of HPSs

While renewable energy sources offer promising solutions for electricity generation, their use in standalone systems may be limited by their inherent variability and unpredictability. Hybrid Power Systems address this challenge by combining diverse renewable energy sources within a single integrated framework. By harnessing the synergies between different energy sources, HPS enhance system reliability and performance, presenting a more consistent and dependable supply of energy compared to standalone renewable energy systems (Mtshali, et al., 2011).

The combination of multiple renewable energy sources in HPS not only increases system reliability but also optimizes energy utilization, resulting in improved cost-effectiveness and efficiency. Additionally, the inclusion of energy storage systems, such as batteries or pumped hydro storage, further enhances the flexibility and resilience of HPS by enabling energy to be stored during periods of excess generation and discharge during high demand periods (Coppez, et al., 2010).

2.3.2 Applications of Standalone HPS

Standalone Hybrid Power Systems (HPS) find diverse applications in off-grid or remote locations where access to central electricity grids is limited or unavailable (Yang, et al., 2022). These systems integrate multiple sources of renewable energy, such as wind and PV solar, along with battery storage, to meet the electricity demands of isolated communities or facilities.

In a standalone HPS configuration, the interplay between wind, PV solar, and battery storage components ensures a continuous and reliable electricity supply to meet the mandatory load demand. The capacity and performance of the HPS are tailored to the specific energy needs of the intended application, whether it be powering remote villages, telecommunications towers, or off-grid industrial operations.

However, the operational efficiency and effectiveness of standalone HPS depend on numerous factors, including the accessibility of renewable energy resources, the sizing of components, and the implementation of efficient energy management strategies. By harnessing renewable energy and storage technologies, standalone HPS offer sustainable and resilient solutions for decentralized electricity generation in remote environments (Yang, et al., 2022).

2.4 Solar Power Renewable Energy System

Solar energy is one of the amplest sources of renewable energy that exists. This makes it a resource that appealing to be used as a vital part of the renewable energy system. The cost of solar panels is declining over the years while its efficiency is on the increase due to improved technologies. Solar power systems have high capital costs, but the appeal lies in their cost-effectiveness, particularly in small-scale implementations compared to large-scale ones (Chowdhury, et al., 2009).

Photovoltaic (PV) systems are a cornerstone of renewable energy technology, harnessing solar energy to generate electricity. Solar energy offers several significant advantages, including its environmentally friendly nature, as it produces no pollution and contributes to reducing carbon emissions (Eynde, et al., 2010). Additionally, minimal maintenance is required by PV systems, making them cost-effective in the long term (Eynde, et al., 2010). Their sustainability is unmatched, as solar energy can be harnessed indefinitely without depletion, contributing to long-term energy security (Eynde, et al., 2010).

Moreover, PV systems are remarkably advantageous in isolated or off-grid locations where traditional grid infrastructure is absent, providing essential access to electricity (Eynde, et al., 2010). The cost efficiency of solar energy is further enhanced when PV systems are located close to the load, reducing transmission and distribution losses and safeguarding a reliable power supply (Eynde, et al., 2010).

However, the deployment of PV systems also comes with challenges. The most significant of these is the inconsistency of solar irradiance, which leads to variable power output. This intermittency can cause disruptions in power supply, making it difficult for PV systems to continuously meet load requirements without supplementary energy storage or backup systems (Eynde, et al., 2010).

In figure 2-1 (Achaibou, et al., 2012), the basic principle of a typical solar PV system is depicted (Mtshali, et al., 2011), showcasing its fundamental operation.

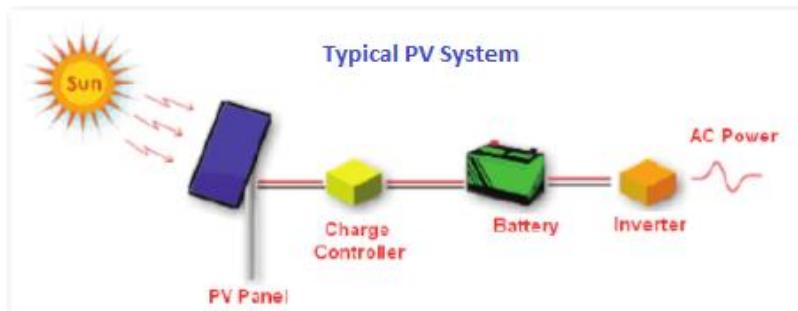


Figure 2-1 Solar PV system basic principle

2.4.1 PV module main components:

Photovoltaic (PV) modules, the building blocks of solar panels, comprise several essential components that work jointly to convert energy from the sun into electricity. The key components of a PV module include:

- **Glass Cover:** A transparent, durable cover made of tempered glass that protects the cells in the panel from environmental elements such as moisture, dust, and impact.
- **Lamination:** Layers of encapsulant material, typically ethylene-vinyl acetate (EVA), that seal and laminate the solar cells and other components together within the module, providing structural integrity and protection against humidity and thermal stresses.
- **Solar Cells:** Crystalline silicon solar cells, either polycrystalline or monocrystalline, are the heart of the PV module. These cells harness the energy from the sun and convert it into direct current (DC) through the photovoltaic effect.
- **Copper Ribbons:** Thin copper strips used to interconnect the solar cells within the module, forming a parallel or series arrangement to accomplish the desired current and voltage output.
- **Plastic Backing:** A durable, waterproof backing layer made from materials such as polyvinyl fluoride (PVF) or polyethylene terephthalate (PET), which provides additional protection and insulation for the solar cells and other internal components.
- **Junction Box:** An enclosure located behind the PV module that stores electrical connections, diodes, and bypass diodes. The junction box serves to protect the internal wiring and facilitate the connection of multiple modules into a solar array, enabling efficient electrical wiring and maintenance.

In Figure 2-2 below, these components produce a robust and efficient PV module capable of harnessing solar energy to generate clean and renewable electricity for numerous applications, ranging from utility-scale solar farms to residential rooftop installations.

The figure 2-2 below presents the design of a solar PV module (Dubey, et al., 2013):

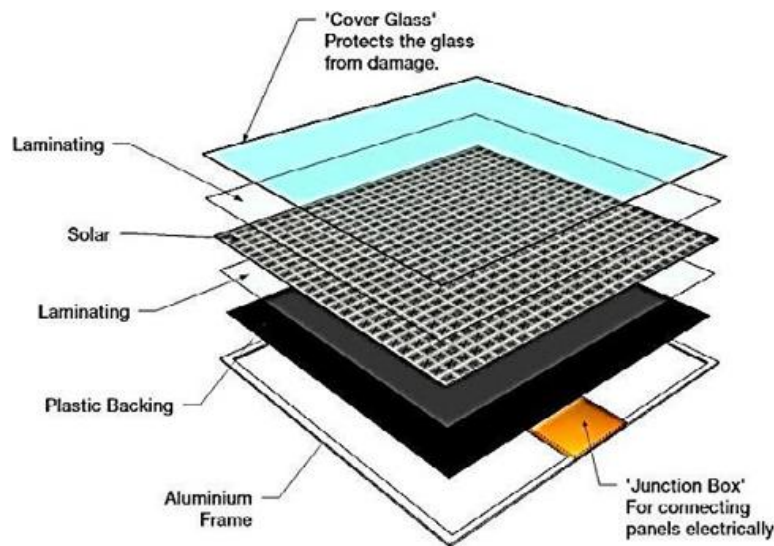


Figure 2-2 components of a PV module

2.4.2 Limitations of solar energy

- Weather conditions dependency

Solar energy is a resource in abundance and virtually infinite. However, the energy from the sun can only be harnessed significantly on clear sunny days compared to cloudy days. On bad weather days, the solar energy captured is significantly reduced. Therefore, the variation in solar irradiance impacts the efficiency of the generation of electricity using solar energy.

- Daytime impact

Solar energy can't be harnessed at night due to levels of solar irradiance being too low for efficient energy generation. During the night, the output is virtually zero which results in not being able to supply a load of any kind.

- Solar energy distribution

Solar PV can supply the load when the demand and supply are equal. However, when the supply is greater than the demand, the excess energy is 'dumped' or wasted. Solar PV on its own does not have a means to store the excess energy for a future stage when required.

2.4.3 PV Module Types

Photovoltaic (PV) modules are offered in several types, each with apparent characteristics and performance attributes:

- **Monocrystalline PV Modules:** Monocrystalline solar panels are manufactured from single-crystal silicon, which is cut into wafers to form individual cells. These cells have a uniform dark colour and rounded edges, giving monocrystalline modules a sleek

appearance. Monocrystalline panels have a high efficiency and space-saving design, which makes them ideal for installations with limited space, such as rooftops (Marsh, 2023).

- **Polycrystalline PV Modules:** Polycrystalline solar panels are made by melting silicon crystals together to form ingots, and then sliced into wafers. Polycrystalline cells have a blueish appearance and square edges due to their manufacturing process. While polycrystalline modules generally have an efficiency lower than monocrystalline panels, they offer a cost-effective option for large-scale installations where space isn't a constraint (Marsh, 2023).
- **Multi-crystalline PV Modules:** Multi-crystalline solar panels are similar to polycrystalline modules, by melting silicon crystals together to form ingots. However, multi-crystalline cells have a more irregular and fragmented structure compared to polycrystalline cells. Multi-crystalline modules typically offer moderate efficiency and performance, appropriate for numerous applications, including installations in residential and commercial applications.
- **Thin-Film PV Modules:** Thin-film solar panels are produced by depositing thin layers of semiconductor materials, like amorphous silicon (a-Si), cadmium telluride (CdTe), or copper indium gallium selenide (CIGS), onto a substrate material. Thin-film modules are lightweight, flexible, and less expensive to produce in comparison to crystalline silicon modules. Nonetheless, they generally have an efficiency that is lower and degrade faster over time, making them better suited for large-scale utility installations or niche applications where cost and flexibility are prioritized over efficiency.

All types of PV modules have its benefits and restrictions, and the selection of module varies based on factors such as space availability, budget, efficiency requirements, and installation conditions.

2.4.4 PV models equivalent circuit designs

Numerous PV circuit models have been developed and each one has its unique advantages in specific applications. Some of the downsides of models are the complexity of the calculations associated with the model equations because of too many unknown variables.

- **Ideal PV model**

The ideal PV model serves as a fundamental representation of a photovoltaic system under ideal conditions. In this model, the PV module is assumed to operate at its maximum power point (MPP) continuously, regardless of environmental factors or load variations. The ideal PV

model simplifies calculations by considering the solar cell as a perfect energy converter with no losses or limitations (Baba, et al., 2020).

The characteristics of the ideal PV model include:

1. **Perfect Conversion Efficiency:** The ideal PV model assumes 100% conversion efficiency, meaning that all solar radiation that is available is converted into electrical energy without any losses.
2. **Constant Maximum Power Point:** In ideal conditions, the PV module operates at its maximum power point (MPP) continuously, providing a constant and predictable output regardless of variations in solar irradiance or temperature.
3. **Current and Voltage Linear Relationship:** The ideal PV model represents the current-voltage (I-V) curve of the PV module as a straight line, simplifying analysis and calculations.

Nevertheless, it's critical to note that the ideal PV model is purely theoretical and does not accurately reflect real-world PV system behaviour. Actual PV modules experience losses due to factors such as temperature variations, shading, and non-uniform irradiance.

Figure 2-3 illustrates the ideal PV model and its simplified representation of the PV module's behaviour under ideal conditions (Eynde, et al., 2010).

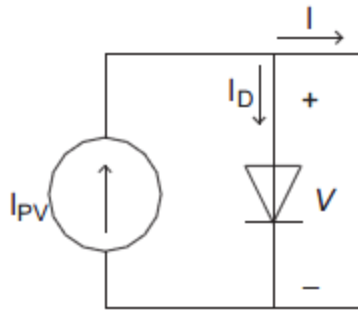


Figure 2-3: Ideal model of solar cell

- Single diode model

The single diode model is a commonly used PV circuit model that strikes a balance between accuracy and simplicity (Eynde, et al., 2010). This model incorporates a single diode to represent the behaviour of the photovoltaic cell under varying operating conditions. While the single diode model grants a simplified representation of the PV module, it may not capture all the intricacies of real-world performance.

The accuracy of the single diode model can be enhanced by adding a shunt resistor (Ishaque, et al., 2011). This addition helps to improve the model's representation of the PV module's behaviour, particularly under non-ideal conditions. However, despite these improvements,

single diode models still have limitations, particularly in accurately accounting for losses related to recombination processes (Ishaque, et al., 2011).

Figure 2-4 illustrates the single diode model for a PV cell with only a series resistor, providing a visual representation of how the model represents the behaviour of the PV module within a circuit under simplified conditions (Ishaque, et al., 2011).

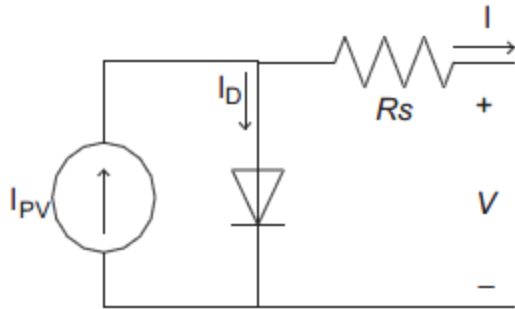


Figure 2-4: PV Cell Single Diode Model with Series Resistor Only

Figure 2-5 depicts the PV cell single diode model with both a shunt and series resistor, offering a more comprehensive representation of the model that accounts for additional factors affecting PV module behaviour (Ishaque, et al., 2011).

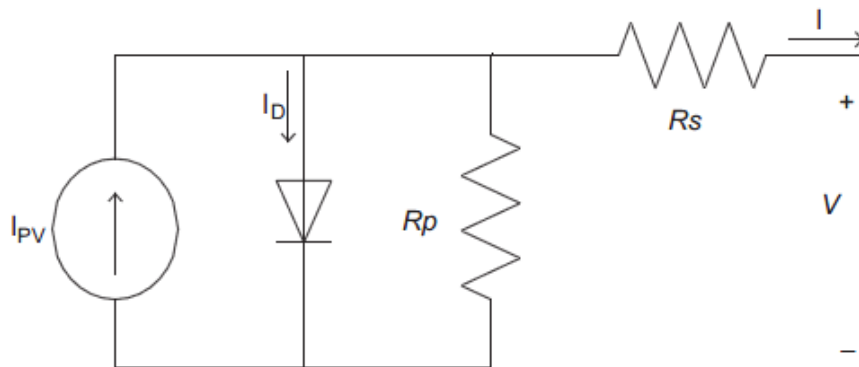


Figure 2-5: PV Cell Single Diode Model with Both Shunt and Series Resistor

By understanding the strengths and limitations of the single diode model in its various configurations, researchers and engineers can make informed decisions when designing and analysing PV systems.

- Double exponential model

The double exponential model is an advanced PV circuit model that incorporates an additional diode to represent the carrier recombination effect (Eynde, et al., 2010). This model provides a comprehensive representation of the behaviour of photovoltaic (PV) cells under varying operating conditions.

Figure 2-6 illustrates the double exponential model of a PV cell, incorporating two diodes along with both shunt and series resistors. This configuration accounts for various factors such as ambient temperatures, irradiance, photocurrent, saturation currents of both diodes, and resistive losses in series and parallel configurations, all of which contribute to the outcome of the I-V curve (Eynde, et al., 2010). The inclusion of these components enhances the accuracy of the model and facilitates the design of more precise PV systems (Eynde, et al., 2010).

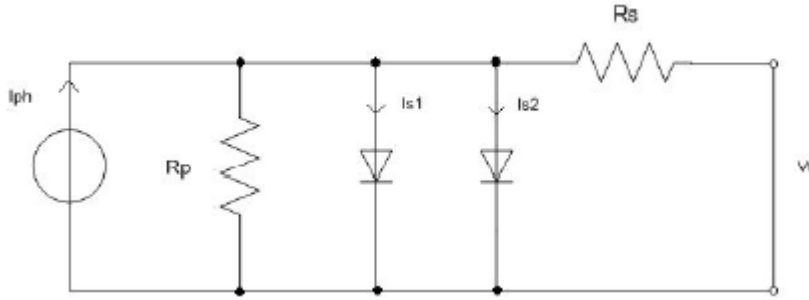


Figure 2-6: Double Exponential Model of a PV Cell

Additionally, the circuit can be utilized in the form of a two-diode model, as illustrated in Figure 2-7. The two-diode model is renowned for its accuracy in representing PV cell behaviour (Ishaque, et al., 2011). However, the calculations associated with this model are complex and often require numerous iterations to converge on accurate results (Ishaque, et al., 2011).

The circuit can also be used as shown below:

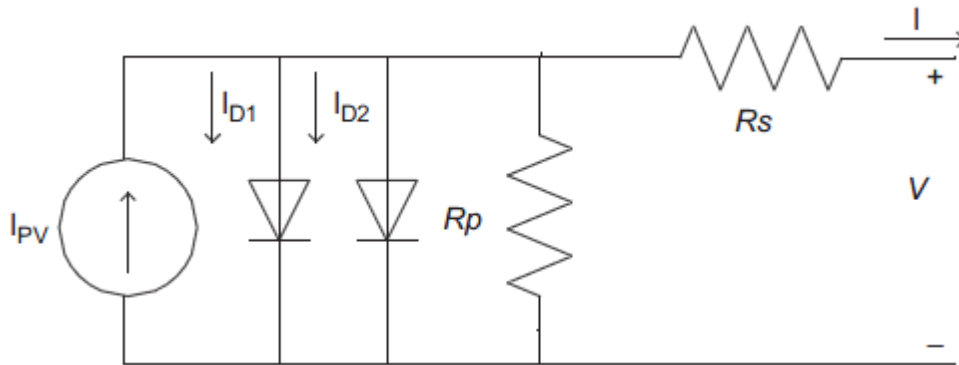


Figure 2-7: Two-Diode Model with Shunt and Series Resistor

Despite the computational complexity, the double exponential model and the two-diode model offer valuable insights into PV system performance, enabling researchers and engineers to optimize system design and operation.

2.4.5 Maximum power point tracking (MPPT) Techniques for PV

Maximum Power Point Tracking (MPPT) is crucial for optimizing the effectiveness of photovoltaic (PV) systems. It ensures that the maximum potential power is extracted from solar panels by dynamically adjusting the operating point of the system under varying environmental

conditions. This optimization is achieved through algorithms that respond to changes in temperature and irradiance, maintaining the highest possible output power for battery charging and other uses (Ayamolowo, et al., 2022). Due to fluctuating weather conditions, the maximum power point (MPP) of a solar panel is not constant. Thus, MPPT systems are essential for maintaining optimal performance. Modern MPPT controllers achieve efficiency rates of 93-97%, potentially increasing energy output by 15% in winter and 35% in summer.

2.4.5.1 MPPT operation

MPPT operates by constantly modifying the PV array's operating point to maintain maximum power output. This involves sensing the current and voltage of the PV array and dynamically adjusting the operating point to track the MPP on the voltage-current curve. Figure 2-8 offers a visual interpretation of the MPPT process/algorithm (Eynde, et al., 2010).

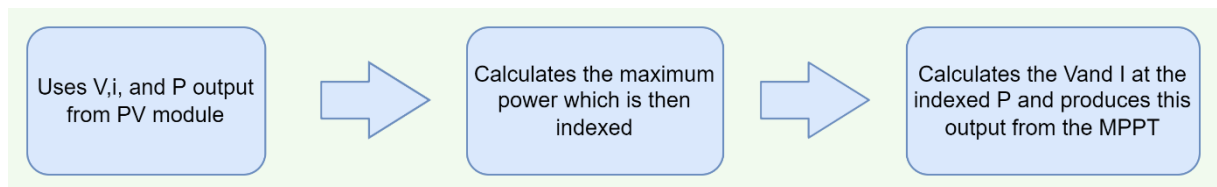


Figure 2-8: Block diagram illustration of the general MPPT process/algorithm

The PV module outputs values for power, current, and voltage, enabling the application of algorithms to enhance system efficiency. Effective MPP tracking is critical for improving the conversion efficiency of the PV system (Ma, et al., 2013). MPP algorithms can be classified into 'off-line' and 'on-line' types, with off-line algorithms not accounting for environmental changes, while on-line algorithms adapt to these changes.

Figure 2-9 below illustrates the current-voltage (I-V) characteristic curve of a photovoltaic (PV) array, which is fundamental to understanding the performance of PV systems (Eltawil & Zaho, 2013). This curve represents the relationship between the output current (I) and voltage (V) of the PV array under a specific set of conditions, such as irradiance and temperature.

The point on the I-V curve where the product of current and voltage is at its maximum corresponds to the Maximum Power Point (MPP). At this point, the PV array operates at its highest efficiency, delivering the maximum possible power output. The significance of identifying and operating at this point is crucial for maximizing the energy harvested from the PV system. The MPP varies with environmental factors like sunlight intensity and temperature, making it essential for the system to continuously track and adjust to these changes to maintain optimal performance. This is where Maximum Power Point Tracking (MPPT) algorithms come into play, as they help the system dynamically locate and operate at the MPP, thereby improving overall energy conversion efficiency (Eltawil & Zaho, 2013).

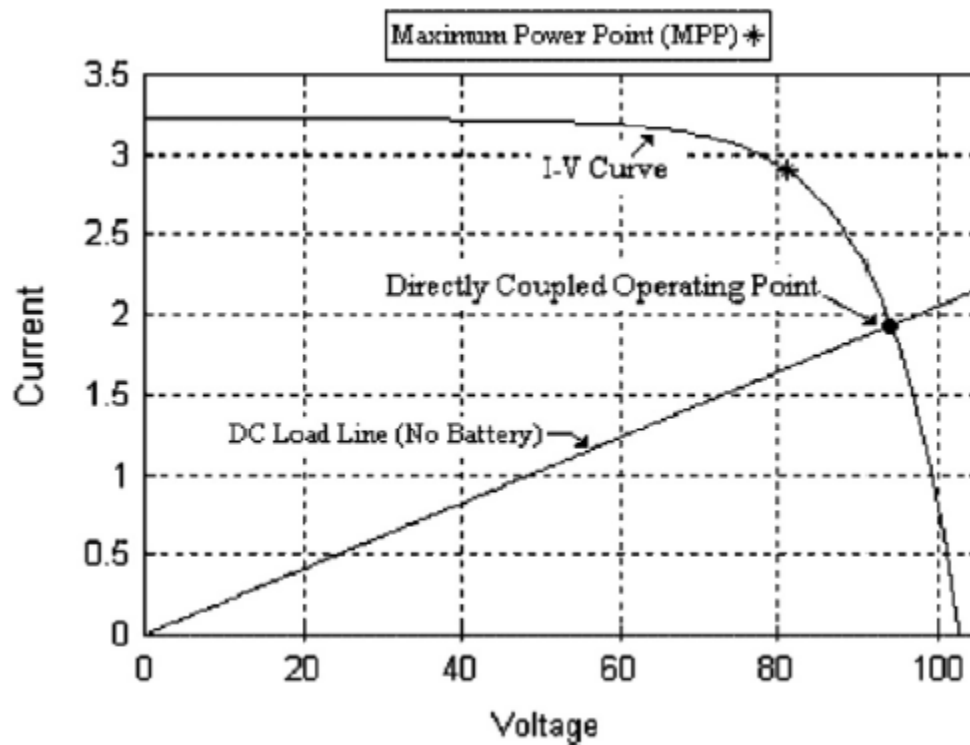


Figure 2-9: current-voltage characteristic for a PV array

2.4.5.2 MPPT techniques/methods

MPPT techniques are diverse and essential for maximizing PV system efficiency. By adjusting the PV system's operating point to track the MPP under varying environmental conditions, these techniques ensure optimal power generation and utilization of solar energy.

- Perturb-and-observe – P&O

The P&O technique adjusts to instant variations in solar radiation, making it suitable for solar energy harnessing. It is efficient, reliable, and simple to implement (Mtshali, et al., 2011). This technique involves measuring the voltage at the PV array's terminals at regular intervals and comparing it with the output power obtained from the previous "perturbation" results (Eltawil & Zaho, 2013).

The flow chart in figure 2-10 below presents the operation of P&O (Eltawil & Zaho, 2013):

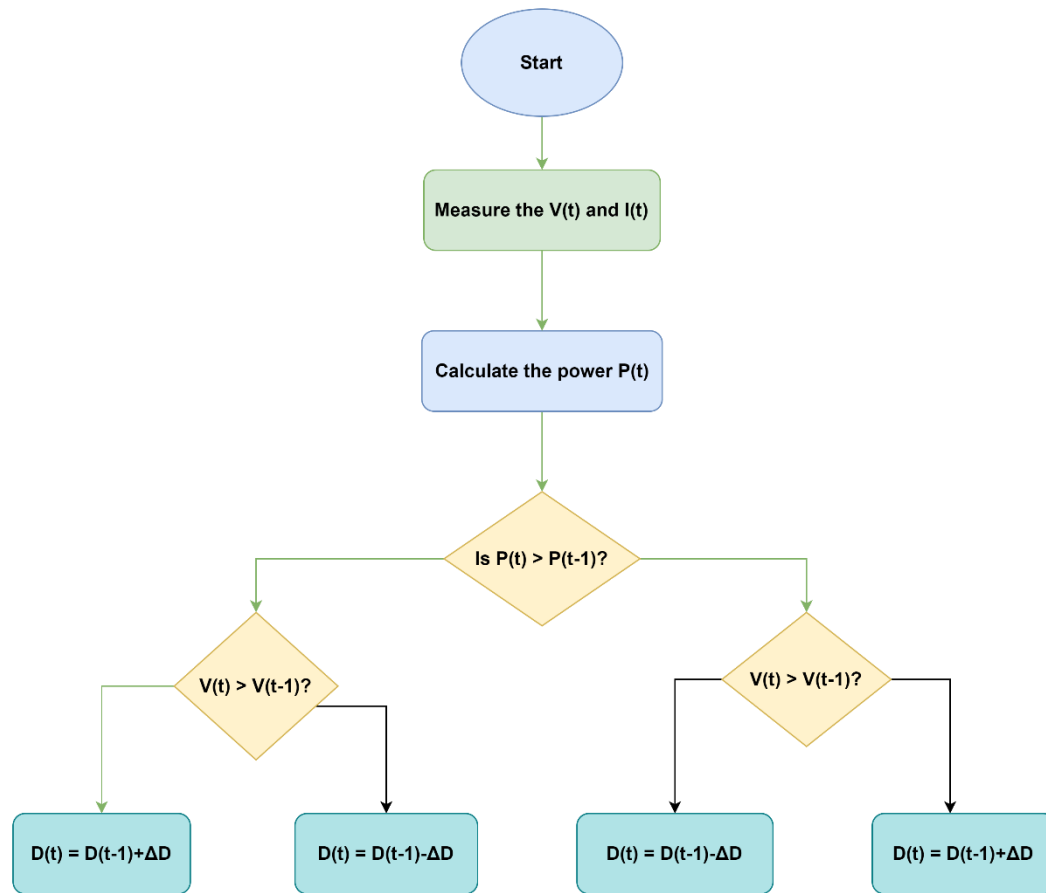


Figure 2-10: Flow chart illustrating the operation of the P&O method/algorithm.

Where P is power, V is voltage, D is the duty cycle, and ΔD is the perturbation step-size.

- Incremental conductance

The Incremental Conductance (IncCond) method is a sophisticated technique employed for Maximum Power Point Tracking (MPPT) in photovoltaic (PV) systems. This method is designed to overcome some of the limitations associated with simpler MPPT techniques like Perturb and Observe (P&O), particularly in quickly changing environmental circumstances such as fluctuating irradiance or temperature.

This technique is focused on satisfying the equation below, where at the MPP (Eltawil & Zaho, 2013):

$$\frac{dP}{dV} = \frac{d(VI)}{dV} = I + V \left(\frac{dI}{dV} \right) = 0 \quad (2.1)$$

Where dP/dV denotes the derivative of power (P) with respect to voltage (V), $d(VI)/dV$ represents the derivative of the product of voltage (V) and current (I) with respect to voltage, I represents the current generated by the PV system at a given operating point, V represents the voltage across the PV system at a given operating point, dI/dV represents the derivative of current (I) with respect to voltage (V).

It requires the slope at the MPP to be zero, with the slope to the right and left of the MPP being negative and positive, respectively. The incremental conductance method determines the direction to perturb the array to reach the MPP optimally (Eltawil & Zaho, 2013).

Figure 2-11 illustrates the flowchart representing the incremental conductance algorithm (Eltawil & Zaho, 2013). This algorithm utilizes both the current and previous values of the solar arrays voltage and current to derive the rates of change (dI and dV). If both dV and dI are equal to zero, it indicates stable atmospheric conditions, affirming that the MPPT remains operational at the MPP. Conversely, if dV equals zero while dI is greater than zero, it suggests an increase in sunlight intensity, consequently elevating the MPP voltage.

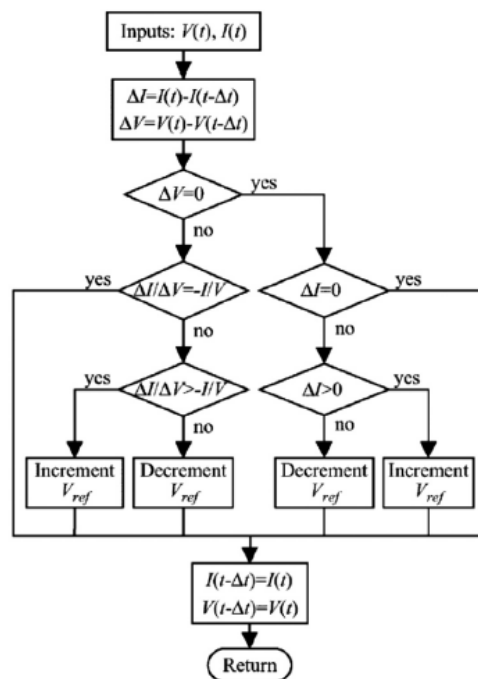


Figure 2-11: Flow chart of the algorithm for the incremental inductance method

2.4.6 PV Controller Designs

The PV controller serves as the brain of the photovoltaic subsystem, actively managing solar energy generation to maximize efficiency and yield. It employs sophisticated algorithms to track the maximum power point (MPPT) of the PV panels, adjusting their operating parameters in response to changing environmental conditions such as solar irradiance and temperature. The MPPT for PV systems is an effective and efficient controller. It ensures optimal power generation with PV solar arrays. Figure 2-12 below presents a feedback control system by (Carbone & Tomaselli, 2011):

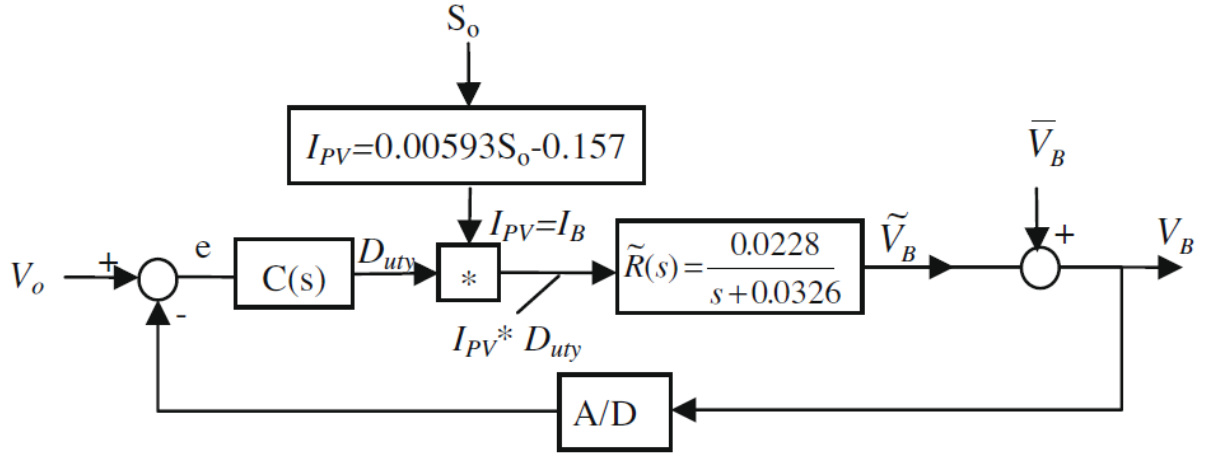


Figure 2-12: A feedback control system of a PV battery charging

2.4.7 Inverter for PV

In a photovoltaic (PV) system, the inverter converts the direct current (DC) power generated by solar panels into alternating current (AC) electricity, making it suitable for use in homes, businesses, and integration with the electrical grid. The inverter's main function is to maintain consistent AC output voltage levels, regardless of temperature changes and fluctuations in solar irradiance. This ensures the reliability and efficiency of the PV system, maximizing energy yield and smooth integration with existing electrical infrastructure (Chowdhury, et al., 2009). Figure 2-13 illustrates an equivalent circuit of a DC-AC inverter linked to a PV array, demonstrating the critical role of the inverter in the overall system setup (Chowdhury, et al., 2009).

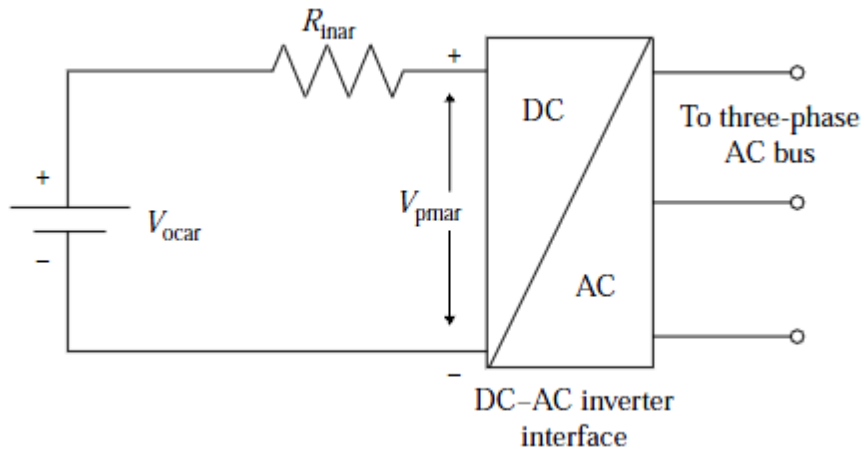


Figure 2-13: An equivalent circuit of a DC-AC inverter connected to a PV array

2.5 Wind Energy

Wind energy is one of the fastest-growing sources of renewable energy (Mtshali, et al., 2011). Although there are some greenhouse gas emissions associated with the production and maintenance of wind energy systems, these emissions are significantly lower than those generated by burning fossil fuels (R.Saidur, et al., 2011).

In a Hybrid Power System (HPS), wind energy is vital as it complements other renewable sources, such as photovoltaic (PV) systems. The availability of wind energy helps to offset the variability and intermittency of solar power, thereby increasing the overall reliability and efficiency of the HPS.

2.5.1 Wind Turbine

Wind turbines generate electricity by converting mechanical power into electrical energy. The system consists of blades that rotate when wind flows over them. These blades are coupled to a gearbox, which is further linked to the generator shaft. As the blades spin, the gearbox increases the rotational speed transferred to the generator. The generators used in wind turbines can be either induction generators or synchronous generators (Chowdhury, et al., 2009).

A wind turbine is an advanced electromechanical system that efficiently captures wind's kinetic energy and converts it into electrical power. It consists of multiple sophisticated components; each meticulously designed to maximize performance and ensure reliability. Figure 2-14

provides an overview of the structure and key components of a typical wind turbine (Encalada, et al., 2022).

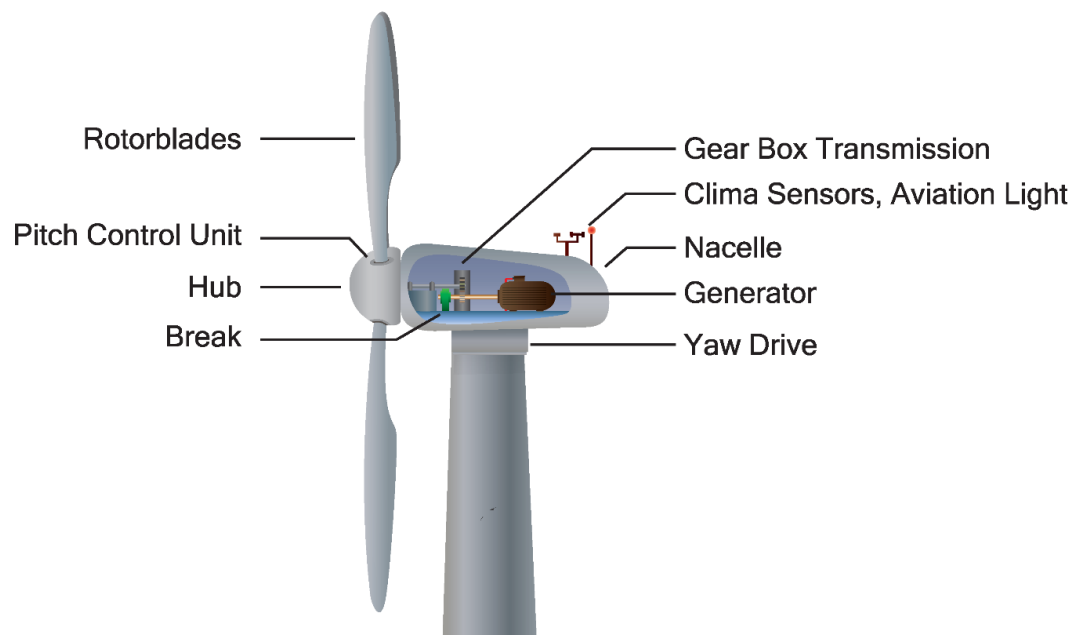


Figure 2-14: Overview of a wind turbine

2.5.2 Components and Operation of Wind Turbines:

Wind turbines are complicated machines designed to convert kinetic energy from the wind into electrical energy efficiently. Understanding the various components of a wind turbine and their roles is essential to grasp how these systems operate and contribute to renewable energy generation. Below is an overview of the key components involved in wind turbine operation and their specific functions:

- 1. Blades:** The blades of a wind turbine capture the kinetic energy from the wind, causing them to rotate as the wind flows over their surface. This rotation is the initial step in the energy conversion process. The design and material of the blades are crucial for maximizing energy capture and minimizing losses due to aerodynamic drag.
- 2. Gearbox:** The gearbox is a vital component that links the rotor (blades) to the generator. It increases the low rotational speed of the blades to a higher speed that is optimal for the generator, as most electrical generators perform more efficiently at higher rotational speeds.
- 3. Generator:** The generator is the component that converts the mechanical energy generated by the rotating blades into electrical energy. Wind turbines commonly utilize either induction generators or synchronous generators for this conversion process:

- **Induction Generators:** Induction generators are simple, robust, and cost-effective. They function based on the principles of electromagnetic induction, where a rotating magnetic field induces an electric current in stationary windings.
- **Synchronous Generators:** Synchronous generators offer high efficiency and precise control over output voltage and frequency, making them ideal for grid-connected applications.
- **Permanent Magnet Synchronous Generators (PMSG):** PMSGs are particularly advantageous in stand-alone wind systems because of their cost-effectiveness, reliability, and high efficiency (Urtasun, et al., 2013) (Dang, et al., 2011). These generators have low mechanical losses and do not require an excitation system, which simplifies the overall design and reduces maintenance needs. PMSGs offer the added benefit of a gearless construction, which not only enhances their efficiency in extracting wind energy but also makes them more compact and appealing for remote area micro plants (Sanchez, et al., 2012) (Hong, et al., 2013). Figure 2-15 presents a block diagram of a PMSG wind energy design (Abdullah, et al., 2012):

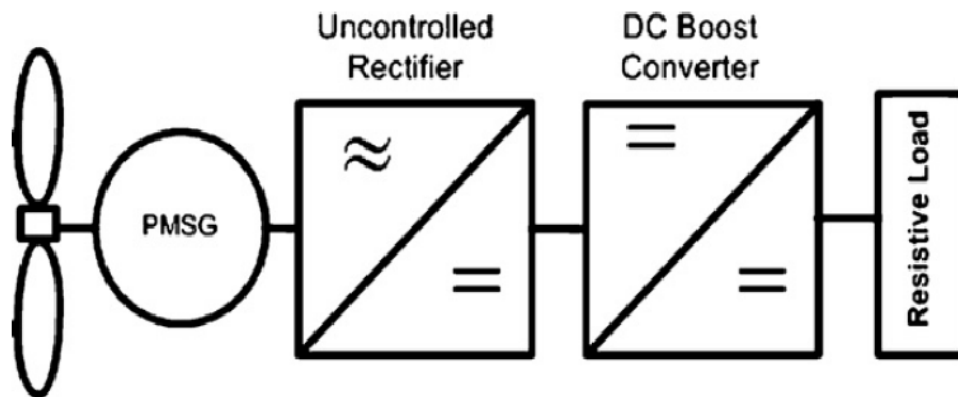


Figure 2-15: Block diagram of a PMSG wind energy design

- **Doubly-Fed Induction Generators (DFIG):** DFIGs are highly popular in modern wind turbine applications due to their ability to operate efficiently under varying wind conditions. This flexibility allows DFIGs to generate more power, thereby improving cost-effectiveness (Babouri, et al., 2013). A key advantage of DFIGs is their ability to produce electricity with constant voltage and frequency, which is essential for grid stability. Additionally, the implementation of DFIGs in wind turbine systems enhances overall efficiency by reducing losses in the power converters. The schematic below illustrates a wind turbine incorporating a DFIG with an AC-DC-AC converter (Abo-Khalil, 2012):

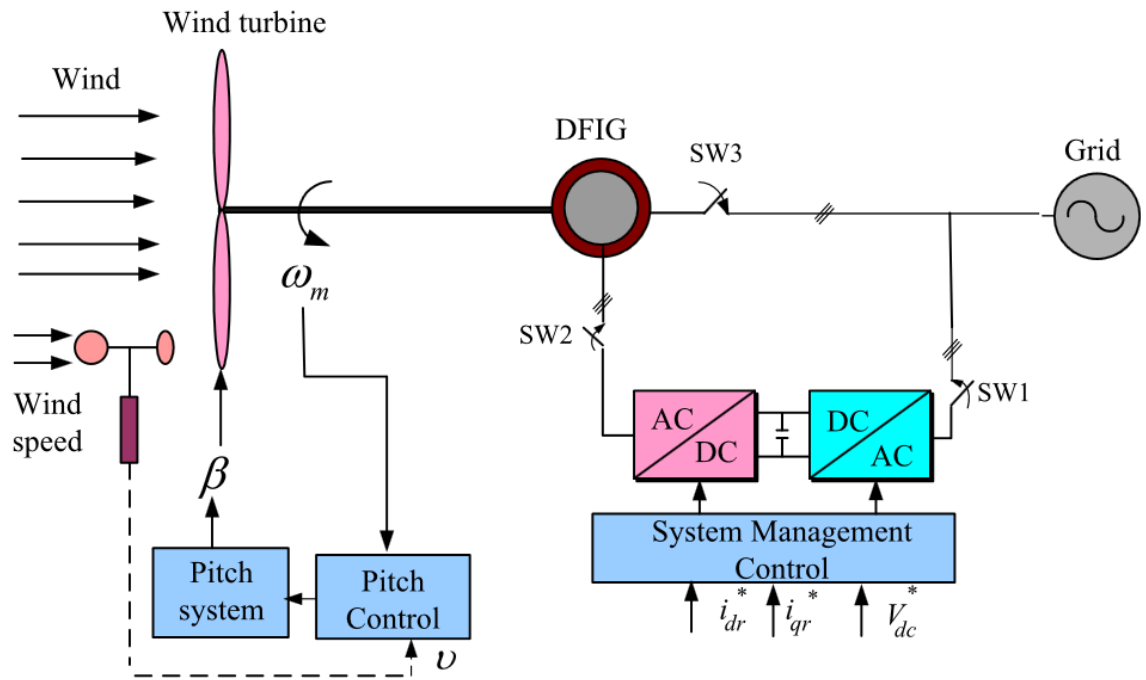


Figure 2-16: Schematic of a DFIG incorporated in a wind energy conversion system

4. **Nacelle:** The nacelle contains the essential components of a wind turbine, such as the gearbox, generator, and control systems. Positioned on top of the tower, it rotates to align the turbine with the wind direction, optimizing energy capture.
5. **Tower:** The tower supports the nacelle and rotor, elevating them to a height where wind speeds are generally higher and more consistent. Taller towers can access stronger and more stable wind flows, increasing the turbine's energy output.
6. **Control Systems:** Modern wind turbines feature advanced control systems that continuously monitor and optimize their performance in real-time. These systems adjust the blade pitch, yaw orientation, and rotational speed to maximize energy capture and ensure safe operation under different wind conditions. Figure 2-17 below illustrates the operation of a typical wind turbine system (Narayana, et al., 2012).

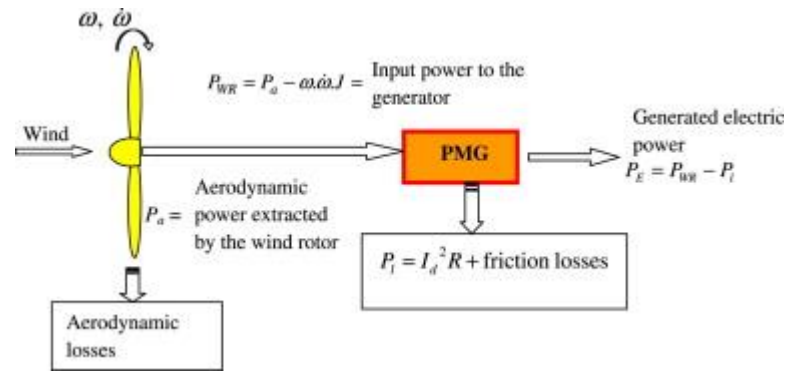


Figure 2-17: Wind Turbine power flow diagram

Variable Speed and Variable Pitch:

- **Variable Speed Turbines:** Rotor speed can be adjusted to maintain ideal tip speed ratio, maximizing power generation efficiency (Manwell, et al., 2009).
- **Variable Pitch Turbines:** Alter blade pitch to control the angle of attack and torque output, enhancing performance under varying wind conditions (Manwell, et al., 2009).

2.5.3 Types of Wind Turbines

Wind turbines are generally classified into two types based on the orientation of their rotational axis: Horizontal-Axis Wind Turbines (HAWT) and Vertical-Axis Wind Turbines (VAWT). Each type has unique characteristics, advantages, and specific applications.

2.5.3.1 Horizontal-axis wind turbine – HAWT

HAWTs have a horizontal axis of rotation, typically parallel to the wind flow direction. They are the most common type of wind turbines and can be positioned either downwind or upwind (S.Mathew & G.S.Philip, 2012) (M.A.Hyams, 2012). HAWTs operate within a wind speed range of 6m/s to 25m/s and are known for generating significant amounts of energy in favourable wind conditions. However, they are not designed to withstand high turbulence (Islam, et al., 2013). Figure 2-18 illustrates an offshore wind farm featuring three-bladed horizontal-axis wind turbines (S.Mathew & G.S.Philip, 2012).



Figure 2-18: An offshore wind farm with three bladed horizontal axis wind turbines

2.5.3.2 Vertical axis wind turbine – VAWT

VAWT has an axis of rotation that is vertical, allowing it to operate in whichever wind direction with no the need for a wind tail (Narayana, et al., 2012). They are suitable for residential areas and small-scale projects, performing well in severe wind conditions. VAWTs operate within wind speeds of 2m/s to 65m/s, offering advantages over HAWTs in certain applications (Islam, et al., 2013). Figure 2-19 shows a vertical axis wind turbine (M.A.Hyams, 2012).



Figure 2-19: Vertical-axis wind turbine

2.5.4 Wind turbine operating systems

Wind turbine operating systems are crucial components that determine how the turbine responds to varying wind conditions and generates electricity. These systems have a vital role in controlling the turbine's operation, optimizing its performance, and ensuring safe and efficient energy generation. There are two main types of wind turbine operating systems, each

defined by its unique control mechanism: pitch control systems and stall control systems. These systems are designed to optimize the turbine's performance and efficiency under varying wind conditions (Chowdhury, et al., 2009):

- **Constant speed turbines**

Constant speed turbines include stall-regulated and pitch-regulated turbines. These turbines consist of fewer parts which results in increased reliability. However, their efficiency regarding aerodynamics is low (Chowdhury, et al., 2009).

- **Variable speed turbines**

Variable speed turbines are known for their efficiency in aerodynamics, allowing them to harness wind energy more effectively. However, this efficiency in aerodynamics is accompanied by lower electrical efficiency (Chowdhury, et al., 2009). Figure 2-20 illustrates the layout and operation of a variable speed pitch-regulated wind turbine (Chowdhury, et al., 2009):

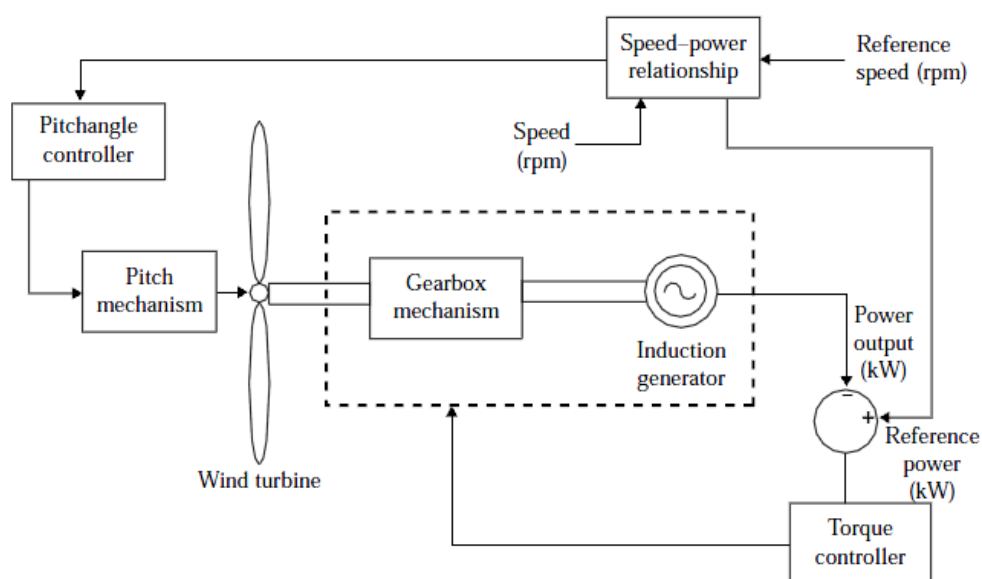


Figure 2-20: Variable Speed Pitch-Regulated Wind Turbine Schematic

2.5.5 Limitations of the wind energy source

- **Weather conditions in harnessing energy for wind systems**

Wind energy is highly dependent on weather conditions and is inherently variable. Wind speeds can fluctuate significantly, leading to inconsistent power generation. Unlike solar power, which can be somewhat predictable based on the time of day, wind can vary drastically over short periods, making it challenging to rely on as a sole power source.

- **Wind turbines dependent on wind speeds**

Wind turbines are dependent on the wind speeds. Wind energy conversion systems have a drawback of being weather dependant which is unpredictable in nature. This is one negative that makes wind that results in push back against wind energy systems.

A traditional wind power generation design for systems incorporates:

- variable pitch and variable speed turbines
- slip ring synchronous generators or squirrel cage induction generators

2.6 Battery Storage

Battery storage is vital in hybrid power systems (HPS) as it stores surplus energy produced during periods of high renewable energy output and provides power during times of low generation or increased demand. This section delves into the significance of battery storage in HPS, detailing its components, operating principles, and its essential role in maintaining a reliable and stable energy supply.

2.6.1 Function of a battery storage unit in a Hybrid Power System

The battery energy storage system (BESS) is employed in a hybrid power system to supply the load in the case where the renewable energy generation is not sufficient. This enhances the reliability of the system as this always ensures that the load demand can be satisfied (Coppez, et al., 2010). A BESS also stores the excess energy generated from the renewable energy sources at a period when electricity demand is low and then compensates for the renewable energy generation deficit when demand is high. In a PV system, the BESS can be optimised with MPPT (Carbone & Tomaselli, 2011).

2.6.2 Battery energy storage system integration in an energy generation system

The battery type used must be compatible with the rest of the system design to ensure system operates as efficiently as possible. It is vital to monitor the depth of discharge using a controller integrated in the system. Monitoring the depth of discharge and cell life of each cell at regular intervals ensures that each cell can reach its end of life simultaneously (Babouri, et al., 2013). These practices will result in increasing the BESS's efficiency.

2.6.3 Battery Controller Designs

Battery controllers are essential for optimizing the performance and lifespan of energy storage systems. They monitor key parameters such as cell voltage, temperature, charging and discharging currents, and state of charge (SOC) to ensure the battery operates efficiently and is protected from potential damage (Qian, et al., 2011).

- State of Charge (SOC) Management

Central to the controller's function is the battery's state of charge (SOC) monitoring and management. SOC represents the quantity of electrochemical energy collected in the battery at any given time (Qian, et al., 2011). The controller continually monitors the SOC and regulates charging and discharging operations to prevent the battery from exceeding predefined SOC thresholds. This careful management helps maximize battery efficiency and lifespan (Qian, et al., 2011).

- Battery Charging Control System

As depicted in Figure 2-27, a battery charging control system, as proposed in (Huang, et al., 2010), consists of several components working in tandem to regulate the charging process effectively. The block diagram illustrates the flow of control signals and feedback mechanisms involved in managing the battery charging process (Huang, et al., 2010). This system ensures precise control over charging operations, optimizing battery performance and longevity.

From (Huang, et al., 2010), figure 2-21 presents a battery charging control system utilizing pulse-width modulation (PWM) to manage the charging current and maintain battery voltage beyond the overcharge threshold V_o . The system employs a Metal-Oxide-Semiconductor-Field-Effect Transistor (MOSFET) to switch the charging current on and off via a PWM signal generated from the solar photovoltaic (PV) source. By adjusting the duty cycle of the PWM signal, the average charging current is regulated, effectively controlling the battery voltage at the desired overcharge point. The controller $C(s)$ is designed to ensure robust performance by using known system dynamics models of the PV and battery components, preventing overcharging. This design optimizes the performance and longevity of the battery within the solar PV system, ensuring efficient and safe operation.

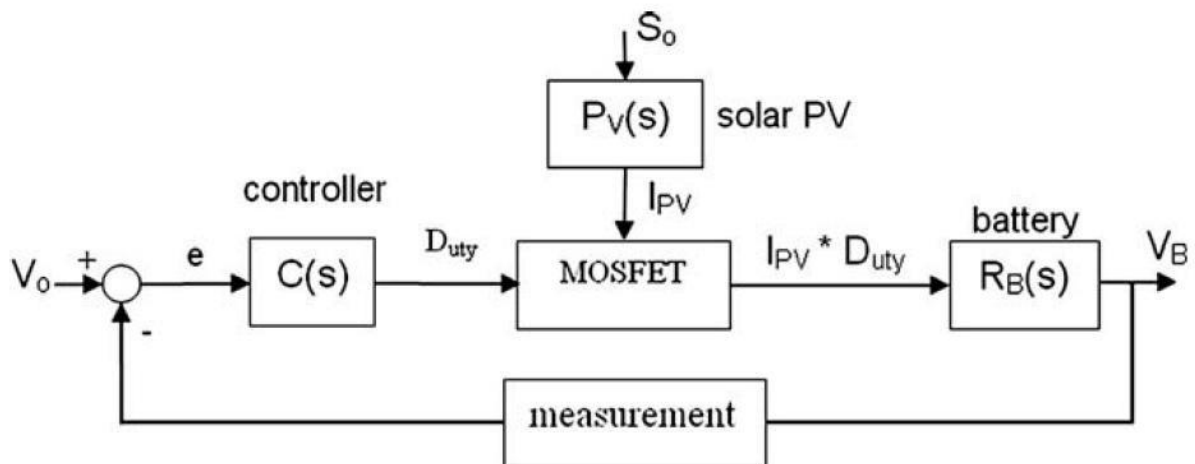


Figure 2-21: Block diagram of a battery charging control system

2.6.4 Advantages and disadvantages of a battery energy storage system

Battery energy storage systems possess numerous advantages, significantly enhancing the performance and reliability of hybrid power systems (HPS). These advantages include:

1. **Enhanced Load Supply:** PV power units experience fluctuations in solar irradiance, particularly during overcast days or evenings. A Battery Energy Storage System (BESS) is designed to store surplus energy generated during peak production periods and release it during times of low generation, ensuring a consistent supply of power and reducing the impact of the variability associated with renewable energy sources (Eynde, et al., 2010).
2. **Supplementary Power Generation:** During periods of inadequate weather conditions when wind or PV systems cannot generate sufficient energy to meet load demand, BESS serves as a supplementary power source, providing backup power to maintain system operation.
3. **Optimized Energy Utilization:** BESS prevents wastage of excess power generated by the HPS during periods of low demand. By storing surplus energy for later use, BESS optimizes energy utilization and improves overall system efficiency (Coppez, et al., 2010).
4. **Improved Power Factor and Load Levelling:** Integration of BESS improves the power factor of the power system, enhancing voltage stability and reducing losses. Additionally, BESS facilitates load levelling by smoothing out fluctuations in energy supply and demand, contributing to a more stable and balanced power system (Coppez, et al., 2010).
5. **Enhanced System Quality and Efficiency:** The incorporation of BESS results in a more resilient and efficient HPS. By providing backup power, load support, and voltage regulation capabilities, BESS enhances system quality and ensures reliable operation under varying conditions (Coppez, et al., 2010).

However, despite these significant advantages, battery storage systems also exhibit certain limitations, including:

Storage Capacity Sensitivity: The rate of discharge of batteries is highly sensitive to their storage capacity. Inadequate storage capacity may lead to insufficient backup power during high-demand periods, limiting the effectiveness of the BESS in providing continuous load support (Eynde, et al., 2010). By leveraging the benefits of battery energy storage systems while addressing their limitations, HPS can achieve improved performance, reliability, and efficiency, contributing to the widespread adoption of renewable energy technologies in the global energy landscape.

2.6.5 Cell batteries

Cell batteries are the most popular types which is often used in HPS's. The following are a few important features to be considered during battery selection (Eynde, et al., 2010), and these

are battery life, depth of discharge, life cycle, cycle of charge and discharge, temperature, rate of discharge, power density and energy density.

The table 2-1 below presents the different types of cell batteries which can be used in a battery energy storage system (Coppez, et al., 2011):

Table 2-1: Comparison of Various Battery Types

Cell type	Efficiency %	Depth of discharge %	Life span (cycles)	Self-discharge	Technology maturity	Cost
Lead acid	72 - 78	75	1000	Average	Mature	Low
Lithium Ion	100	80	3000	Negligible	Immature	Very high
Sodium Sulphur	89	100	2500	Negligible	Mature	High
Nickel Cadmium	72 - 78	100	3000	High	Mature	High
Zinc Bromine	75	100	2000	Negligible	Immature	High

The above-mentioned batteries are typically used in various applications based on their characteristics:

- **Lead Acid** – Commonly used in UPS systems, hospital equipment, and emergency lighting because of their low cost and mature technology (Battery University, 2017).
- **Lithium Ion** – Predominantly used in laptops and mobile phones, benefiting from high efficiency, low self-discharge, and a longer lifespan, despite their very high cost and relatively immature technology (Battery University, 2017).
- **Sodium Sulphur** – Often employed as a standby power source for customer loads, thanks to their high efficiency, negligible self-discharge, and mature technology, though they are costly (Hatta, 2012).
- **Nickel Cadmium** – Utilized in two-way radios, biomedical equipment, and power tools because of their high depth of discharge, mature technology, and long lifespan, despite their high self-discharge and cost (Battery University, 2017).

Based on the tabulated information, while Zinc Bromine batteries offer a high depth of discharge and negligible self-discharge, their immature technology and associated high costs, along with potential toxicity, make them an unsuitable option for widespread use (Coppez, et al., 2010). Lithium-ion batteries would be the most optimal choice as it has a 100% efficiency rating. However, it is very expensive when implementing it in large scale applications which it an undesirable option for a renewable energy system (Coppez, et al., 2010).

Lead Acid batteries are cost-effective with low self-discharge, making them an attractive option. Nickel Cadmium batteries follow, but they do not perform well for long-term energy storage due to their high self-discharge feature, as illustrated in the table above (Coppez, et al., 2010). Based on the comparisons of the batteries' features, lead Acid batteries appear to

be the clear choice for most applications. However, the short lifespan of Lead Acid batteries results in more frequent cell replacements compared to other battery types. This might be seen as a limitation for Hybrid Power Systems (HPS) situated in remote areas, but they are easy to maintain, which is a positive aspect (Nair & Garimella, 2010).

Lead Acid batteries can be expensive in the long term in certain use cases. Therefore, Sodium Sulphur batteries might be a better option, but it must be kept at a temperature of 300 degrees Celsius (Coppez, et al., 2011)

Nickel Cadmium (NiCd) batteries have a longer life cycle and higher energy density compared to lead-acid batteries, making them more suitable for applications requiring extended usage and compact energy storage solutions (Nair & Garimella, 2010). The main negative feature is its high self-discharge. Considering their durability and reliability, they are classified as apposite for applications such as PV systems (Nair & Garimella, 2010) where they will cope with unfavourable weather conditions.

Figure 2-22 below presents the voltage profiles for a few batteries' energy storage system (Nair & Garimella, 2010).

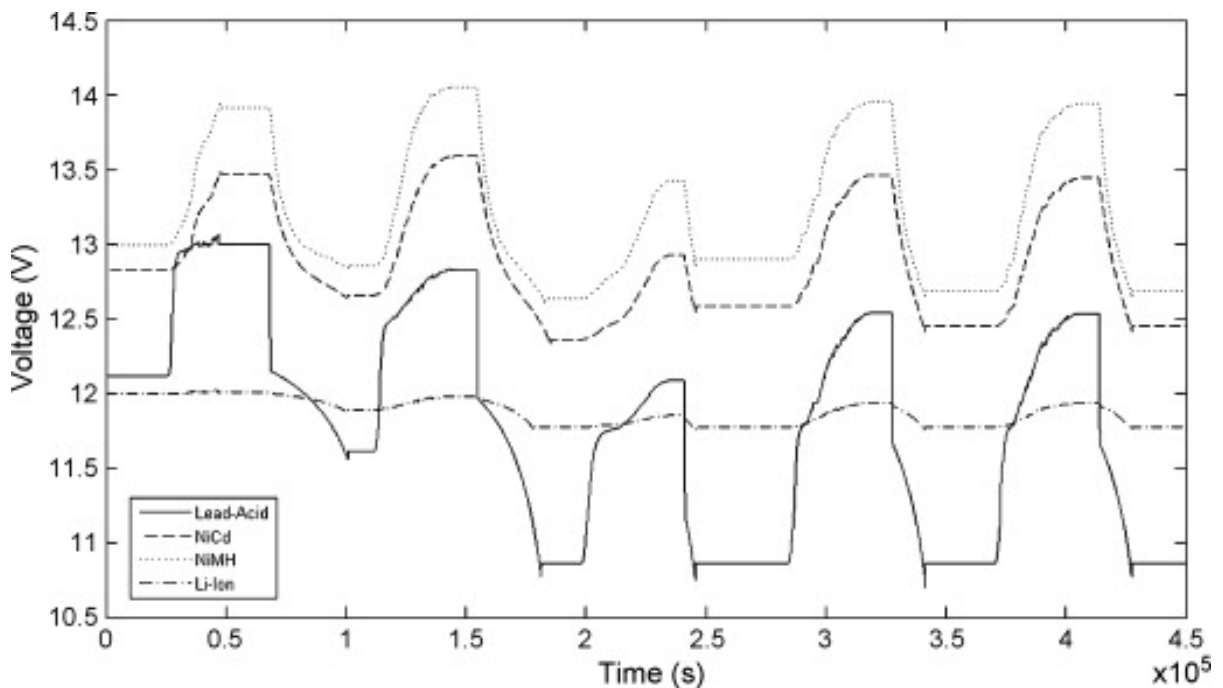


Figure 2-22: Comparison of The Voltage Profiles of Various BESS's

2.6.6 Charging and discharging processes of a battery

The charging and discharging processes of a battery are crucial for understanding its behaviour and functionality within an energy storage system. In the charging process, electrical

energy is transformed into chemical energy and stored in the cells of the battery. This chemical energy is then converted back into electrical energy during the discharging process when the battery powers external devices or systems. The efficiency and performance of these processes are influenced by various factors, including the battery chemistry, charging/discharging rates, temperature, and environmental conditions. Understanding these processes is crucial for optimizing battery usage, extending its lifespan, and maximizing the overall efficiency of the energy storage system.

An active MPPT function can be used which can avoid the battery from over discharging/charging (Carbone & Tomaselli, 2011) This will increase the lifespan of the battery. The following equation conveniently describes the performance of a battery (Achaibou, et al., 2012):

$$V = V_{OC} \pm IR \quad (2.3)$$

Where V_{OC} – open circuit voltage, R – internal resistance, and I – current, positive through the charging phase and negative during the discharge phase.

2.6.7 Discharging of a battery

Discharging of a battery is a critical aspect of its operation within an energy storage system. The discharging process involves converting the stored chemical energy back into electrical energy to supply power to external devices or systems. The rate and efficiency of discharging depend on factors such as the battery chemistry, discharge rate, temperature, and load characteristics. Effective management of the discharging process is crucial for maintaining reliable and consistent power delivery, extending the battery's lifespan, and enhancing the overall performance of the energy storage system. Understanding the discharging behaviour of batteries is crucial for designing efficient energy storage solutions and implementing effective control strategies.

Considering Q , ($Q = It$), the charge provided at a given moment and C , the capacity of the battery, the ratio Q/C represents the depth of discharge which can then be used to calculate the state of charge, SOC (Achaibou, et al., 2012):

$$SOC = 1 - * Q/C \quad (2.4)$$

The discharging of the battery can be given as (Achaibou, et al., 2012):

$$V = [2.085 - 0.12(1 - SOC)] - \frac{1}{C^{10}} \left(\frac{4}{1+I^{1.3}} + \frac{0.27}{SOC^{1.5}} + 0.02 \right) * (1 - 0.007 * \Delta T) \quad (2.5)$$

where temperature variation $\Delta T = T - 25$ (Achaibou, et al., 2012)

and

$$\frac{C}{C_{10}} = \frac{1.67}{1 + 1.67 * \left(\frac{I}{I_{10}}\right)^{0.9}} * (1 + 0.005\Delta T) \quad (2.6)$$

2.6.8 Charging of a battery

The charging of the battery can be given as (Achaibou, et al., 2012)

$$V = [2 - 0.16SOC] + \frac{1}{C_{10}} \left(\frac{6}{1 + I^{0.86}} + \frac{0.48}{(1 - SOC^{1.2})} + 0.036 \right) * (1 - 0.025 * \Delta T) \quad (2.7)$$

with the State of Charge (SOC) as (Achaibou, et al., 2012):

$$SOC = SOC_0 + \frac{\eta c * Q}{C} \quad (2.8)$$

where the efficiency equation can be expressed as (Achaibou, et al., 2012):

$$\eta c = 1 - \exp \left[-\frac{20.73}{\frac{I}{I_{10}} + 0.55} * (SOC - 1) \right] \quad (2.9)$$

2.7 Energy Management Systems in Hybrid Power Systems

In the contemporary landscape of renewable energy integration, hybrid power systems (HPS) emerge as pivotal solutions for enhancing energy resilience, sustainability, and autonomy. Hybrid configurations, for instance combining photovoltaic (PV) solar panels, wind turbines, and battery storage, offer synergistic advantages by leveraging diverse energy sources and storage technologies. However, the optimal utilization of these components necessitates sophisticated control strategies that can adapt to dynamic environmental conditions, fluctuating energy generation, and varying load demands. In this context, Energy Management Systems (EMS) play a fundamental role in orchestrating the efficient management of hybrid power systems by intelligently managing energy generation, storage, and distribution (Olabode, et al., 2021).

The primary objective of an EMS in a hybrid PV-wind-battery system is to maximize energy utilization while ensuring system stability, reliability, and cost-effectiveness. By continuously monitoring system parameters, such as renewable energy generation, battery state of charge, and load requirements, an EMS can dynamically adjust control actions to optimize energy flow and balance supply with demand. This entails making real-time decisions on energy dispatch, storage, and conversion based on predictive models, historical data, and user-defined objectives.

The complexity of EMS design lies in the need to reconcile competing priorities, such as maximizing energy efficiency, minimizing operating costs, and mitigating environmental impacts, while adhering to technical constraints and regulatory requirements. Moreover, the

dynamic and stochastic nature of renewable energy sources poses additional challenges for EMS implementation, necessitating adaptive and robust control strategies capable of handling uncertainty and variability.

Energy Management Systems are essential for optimizing hybrid power systems (HPS) that combine multiple renewable energy sources like photovoltaic (PV) solar panels, wind turbines, and battery storage. This section offers an in-depth review of different EMS approaches, including rule-based systems, Model Predictive Control (MPC), and fuzzy logic control. It examines their methodologies, challenges, outcomes, and relevance to the development of an EMS for a PV-wind-battery HPS.

2.7.1 Rule-Based Energy Management Systems

Rule-based EMS rely on predefined sets of rules or heuristics to make decisions regarding energy generation, storage, and distribution within the HPS. These systems are characterized by their simplicity, ease of implementation, and transparency, making them suitable for smaller-scale HPS deployments where real-time computational resources are limited.

In (Kayaalp, et al., 2023), the authors highlight the simplicity and effectiveness of rule-based EMS in ensuring reliable power supply for critical loads. The study underscores the ease of implementation and low computational requirements of this approach, though it notes the limitations in adaptability to rapidly changing environmental conditions.

Similarly, the work in (Kayaalp, et al., 2023) demonstrates the robustness of rule-based EMS in optimizing energy distribution in a solar power system. The fixed nature of the rules, however, can hinder the system's ability to adapt to real-time variations in energy supply and demand.

In the work in (Wang, et al., 2019), the authors explore combining rule-based strategies with Model Predictive Control (MPC) for enhanced energy management. This hybrid approach leverages the simplicity of rule-based systems for initial decision-making and the optimization capabilities of MPC for fine-tuning control actions.

In summary, rule-based EMS offer simplicity, transparency, and robustness in coordinating energy generation, storage, and distribution within hybrid PV-wind-battery systems. However, their limited adaptability to changing conditions can lead to suboptimal performance in dynamic environments.

2.7.2 Model Predictive Control (MPC)

Model Predictive Control (MPC) is an advanced control strategy that utilizes dynamic models of Hybrid Power System (HPS) components to predict future system behaviour and optimize control actions over a specific time horizon. MPC algorithms solve an optimization problem to minimize a predefined cost function while adhering to system constraints.

In (Wang, et al., 2019), the authors highlight the advantages of integrating MPC with rule-based strategies. The hybrid approach improves system performance under dynamic conditions but requires accurate models and significant computational resources for real-time implementation.

MPC offers several benefits, including dynamic optimization, constraint handling, and adaptability to varying operating conditions. By considering future system states and objectives, MPC can proactively adjust control actions to optimize system performance, improve energy efficiency, reduce operating costs, and enhance system reliability.

However, MPC requires accurate dynamic models and significant computational resources, posing challenges for real-time implementation, especially in large-scale HPS deployments.

In summary, MPC offers dynamic optimization and proactive control capabilities for complex hybrid PV-wind-battery systems, enabling optimal operation under dynamic and uncertain conditions. Its ability to handle nonlinearities and uncertainties makes it well-suited for optimizing hybrid energy systems, despite the challenges in model accuracy and computational requirements.

2.7.3 Fuzzy Logic Techniques

Fuzzy logic systems offer an adaptive and heuristic-based approach to EMS design in hybrid power systems. These systems use fuzzy sets and rules to handle uncertainties and nonlinearities, making them suitable for complex and variable conditions typical of HPS.

In (Wasim, et al., 2024), the authors demonstrate that fuzzy logic can effectively handle the uncertainties and variabilities of renewable energy sources. The study shows that fuzzy logic provides a robust control strategy for hybrid systems, although implementation requires careful tuning and extensive training data.

Fuzzy logic systems are constructed to handle uncertainty and imprecision, which makes them ideal for managing the variability inherent in renewable energy sources. By using fuzzy sets

and rules, these systems can model complex relationships and make decisions based on ambiguous or incomplete information.

Fuzzy logic systems mimic human decision-making processes, incorporating expert knowledge and heuristics into the control strategy. This enables intuitive and flexible control, which is particularly beneficial for systems with dynamic and unpredictable behaviours.

In summary, fuzzy logic techniques offer adaptive and heuristic-based approaches to EMS design in hybrid PV-wind-battery systems, enabling robust and flexible control strategies under dynamic and uncertain conditions. Their adaptability, robustness, and ease of implementation make them well-suited for optimizing the performance of complex energy systems.

2.7.4 Optimization Algorithms

Optimization algorithms, such as particle swarm optimization, genetic algorithms, and linear programming, provide systematic approaches to EMS design by searching for the optimal set of control parameters to maximize predefined objectives.

The study in (Modu, et al., 2024) examines the use of optimization algorithms in EMS. The authors demonstrate that genetic algorithms and particle swarm optimization can effectively optimize energy management strategies, improving system efficiency and reliability. However, they note the significant computational resources and time required for convergence, which can be a limitation for real-time applications.

Optimization algorithms offer robustness to uncertainties, scalability to large-scale HPS deployments, and global convergence properties. However, they may require significant computational resources and time for convergence, particularly for high-dimensional or nonlinear optimization problems.

In summary, optimization algorithms provide systematic approaches to EMS design in hybrid PV-wind-battery systems, enabling the optimization of control actions to maximize energy efficiency, minimize costs, or satisfy system requirements. While they require significant computational resources and time for convergence, their robustness and scalability make them well-suited for optimizing complex energy systems.

2.8 Comparison and Evaluation of EMS Approaches for Hybrid Power Systems

This section compares and evaluates different Energy Management System (EMS) approaches, focusing on their suitability for (HPS), particularly hybrid PV-wind-battery storage systems. EMS approaches are critical for optimizing energy utilization, ensuring system reliability, and managing variability in renewable energy sources.

Given the context of a hybrid PV-wind-battery system, rule-based EMS stands out for its simplicity and low computational requirements, making it a practical choice for smaller-scale systems. However, more advanced approaches, such as Model Predictive Control (MPC), Artificial Intelligence (AI) techniques, and optimization algorithms, are also considered for their potential to improve system performance in more complex or dynamic environments.

The table below provides a consolidated comparison of these EMS approaches, highlighting their suitability, advantages, and limitations.

Table 2-2: Comparison of EMS Approaches

EMS Approach	Suitability	Advantages	Limitations
Rule-Based Systems	<ul style="list-style-type: none">- Suitable for smaller-scale HPS with limited computational resources and a need for simplicity.	<ul style="list-style-type: none">- Simple, transparent, and easy to implement.- Low computational complexity with minimal resources required for real-time decisions.	<ul style="list-style-type: none">- Lacks flexibility and adaptability to dynamic changes.- May lead to suboptimal performance in complex environments.
Model Predictive Control (MPC)	<ul style="list-style-type: none">- Suitable for complex HPS requiring advanced control and optimization capabilities.	<ul style="list-style-type: none">- Provides advanced optimization and predictive control.- Optimizes system performance over time with adaptability to changes.	<ul style="list-style-type: none">- Requires accurate models and significant computational resources.- Real-time implementation is challenging.
Artificial Intelligence (AI) Techniques)	<ul style="list-style-type: none">- Suitable for adaptive and robust control in dynamic conditions but requires significant computational resources.	<ul style="list-style-type: none">- Adaptive, robust, and data-driven, capable of handling uncertainties.- Scalable for complex scenarios.	<ul style="list-style-type: none">- High computational and extensive training data requirements.- May lack transparency and interpretability.
Optimization Algorithms	<ul style="list-style-type: none">- Suitable for systematic optimization in complex systems but may be too computationally intensive for real-time use.	<ul style="list-style-type: none">- Explores large solution spaces systematically for optimal control policies.- Scalable to complex systems.	<ul style="list-style-type: none">- Computationally intensive and slow to converge.- Not suitable for real-time applications in smaller-scale systems.

2.9 Evaluation for Hybrid PV-Wind-Battery Systems with Rule-Based EMS

For hybrid PV-wind-battery systems, the choice of EMS depends on system characteristics, resource constraints, and operational requirements. Rule-based systems are particularly advantageous for smaller-scale systems due to their simplicity and minimal computational demands. They are well-suited for applications where transparency and ease of implementation are priorities.

However, for more complex hybrid power systems, approaches such as MPC or AI techniques may be preferred to achieve better optimization and adaptability. While these methods require greater computational and data resources, they can significantly enhance performance in dynamic or large-scale environments.

The comparison above underscores the trade-offs between computational complexity, adaptability, and suitability for specific applications, aiding in the selection of an appropriate EMS approach based on system requirements.

2.10 Conclusion

This chapter conducts an ample literature review focusing on the development and management of hybrid power systems (HPS) integrating wind turbines, photovoltaic (PV) solar panels, and battery storage. The review is segregated into two main categories. The first category provides a detailed explanation of the several components used in the hybrid power system, offering accurate and updated information about these elements. This includes the technical specifications and operational principles of PV systems, wind turbines, and battery storage units, as well as their integration within the HPS.

The second category examines the key energy management techniques for hybrid power systems available in literature. This includes a critical review of different energy management strategies (EMS), such as rule-based systems, Model Predictive Control (MPC), and fuzzy logic techniques. The review highlights the methodologies, challenges, results, and applicability of these approaches to the hybrid PV-wind-battery system.

Given the advantages of rule-based EMS, this approach is well-suited for the hybrid PV-wind-battery storage system. While rule-based EMS may lack the adaptability and optimization capabilities of more advanced methods like MPC or AI techniques, its simplicity, transparency, and low computational complexity make it the preferred choice for smaller-scale or less complex hybrid systems. The selection of rule-based EMS aligns with the system's requirements for real-time decision-making and ease of implementation, providing a

straightforward energy management strategy for efficient operation and control of the hybrid power system.

This literature review not only provides a thorough understanding of the components and EMS methodologies but also justifies the choice of a rule-based approach for this study, ensuring the development of an efficient and reliable energy management system for the proposed hybrid power system.

CHAPTER THREE: MATHEMATICAL MODELLING OF PROPOSED ENERGY MANAGEMENT STRATEGY

3.1 Introduction

Chapter three focuses on mathematical modelling and developing the HPS and the associated energy management strategy. The main goal is to develop a comprehensive model which effectively integrates the various sources of renewable energy, such as PV, wind, and battery storage, ensuring that the load demand is satisfied consistently and efficiently. The chapter starts by reviewing the development of the HPS model, including the individual components and their interactions within the system. The mathematical formulations necessary to simulate the performance and behaviour of these components under different operating conditions are also presented. These formulations lay the groundwork for the energy management strategy that is designed to optimize the system's operation.

3.2 Development of the HPS model

The Hybrid Power System (HPS) in this study integrates multiple energy sources, including PV panels, wind turbines, and battery storage, to provide a reliable and sustainable energy solution. This section outlines the development of the HPS, focusing on the modelling and design of the PV, wind, and battery models along with the event-based controller, which performs a critical part in energy generation and management.

- The objectives of the HPS development are:

- 1 Creating a balanced energy system capable of effectively managing renewable energy sources to meet energy demands.
- 2 Ensuring stability and reliability by coordinating the operations of PV, wind, and battery storage.

- The scope of the HPS development involves:

- Designing a hybrid system that operates efficiently under varying environmental conditions and energy demands.
- Incorporating control systems that can adapt to fluctuations in renewable energy generation and load requirements.

3.3 System Model

To accurately simulate and analyse the performance of the hybrid PV-wind-battery system, a comprehensive system model was developed using MATLAB/Simulink. This model integrates the individual models of PV, wind, and battery storage into a single framework that can simulate the dynamic interactions between these components under various operating conditions.

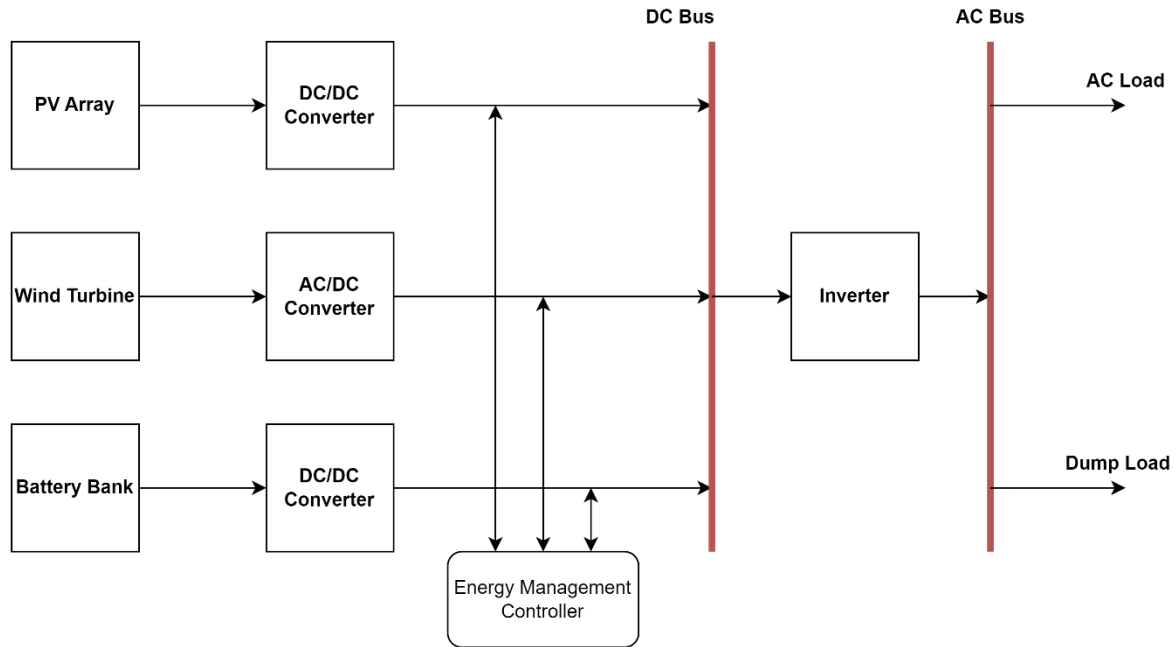


Figure 3-1: Schematic of the HPS System Model

3.4 PV Model Design

The objective of the PV model developed in this thesis is to accurately simulate a photovoltaic (PV) system, capturing irradiance and temperature data to determine the appropriate current output based on given conditions. The PV model subsystem, as depicted in Figure 3-1 in MATLAB Simulink, incorporates switches to adjust inputs for different irradiation and temperature scenarios, providing a flexible environment for comprehensive testing.

The PV model is designed based on parameters from the selected Monocrystalline PV module, specifically the CS6P-250M 250-watt solar panel provided by Canadian Solar (refer to Appendix A for detailed specifications). Standard test conditions (STC) are used to operate the model, which consist of 1000W/m^2 irradiance, Air Mass (AM) = 1.5, and an ambient temperature of 25 degrees Celsius.

3.4.1 Assumptions for the PV model:

The assumptions below were comprised for the PV model:

- The model serves as a representation of each module within the PV system. Therefore, when the model detects an input, it implies that all the modules in the actual system would react similarly, generating electrical energy.
- The operating conditions are based on typical irradiance and temperature ranges, allowing for testing under various scenarios to ensure the model's accuracy and reliability.

3.4.2 Model Selection for PV model

The PV module will be modelled using an equivalent circuit, chosen for its simplicity and ease of implementation in MATLAB Simulink. To simplify the system further, the shunt resistance is excluded. the two-diode model with shunt resistance requires an extensive number of iterations which creates significant modelling complications. Therefore, a single-diode model with only a series resistance, the series resistance can be assumed as negligible which results in easier MATLAB modelling and calculations. Figure 3-2 shows a PV solar cell with single-diode and series resistance (Rodrigues, et al., 2011).

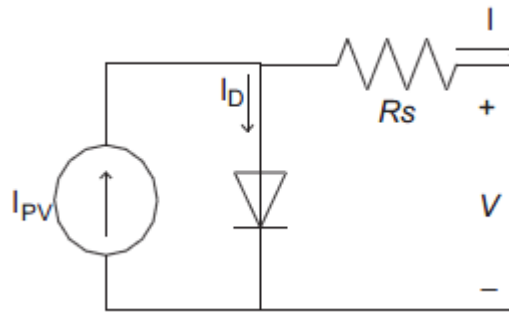


Figure 3-2: PV solar cell with single-diode and series resistance

3.4.3 Design of the PV Model

Figure 3-3 shows the Simulink PV Model, displaying the configuration and the key components used to simulate a PV system. This diagram includes the necessary blocks and subsystems that facilitate the calculation of current output based on input data.

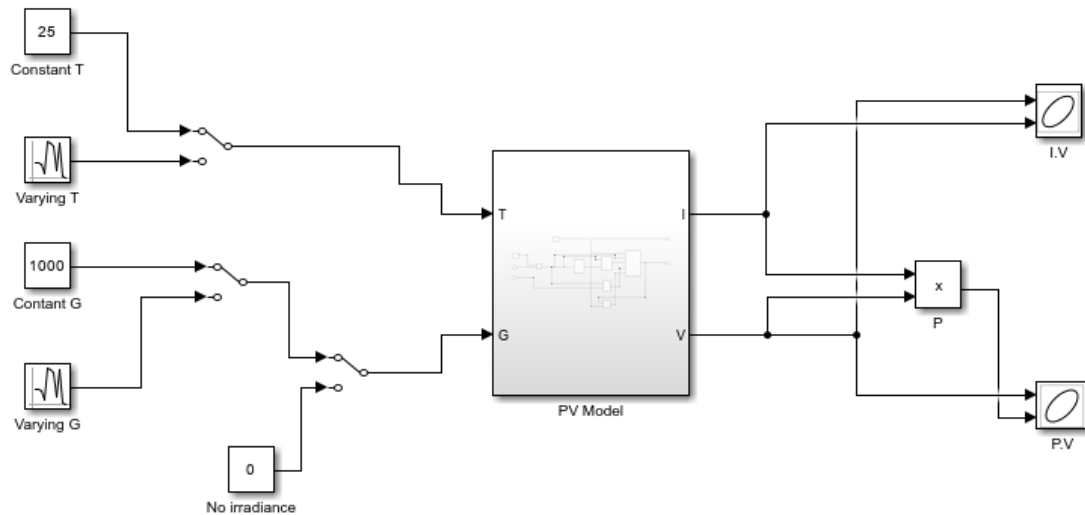


Figure 3-3 MATLAB Simulink PV Model

The required inputs for the PV model are:

- **Irradiance:** This parameter varies from 200 W/m² to 1000 W/m², representing different levels of sunlight intensity.
- **Temperature:** This parameter ranges from 25 degrees Celsius to 70 degrees Celsius, allowing for a comprehensive analysis of temperature effects on PV performance.
- **Voltage:** This parameter should not exceed the open-circuit voltage (Voc) as specified in the PV module datasheet in Appendix A.

3.4.4 Results and Its Significance

The results obtained from this PV model will provide insight into how the system responds to different conditions. By analysing the model's outputs, such as current and voltage, we can understand the impact of varying irradiance and temperature on the PV system's performance. These results help determine whether the system can meet energy demands and integrate with other components in the HPS.

The primary goal is to achieve a comprehensive understanding of the PV system's behaviour under different scenarios, allowing for effective energy management and optimal operation of the HPS. The results are intended to inform control strategies and guide the development of robust EMS for the HPS, ensuring reliability and efficiency in energy generation and storage.

3.4.5 Mathematical models for PV design

In this section, the mathematical models developed to simulate various aspects of the Photovoltaic (PV) system is discussed. These models are designed to provide a comprehensive understanding of the PV system's behaviour under various conditions and for performance evaluation. The models were implemented in MATLAB Simulink, following the equations and concepts outlined in reference (Pandiarajan & Muthu, 2011).

To begin with, temperature performs a substantial role in the operation of PV systems. The temperature-related calculations within the PV model convert temperature from degrees Celsius to Kelvin, which is the standard unit for thermodynamic calculations. This conversion is necessary for further computations within the PV model that require temperature in Kelvin. The equations used for this conversion are:

$$T_{\text{Kelvin}} = 273 + T \quad (3.1)$$

$$T_{\text{Ambient(Kelvin)}} = 273 + T_{\text{Ambient}} \quad (3.2)$$

Next, the Photon Current subsystem is critical for determining the PV system's output current. The photon current is computed from the given irradiance and temperature, using the equation (3.3):

$$I_{ph} = [I_{SCRr} + K(T - 298) * \frac{\lambda}{1000}] \quad (3.3)$$

Equation 3.3 represents the photon current where I_{ph} represents photon current, I_{SCr} is short-circuit current, K is short-circuit current temperature coefficient, T is measured temperature, and λ is irradiance.

In modelling the PV system's electrical behaviour, the Reverse Saturation Current is another essential factor. This current is modelled using the following equation in (3.4):

$$I_{rs} = \frac{I_{SCRr}}{[\exp(\frac{qV_{oc}}{N_s k A T}) - 1]} \quad (3.4)$$

Equation 3.4 represents the reverse saturation current where I_{rs} denotes the reverse saturation current, V_{oc} is open-circuit voltage. N_s is number of cells in series, k is Boltzmann's constant, A is ideality factor of the diode, and T is measured temperature.

Further extending the electrical modelling, the Module Saturation Current is calculated to account for temperature-related variations affecting the PV system's overall performance. The equation (3.5) was used as seen below -

$$I_0 = I_{rs} \left[\left(\frac{T}{T_r} \right)^3 \cdot \text{Exp} \left(\frac{q \cdot E_{go}}{Bk} \cdot \left(\frac{1}{T_r} - \frac{1}{T} \right) \right) \right] \quad (3.5)$$

The equation 3.5 represents the module saturation current where I_0 is module saturation current, q is charge of an electron, E_{go} is energy band gap, B is ideality factor of diode, k is Boltzmann's constant, and T_r is reference temperature.

This subsystem is vital for modelling the temperature-related variations in the module saturation current, which affects the overall performance of PV systems.

Finally, the Current Output of PV is a critical metric for evaluating the system's performance. The current output of the PV model is calculated as follows: The equation used is:

$$I_{PV} = N_p \cdot I_{ph} - N_p \cdot I_0 \cdot \left[\exp \left(\frac{q \cdot (V_{pv} + I_{pv} R_s)}{N_s A k T} \right) - 1 \right] - I_{sh} \quad (3.6)$$

Equation 3.6 represents the PV current output where I_{PV} represents the PV model output current, N_p is the parallel number of cells, V_{PV} is output voltage of PV model, I_{ph} is photo-current of PV model, R_s is resistance in series, and I_{sh} is shunt current.

In this model, the R_s value was estimated at 0.000018 ohms, as this parameter can be considered negligible. The R_s parameter is included in the subsystem as a gain in the feedback loop to maintain accuracy.

These mathematical models collectively simulate the key aspects of the PV system's operation, ensuring that the system can be accurately analysed and optimized for different scenarios and environmental conditions.

3.4.6 Purpose of the Mathematical Models

The mathematical models described above aim to simulate various aspects of the PV system's operation. The results obtained from these models are crucial for understanding the PV system's behaviour under different conditions and for evaluating its performance.

By modelling different subsystems, including temperature, photon current, reverse saturation current, module saturation current, and current output, we can determine the impact of varying conditions on the PV system's output. This analysis helps predict how the PV system will perform when integrated into the hybrid power system, providing insights into energy management and system optimization.

Ultimately, the purpose of these mathematical models is to guide the model and control of the PV system within the broader hybrid power system, ensuring efficient energy generation,

stability, and reliability. By accurately modelling these critical components, the overall energy management strategy can be optimized for real-world application.

3.4.7 Maximum Power Point Tracking (MPPT) Controller Design for the PV Model

To ensure that the Photovoltaic (PV) system operates at its MPP, a MPPT controller is required. The MPPT controller optimizes PV system output by adjusting the operating conditions dynamically to maximize power generation. This section describes the development and design of the MPPT controller, outlining the algorithm used and how it interacts with the PV model.

3.4.7.1 MPPT Algorithm Selection

The Incremental Conductance (IncCond) algorithm was selected for MPPT due to its enhanced accuracy and ability to handle adjusting environmental conditions, for instance fluctuations in solar temperature and irradiance. Unlike the P&O algorithm, IncCond accounts for instantaneous changes in power with respect to both voltage and current, allowing for a more precise adjustment of the operating point and leading to more efficient utilization of available solar power.

IncCond also reduces oscillations around the MPP compared to P&O, enhancing system stability. Moreover, it balances accuracy and computational complexity, making it a suitable choice for both academic research and practical implementations. The algorithm will be coded in MATLAB and integrated into the HPS design.

3.4.7.2 Algorithm for the MPPT Controller

A MATLAB script was developed to implement the MPPT controller, ensuring that the PV system consistently runs at its MPP. The algorithm dynamically adjusts the operating voltage

based on incremental conductance, continuously seeking to maximize power output under varying conditions.

The following flowchart (Figure 3-4) illustrates the MPPT controller algorithm used in the MATLAB script.

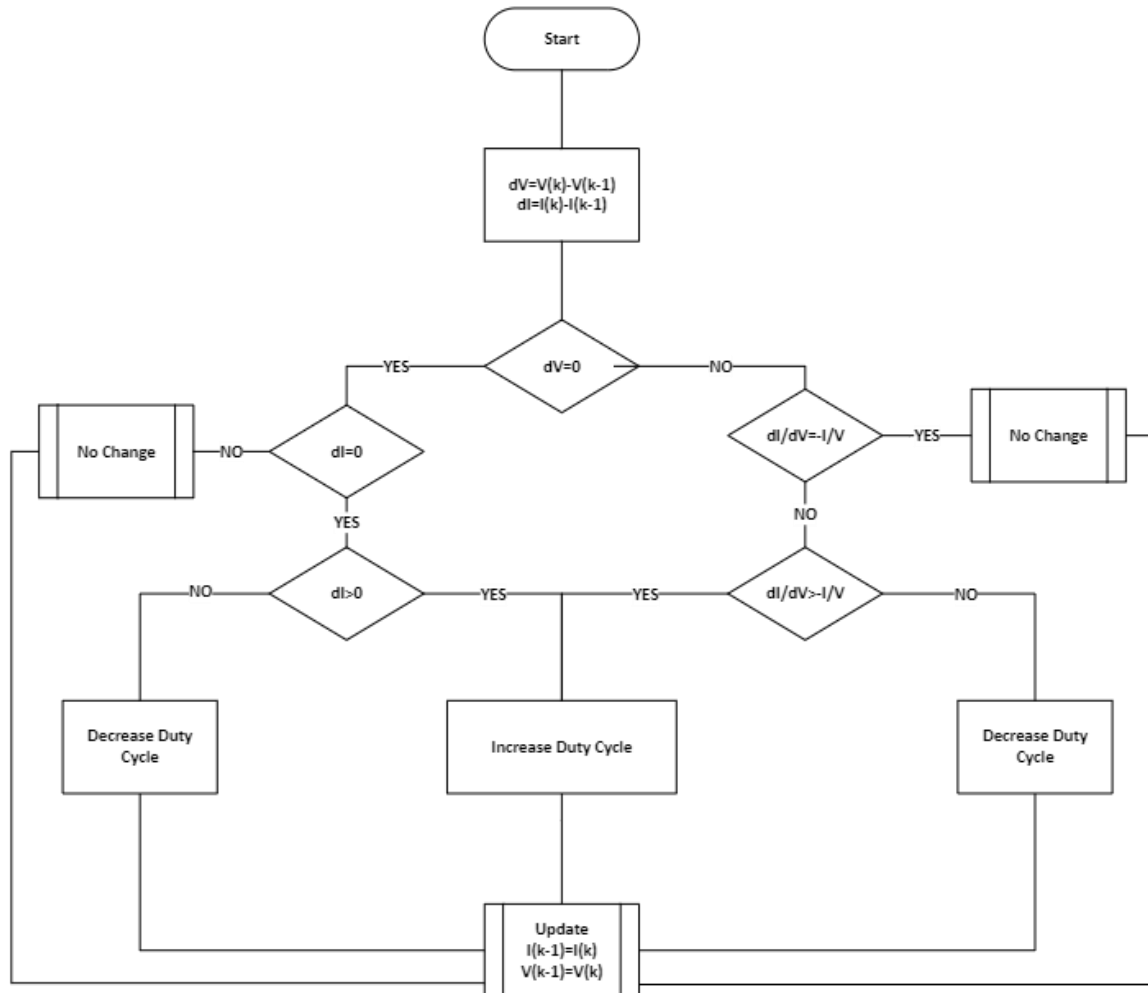


Figure 3-4 MPPT controller algorithm for the PV system

3.4.7.3 Importance of the MPPT Controller

The MPPT controller permits the PV system to adapt to varying conditions and maximize energy production. By continuously tracking the MPP, the controller ensures peak efficiency of the PV system. The implementation of the MPPT controller brings several benefits to the hybrid power system:

- **Optimized Energy Output:** By maintaining the MPP, the PV system can generate the maximum possible power under given conditions, increasing overall system efficiency.
- **Dynamic Response:** The MPPT controller can adapt to changes in irradiance and temperature, ensuring optimal performance in a range of scenarios.

- **Improved Reliability:** Adds to the stability and dependability of the HPS, reducing the risk of power fluctuations.

The MPPT controller plays a crucial role in the hybrid power system by ensuring maximum utilization of renewable energy. It works in coordination with other components, such as wind turbines and battery storage, to balance and optimize energy flow, thereby contributing to the stable, reliable, and efficient operation of the entire HPS.

3.5 Development of the Wind Energy System

The wind energy system development within this hybrid power system focuses on selecting and integrating a suitable wind generator. The chosen generator must convert wind energy efficiently into electrical energy while being compatible with the other components of the hybrid system.

3.5.1 Wind Generator Selection

The DFIG (double-fed induction generator) was chosen since it is suitable for variable wind speed applications. They are efficient for these types of applications seeing as the wind energy can be harnessed effectively without leaving the resource to be wasted. Essentially, the concept of DFIG makes for an appealing option given that it is cost-effective whilst producing a large output power.

3.5.2 Wind Turbine Selection

The HAWT was selected because it is more efficient than the VAWT design. Although the VAWT occupies less space, which is an appealing feature for implementation in remote areas, the HAWT can withstand severe weather conditions. Keeping in mind that PV plants are preferably situated in areas that are exposed to more sunny days, the HAWT therefore stands less chance of being exposed to unfavourable weather conditions when integrated with a PV plant.

3.5.3 Designing the wind energy system

The wind energy system in this study utilizes a Doubly-Fed Induction Generator (DFIG) in its turbine design, as illustrated in Figure 3-5 (Gagnon, et al., 2002) (The MathWorks, Inc., n.d.). This system features a wound rotor induction generator that has a rotor that receives power from the wind's variable frequency. This configuration allows for operation with variable speed, enabling the wind turbine to modify the rotor speed to match wind conditions and optimize its efficiency.

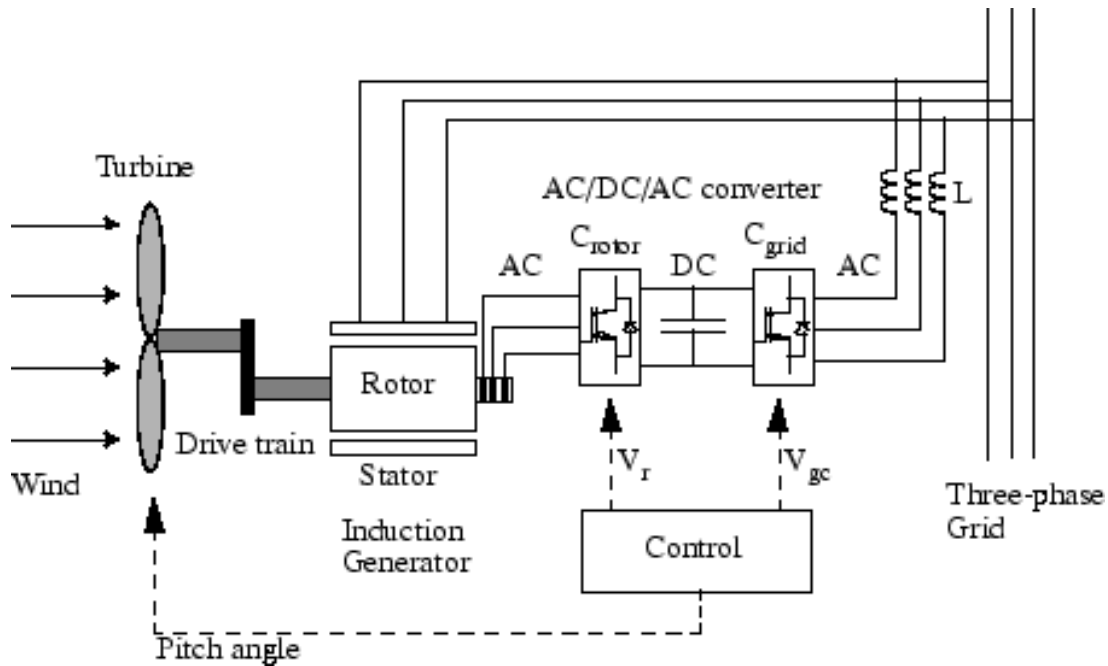


Figure 3-5: Doubly-fed induction generator and wind turbine schematic

A key feature of the DFIG system is its capability to keep a consistent speed of 1.2 p.u. with the help of a torque controller (The MathWorks, Inc., n.d.). This controller adjusts the torque employed on the rotor to uphold synchronous speed with the grid, ensuring stable and efficient power output. This speed setting enhances power generation by allowing the DFIG to operate slightly above the synchronous speed, thereby converting more mechanical energy from wind via the turbine into electrical energy efficiently. The system achieves this consistent speed with the help of a torque controller, which adjusts the torque applied to the rotor. This adjustment ensures that the generator remains stable and synchronized with the grid, even as wind speeds fluctuate, thus maintaining a steady and efficient power output. The controlled speed also lessens mechanical stress on the generator and turbine, improving overall reliability and longevity of the system while allowing for better reactive power control, crucial for grid stability.

The pitch control system for the DFIG is another essential aspect of wind energy systems. This system regulates the wind turbine blades pitch angle based on the speed of the turbines. Figure 3-6 shows the pitch control system implemented with the DFIG (The MathWorks, Inc., n.d.).

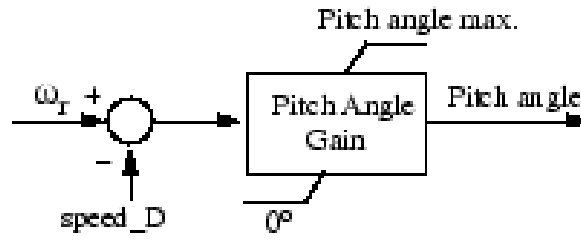


Figure 3-6: The pitch control system implemented with the DFIG

The pitch control system portrays a critical role in retaining optimum performance. It adjusts the pitch angle according to the speed of the turbine's, which is influenced by the speed of wind. Figure 3-16 illustrates the power characteristics of the wind turbine, indicating the correlation between turbine speed and output power.

The power output of the wind turbine is affected by several factors, which includes wind turbine efficiency, wind speed, pitch angle, and tower height (Rodrigues, et al., 2011). The power produced by wind turbines can be expressed by the following equation:

$$P_w = \frac{1}{2} \rho A C_p(\lambda, \beta) v^3 \eta_t \quad (3.7)$$

Equation 3.7 represents the output power for a turbine where P_w is power produced by the turbine, ρ is density of air at turbine hub height (kg/m^3), A is the blades swept area (m^2), $C_p(\lambda, \beta)$ is the turbine power coefficient, which is a function of the blade pitch angle (β) and the tip speed ratio (λ), v is velocity of the wind (m/s), η_t is turbine efficiency, β is blade pitch angle, and λ is tip speed ratio of the rotor blade tip speed to wind speed.

The average power in terms of the average wind speed (m/s) can be expressed by equation 3.8 as: (Rodrigues, et al., 2011)

$$P_{avg} = \frac{1}{2} \rho A C_p(\lambda, \beta) v_{avg}^3 \eta_t \quad (3.8)$$

The tower hub wind speed can be calculated using equation (3.9) (Rodrigues, et al., 2011)

$$v_h = v_r \left(\frac{H_h}{H_r} \right)^\alpha \quad (3.9)$$

Equation 3.9 represents the tower hub wind speed where v_h is the hub height wind speed (m/s), v_r is the reference height wind speed (m/s), H_h is turbine hub height (m), H_r is reference height (m), and α is a surface roughness coefficient that reflects the effects of the land.

The wind turbine power coefficient (C_p) is calculated as below:

$$C_p(\lambda, \beta) = C_1(\frac{C_2}{\lambda_1} - C_3\beta - C_4\beta_5^c - C_6)\exp(\frac{-C_7}{\lambda_i}) \quad (3.10)$$

Equation 3.10 represents the wind turbine power coefficient where:

$$\lambda_i = \frac{1}{\frac{1}{\lambda + 0.08\beta} - \frac{0.035}{\beta^3 + 1}} \quad (3.11)$$

Equation 3.11 represents the tip speed ratio of a wind turbine.

To maximize rotor efficiency, the tip speed ratio (λ) must be optimized. Also, the power coefficient can be calculated as in equation 3.12 below (Rodrigues, et al., 2011):

$$C_p(\lambda, \beta) = 0.22((\frac{116}{\lambda_1} - 0.4\beta - 5)\exp(\frac{-12.5}{\lambda_i})) \quad (3.12)$$

The number of wind turbines needed to satisfy a specific load demand is expressed by Equation 3.13 (Rodrigues, et al., 2011):

$$N_{Turbines} = \frac{P_L \times SF}{P_w} \quad (3.13)$$

Equation 3.13 calculates the number of wind turbines required where $N_{turbines}$ is quantity of required wind turbines, P_L is load demand (W), SF is the safety factor, typically around 120%, and P_w is power produced by a single wind turbine (W).

These equations provide a comprehensive framework for modelling the output power and wind turbine efficiency in a hybrid power system. By understanding and applying these mathematical models, we can better design and optimize the wind energy integration into the overall HPS, safeguarding a reliable and efficient energy supply.

3.6 Development of the battery storage unit

In this thesis, a Nickel-Metal Hydride (NiMH) battery model provided by MATLAB Simulink was employed to simulate the performance and battery storage unit characteristics. However, to align with the requirements of this study and to accurately simulate a Lithium-Ion battery, significant adjustments were made to this existing model.

3.6.1 Battery Selection

In table 3-1 below, the blocks are marked to indicate the benefits offered by each of the five batteries.

Table 3-1: Battery selection weighting

Cell Type	Efficiency %	Depth of Discharge %	Life span (cycles)	Self-Discharge	Technology Maturity	Cost	Suitability	Score
Lithium Ion	✓	✓	✓	✓			✓	5
Lead Acid		✓		✓	✓	✓	✓	5
Zinc Bromine				✓				1
Nickel Cadmium			✓		✓			2
Sodium Sulphur	✓		✓	✓	✓		✓	5

After considering these results, the battery selection has come down to Lead-Acid, Lithium-Ion, and Sodium-Sulphur. Sodium-Sulphur dominates in the efficiency and life span columns where Lead-Acid batteries dominate in the depth of discharge and cost column. Lithium-ion batteries offer several operational benefits. They have a lower self-discharge rate, which allows for energy to be stored longer with less periods of recharging. A faster charging rate is also apparent in lithium-ion batteries, enabling quicker replenishment of energy compared to lead-acid and sodium-sulphur batteries. Moreover, lithium-ion batteries require less maintenance, unlike lead-acid batteries that require periodic electrolyte checks and water refilling. In South Africa, efficient and effective proposals seem more desirable and are opted for more readily than the proposals that are more cost effective upfront. It is for this reason that Lithium-Ion was selected for energy storage in this thesis.

3.6.2 Adjustments for the Lithium-Ion Battery Model

To convert the NiMH battery model into a Lithium-Ion battery model, various parameters were modified to exhibit the qualities of Lithium-Ion technology. These changes were necessary to ensure the model accurately represented the performance and behaviour of a Lithium-Ion battery within the HPS.

3.6.3 Mathematical Equations for the Battery Model

The battery model equations implemented differ based on whether the battery is in a discharging or charging state. Below are the equations for both scenarios (The MathWorks, Inc., n.d.):

Discharge model ($i^* > 0$)

$$f_1(it, i^*, i) = E_0 - K \cdot \frac{Q}{Q-it} \cdot i^* - K \cdot \frac{Q}{Q-it} \cdot it + A \cdot \exp(-B \cdot it) \quad (3.14)$$

Equation 3.14 represents the discharge modelling equation where E_0 is Constant voltage (V), Q is Maximum battery capacity (Ah), it is Extracted capacity (Ah), K is Polarization resistance (Ohms), $\text{Exp}(s)$ is the Exponential zone dynamics (V), and i^* is the Low frequency current dynamics (A).

Charge Model ($i^* < 0$)

$$f_2(it, i^*, i) = E_0 - K \cdot \frac{Q}{it+0.1 \cdot Q} \cdot i^* - K \cdot \frac{Q}{Q-it} \cdot it + A \cdot \exp(-B \cdot it) \quad (3.15)$$

Equation 3.15 represents the charge modelling equation.

These equations represent the battery's behaviour under charging and discharging conditions, providing a detailed model of its performance.

3.6.4 State of Charge (SOC) and Battery Protection

To protect battery overcharging and discharging, the battery model incorporates State of Charge (SOC) limits. The SOC is a measure of the remaining capacity in batteries as a percentage of its total capacity. By monitoring the SOC, the system can determine when to stop charging or discharging to avoid damage and prolong the battery's lifespan.

Table 3-2 presents the specific parameters for the lithium battery model used in the HPS. These parameters include the SOC limits, nominal voltage, rated capacity, nominal discharge current, and internal resistance.

Table 3-2 Battery parameters implemented in the NiMH battery model

SOC %	Starting Value	100
	Maximum (charge) limit	90
	Minimum (discharge) limit	40
Nominal Voltage (volts)		200
Rated Capacity (Ah)		6.5
Nominal discharge current (A)		1.3
Internal Resistance (ohms)		0.3

The availability of battery capacity banks has to be kept between the minimum and maximum capacity limits to guarantee peak performance and durability. The battery discharge minimum limit is set at 40%, and the maximum state of charge (SoC) is set at 90%. This range is

designed to prolong the battery life cycle by avoiding deep discharges and overcharging (Rodrigues, et al., 2011).

The depth of discharge (DoD) and the (SoC) are defined by the following equations:

$$SOC_{min} \leq SOC(t) \leq SOC_{max} \quad (3.16)$$

$$SOC_{min} = (1 - DOD)SOC_{max} \quad (3.17)$$

Equation 3.16 represents the state of charge equation and Equation 3.17 represents the depth of discharge equation where SOC_{min} is the lowest state of charge of the battery, SOC_{max} is the highest state of charge of the battery, and DOD is depth of discharge of the battery.

The battery capacity needed in ampere-hours (Ah) is calculated using the following equation (Rodrigues, et al., 2011):

$$C_{bat} = \frac{A_d E_L}{\eta_{bat} \eta_{inv} DOD v_s} \quad (3.18)$$

Equation 3.18 represents the battery capacity equation where C_{bat} is battery capacity needed (Ah), E_L is load energy (Wh), A_d is autonomy duration, the maximum time the battery can operate without any support from other sources (s), v_s is the system voltage (V), and DoD is the depth of discharge of the battery.

These equations are critical for designing the battery storage component of the HPS, ensuring that the system has sufficient capacity to meet energy demands while maintaining battery health and efficiency. By understanding and applying these mathematical models, we can optimize the battery storage design, contributing to the overall reliability and effectiveness of the hybrid power system.

3.7 Development Of Event-Based Availability Controller

An efficient controller is crucial for managing a HPS that integrates multiple sources of energy, such as PV panels, turbines, and battery units. In this work, the controller to be employed is an event-based availability controller. The primary role of this controller is to analyse the system's inputs, including the availability of energy from the PV panels, turbines, and batteries, and determine which energy source should be used to supply the load.

The event-based availability controller was chosen for its aptitude to react dynamically to variations in energy availability and load demand. Unlike time-based controllers, which operate

on a fixed schedule, the event-based approach allows the controller to make decisions based on real-time events within the system, like fluctuations in the speed of wind, changes in solar irradiance, or the SOC of the battery. This makes it particularly well-suited for hybrid power systems, where the obtainability of renewable sources of energy can be highly variable.

The motivation for selecting this controller lies in its efficiency and flexibility. The event-based availability controller is designed to expand the use of renewable sources of energy when they are available while ensuring that the load is always supplied with power, either from renewables or from the battery storage when necessary. By prioritizing renewable sources, the controller reduces reliance on the battery, thereby extending its lifespan and improving the overall sustainability of the HPS. Additionally, this approach minimizes energy wastage and enhances system reliability by seamlessly switching between energy sources as needed.

3.7.1 Controller Functionality and Scenarios

The HPS controller evaluates the inputs from the photovoltaic (PV), wind energy (WE), and battery storage (BS) units to determine the system's current scenario. The anticipated scenarios and their corresponding cases are outlined in Table 3-3, which illustrates the potential combinations of energy sources available to supply the load. The table displays the different cases tested, with each case showing the input availability and output supply of the PV system, WE system, and BS system. The 'InPV,' 'InWE,' and 'InBS' columns indicate whether each energy source is available ('1' for available, '0' for not available), while the 'OutPV,' 'OutWE,' and 'OutBS' columns represent whether each energy source is actively supplying energy to the load ('1' for supplying, '0' for not supplying).

Table 3-3: HPS controller possible inputs and corresponding outputs

Cases	InPV	InWE	InBS	OutPV	OutWe	OutBS
Case 1	0	0	0	0	0	0
Case 2	0	0	1	0	0	1
Case 3	0	1	0	0	1	0
Case 4	0	1	1	0	1	0
Case 5	1	0	0	1	0	0
Case 6	1	0	1	1	0	0
Case 7	1	1	0	1	0	0
Case 8	1	1	1	1	0	0

In table 3-3, a value of "1" designates the respective energy source is available to supply the load, while a "0" indicates that it is unavailable. The yellow-highlighted blocks represent the chosen energy source for each case.

Based on the above scenarios, the HPS controller has been designed to operate as follows:

- **Case 1** represents a base case scenario where the load is entirely supplied by the grid, as none of the renewable energy sources are utilized in this condition.
- **Case 2** reflects a situation where only the battery storage unit is available to supply the load.
- **Case 3** indicates that only wind energy is available to supply the load, with no solar energy or battery storage.
- **Case 4** shows wind energy and battery storage are available.
- **Case 5** represents only the PV system to supply the load.
- **Case 6** indicates that both PV and battery storage are available, with no wind energy.
- **Case 7** represents a scenario where both PV and wind energy are available, but no battery storage.
- **Case 8** signifies a scenario where all sources—PV, wind, and battery storage—can supply the load.

3.7.2 Anticipated Scenarios and K-Maps

The controller evaluates a range of scenarios, with each scenario representing a specific combination of available energy sources. These scenarios are outlined in Table 3-3 which shows the inputs and corresponding outputs for the HPS controller.

The scenarios are derived using Karnaugh maps (K-maps), which help to simplify the Boolean expressions that govern the controller's operation. The simplified Boolean expressions are used to design a logic-based control system that selects the appropriate energy source based on the detected scenario.

3.7.3 K-maps and Simplified Boolean Expressions

The K-maps for determining the controller's outputs are constructed based on the inputs from the PV, wind, and battery storage units. Here are the simplified Boolean expressions derived from the K-maps:

- $\text{OutPV} = \text{InPV}$
- $\text{OutWE} = \text{InPV} \cdot \text{InWE}$
- $\text{OutBS} = \text{InPV} \cdot \text{InWE} \cdot \text{InBS}$

These expressions indicate the conditions under which each energy source becomes available to supply the load. For example, if the PV system is available, it will supply the load (OutPV).

If both the PV and wind sources are available, wind energy can also supply the load (OutWE). Similarly, the battery storage system can supply the load only when all three inputs (InPV, InWE, InBS) are true (OutBS).

Figure 3-7 represents the simplified Boolean expressions that determine the HPS controller's operation. It provides a clear visualization of the relationship among the expected inputs and outputs for the controller.

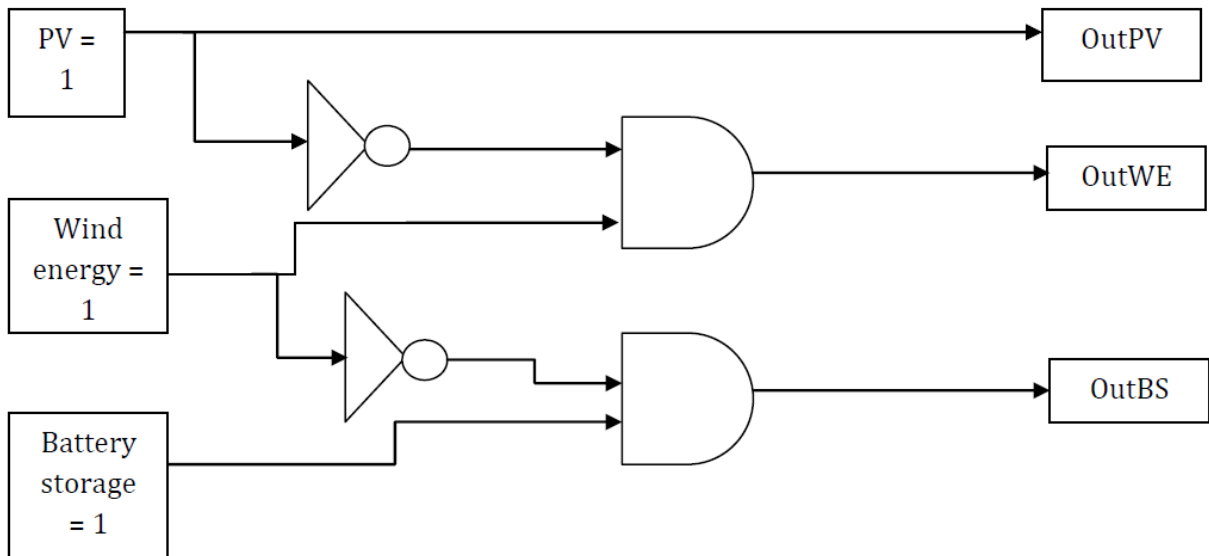


Figure 3-7: Boolean expression depicting the relationship among the expected inputs and outputs of the HPS controller

Controller Algorithm and Implementation

The MATLAB Simulink algorithm designed for the controller operation is shown in Figure 3-8. This algorithm determines the appropriate source of energy based on the inputs from the PV, wind, and battery units, and manages the load accordingly.

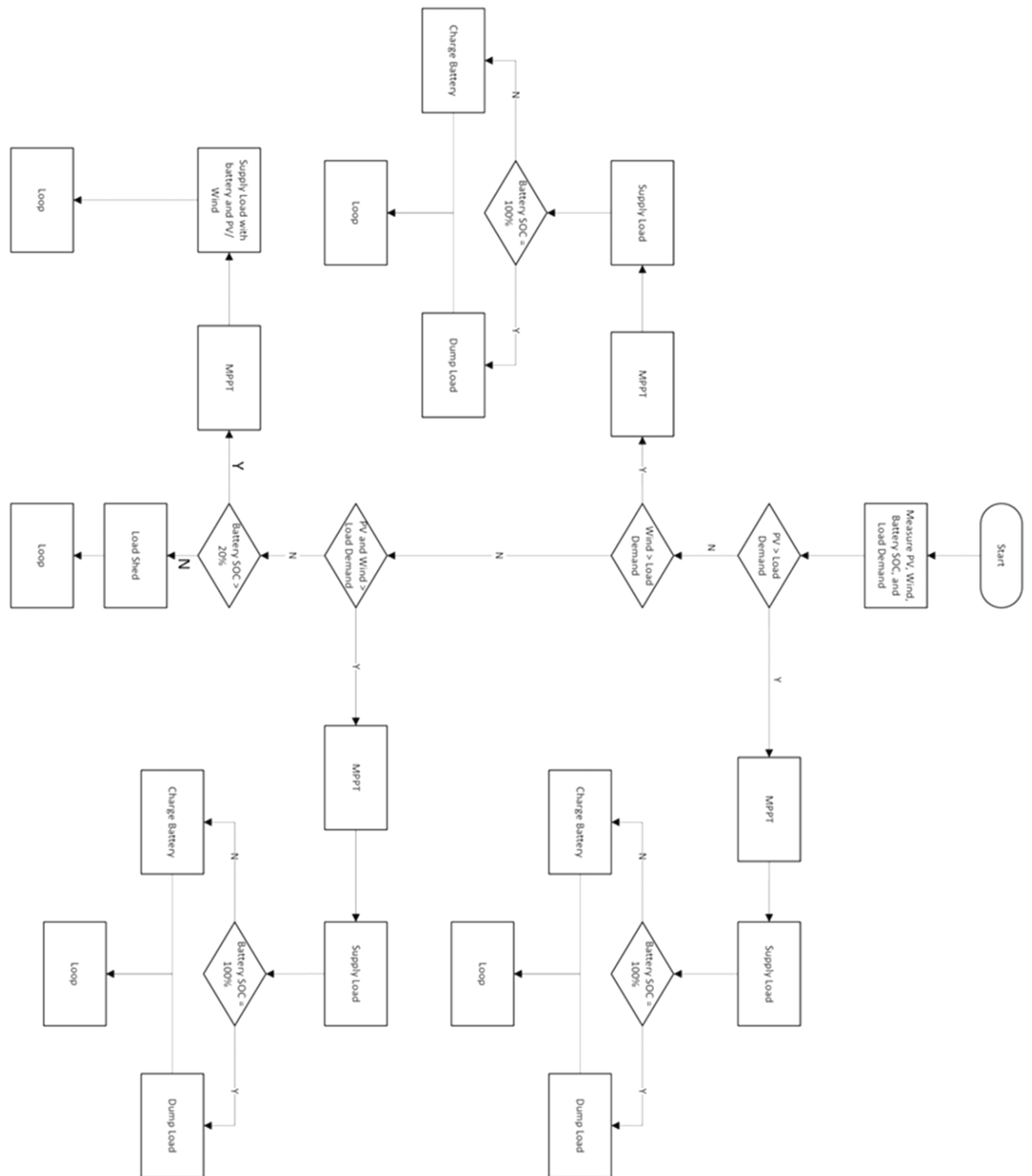


Figure 3-8 The MATLAB Simulink flowchart for controller operation

The above flowchart shows the decision flow that the controller will follow to ensure the load is supplied by renewable energy while using the battery to supplement the supply in the case where renewable sources are insufficient.

The control system should be able to decide based on the weather conditions which combination of the sources is best to supply the load.

1. Measure the PV, wind, battery SoC, and load demand.

2. Check if the PV is generating sufficient power.
 - If yes, supply the load with PV power.
 - If no, proceed to the next step.
3. Check if the wind is generating sufficient power.
 - If yes, supply the load with wind power.
 - If no, proceed to the next step.
4. If either PV or wind power is available, supply the load.
5. Check if battery SoC is above 20%.
 - If yes, the battery can assist in supplying the load demand.
 - If no, proceed to the next step.
6. Check if the battery SoC is below 20%.
 - If yes, excess power should charge the battery as a secondary priority to meet the load demand.
 - If no, proceed to the next step.
7. If the battery and sources of renewable energy are unable to supply the demand, load shedding must be implemented.
8. In the cases where the renewables can supply demand, if demand is met and the battery SoC is 100%, excess power should be sent to the dump load (a resistive load used to dissipate excess power).

The controller's algorithm processes the given inputs and determines the appropriate energy source to supply the load, following the scenarios. It uses these inputs to generate signals for the load supply, ensuring that the HPS operates efficiently and avoids conflicts between energy sources.

To facilitate decision-making, the algorithm considers various weather scenarios that the HPS may encounter. These scenarios are categorized based on the availability of wind, sunlight, and battery power. By analysing these scenarios, the algorithm determines the most appropriate course of action to optimize energy utilization and system performance.

Overall, the algorithm serves as a crucial component of the HPS controller, providing intelligent control and coordination of energy sources to guarantee consistent and efficient operation of the HPS.

CHAPTER FOUR: MODEL AND ANALYSIS OF THE HPS

To simulate the HPS, the PV, wind, and battery storage systems were individually modelled in MATLAB Simulink and later integrated to form the complete HPS configuration. This chapter provides an overview of the modelling process for these components, focusing on the PV system and its integration into the HPS.

4.1 Modelling the PV System

To create the PV system model, several assumptions were made to ensure consistent behaviour within the hybrid system:

1. **Maximum Power Point Tracking (MPPT):** The PV system operates at MPPT, and when the PV source is available, the input "In1" remains constant at "1," indicating the MPP condition. This assumption allows the PV system to generate optimal energy when it is activated.
2. **PV Source Availability:** When the PV source is identified as "available" by the HPS controller, it is assumed to generate sufficient energy to meet the load requirements.
3. **Equivalent PV Model:** The equivalent model for the PV system consists of an AC source, a step-down transformer, and a rectifier, designed to represent the electrical characteristics of a typical PV system. This configuration provides a simplified but effective representation for integration into the HPS.
4. **Load Demand Fulfilment:** It is assumed that the PV model, when active, can supply enough energy to meet the load demand.
5. **Steady-State Conditions:** The model operates under steady-state conditions, focusing on stable behaviour during energy production and distribution.

The PV system model, including the configuration for integration with other components, is illustrated in Figure 4-1.

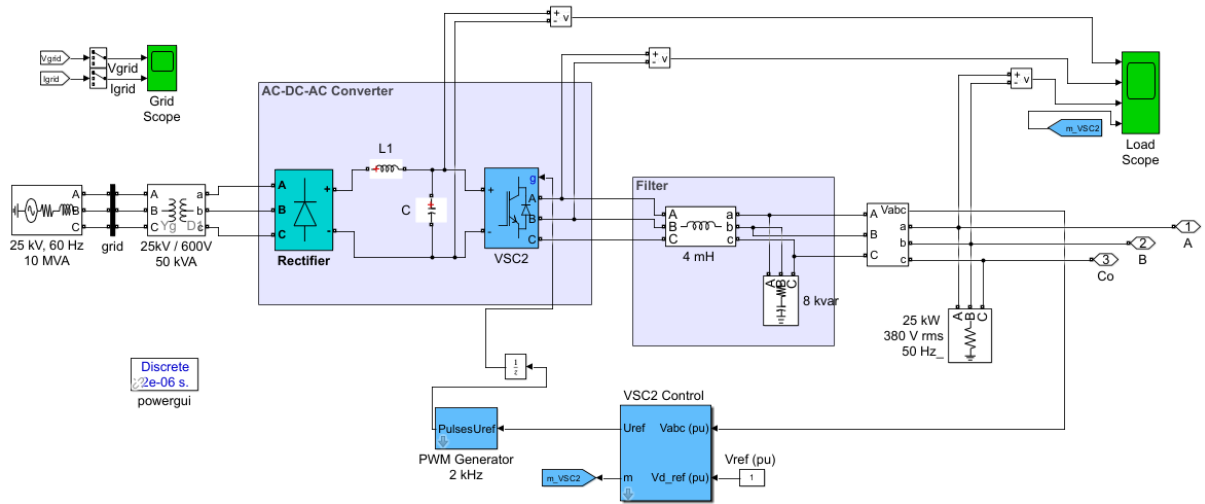


Figure 4-1: AC/DC/AC PWM converter as an equivalent PV model and DC/AC converter

Figure 4-1 presents the integration of the PV system components, where the AC source, step-down transformer, and rectifier blocks form the equivalent model for the PV system, with a DC/AC converter used for output power conversion. This design ensures compatibility with the broader hybrid power system and allows for seamless integration with other energy sources.

In this model, the MPPT controller determines the MPP based on inputs obtained from the actual PV system. Once the MPP is calculated, the controller sends a signal to the "In1" input, which is connected to a switch. When the switch is activated (input value "1"), the circuit breaker closes, allowing the equivalent PV system to run at its MPP, thereby supplying the load with maximum power.

The simulation of the equivalent PV system is designed to verify the MPPT functionality and its effectiveness in maintaining optimal power output. Figure 4-2 illustrates the complete integration of the modelled PV system with the DC/AC converter and load.

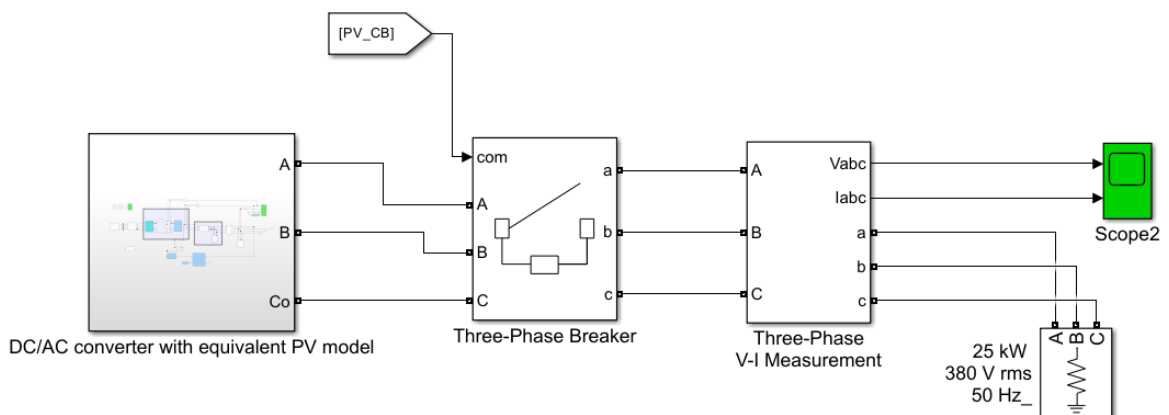


Figure 4-2: Integration of the equivalent PV model with the DC/AC converter and load

In Figure 4-2, the three-phase circuit breaker operates based on input from the controller. When the input is set to "1," the circuit breaker closes, allowing the load to be supplied by the PV system. The controller's decision to close the circuit breaker depends on weather conditions and other inputs to the HPS.

The results obtained from simulating the PV system model were favourable, providing a basis for further analysis and discussions in Chapter 5. The MPPT controller was implemented using a MATLAB script file, and the code for this implementation can be found in Appendix B. This script file demonstrates the tracking of the MPP for varying irradiance conditions, indicating the controller's capability to maintain optimal performance under different scenarios.

4.2 Testing PV Model Methodology

The PV model, developed and discussed in Chapter 3, underwent extensive testing to verify its performance before integration with the DC/AC PWM converter. This section shows results found from testing the PV model with varying irradiance and temperature conditions, providing insights into its behaviour and performance under different scenarios.

Testing with Varying Irradiance

The first set of tests was conducted to examine the PV model's response to varying levels of solar irradiance while maintaining a constant temperature. The voltage versus power trend for these tests is shown in Figure 4-3.

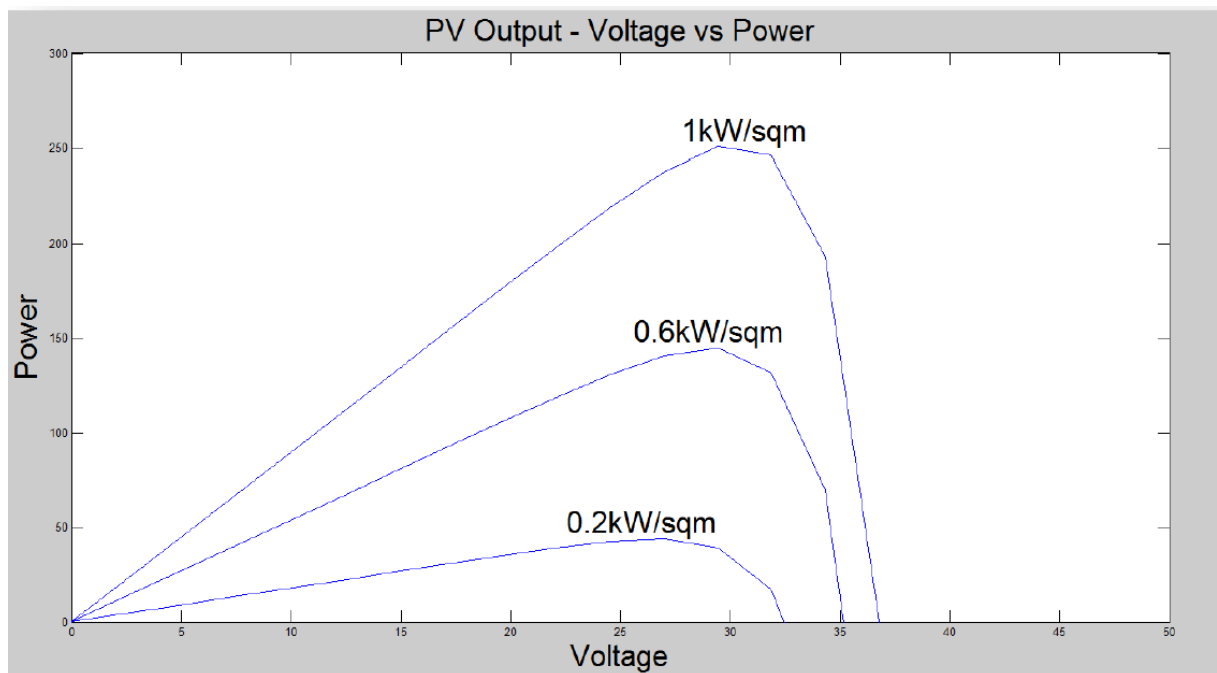


Figure 4-3: Voltage vs power trend for the designed PV model with varying irradiance

From Figure 4-3, the following observations can be made:

- The voltage versus power relationship exhibits a significantly higher peak at 1kW/m^2 compared to lower irradiance levels, such as 0.6kW/m^2 and 0.2kW/m^2 .
- The power output increases as irradiance levels rise, indicating that the PV model accurately captures the impact of varying solar energy.

Next, the voltage versus current trend for varying irradiance levels is shown in Figure 4-4.

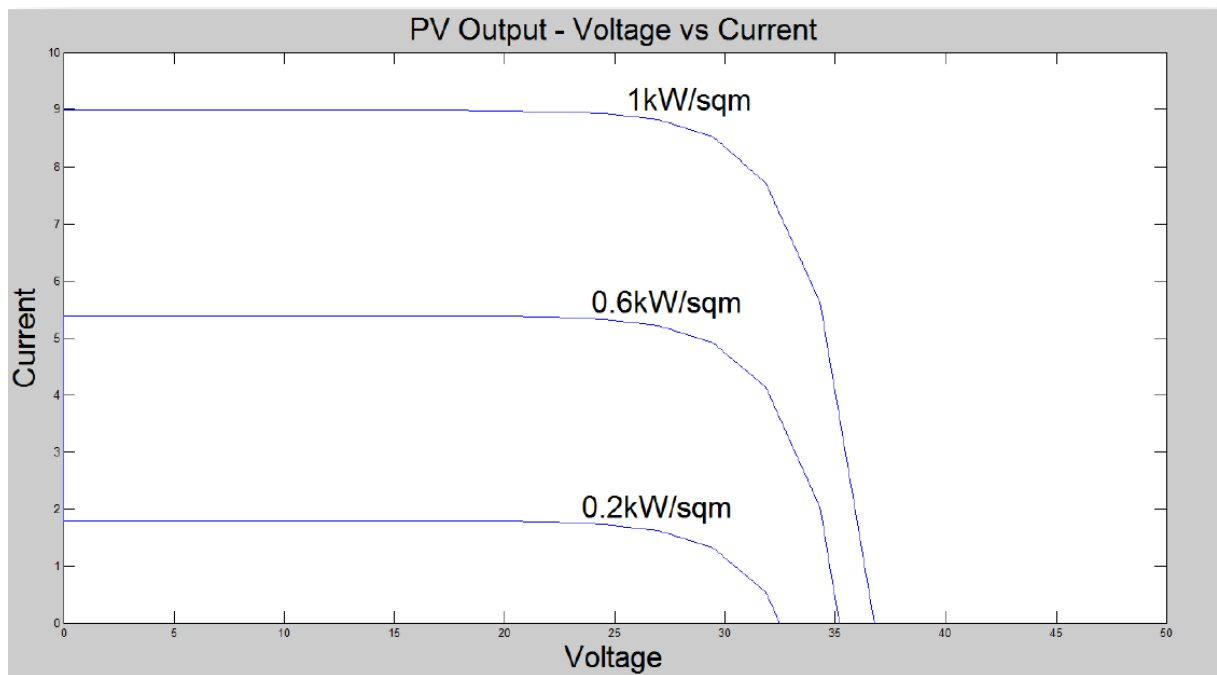


Figure 4-4: Voltage versus current trend for the designed PV model with varying irradiance

In Figure 4-4, the relationship between current and voltage is as follows:

- When the irradiance level is 1kW/m^2 , the voltage versus current trend starts at a higher point, indicating a more significant current flow.
- Lower irradiance levels (0.6kW/m^2 and 0.2kW/m^2) show a reduction in current flow, which is consistent with expectations.

Testing with Varying Temperature

The second set of tests focused on varying the temperature while keeping the irradiance constant. The results for the voltage versus power trend with varying temperature is displayed in Figure 4-5.

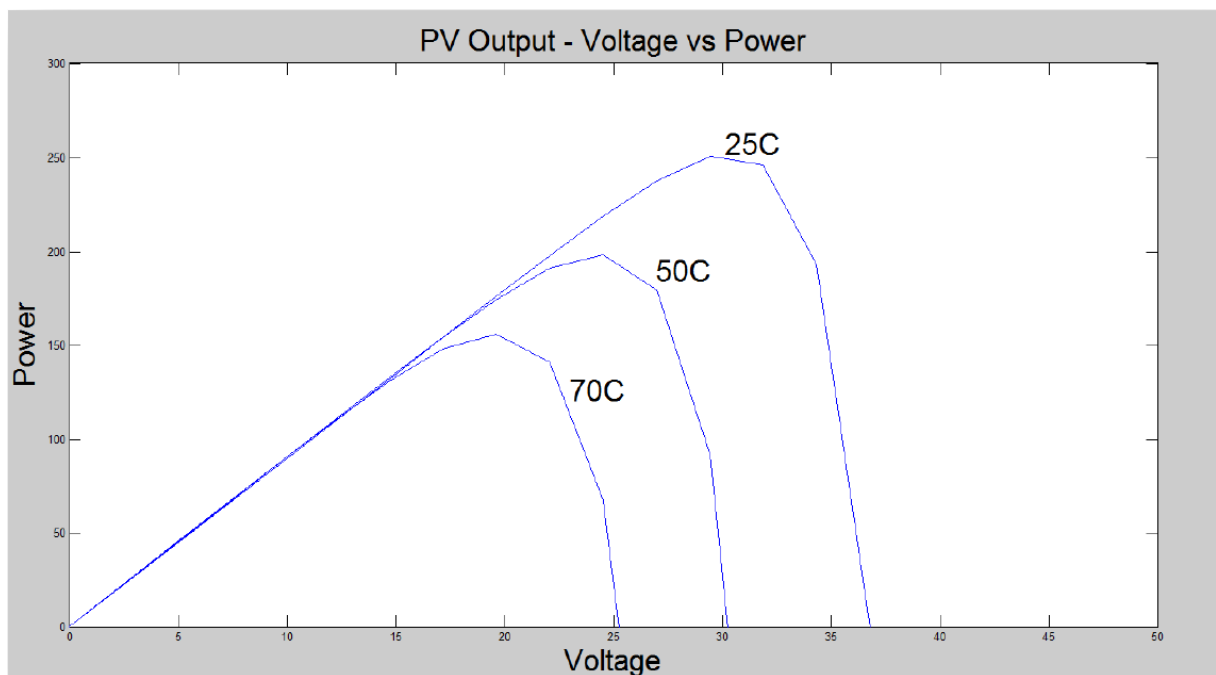


Figure 4-5: Voltage versus power trend of the designed PV model with varying temperature

Observations from Figure 4-5 include:

- When the temperature is 25°C, the voltage versus power relationship reaches a higher peak compared to the results at 50°C and 70°C. This suggests that lower temperatures allow the PV system to operate more efficiently.
- The power output decreases with increasing temperature, reflecting the expected behaviour of PV systems, as higher temperatures typically reduce efficiency.

The voltage versus current trend for varying temperature is represented in Figure 4-6.

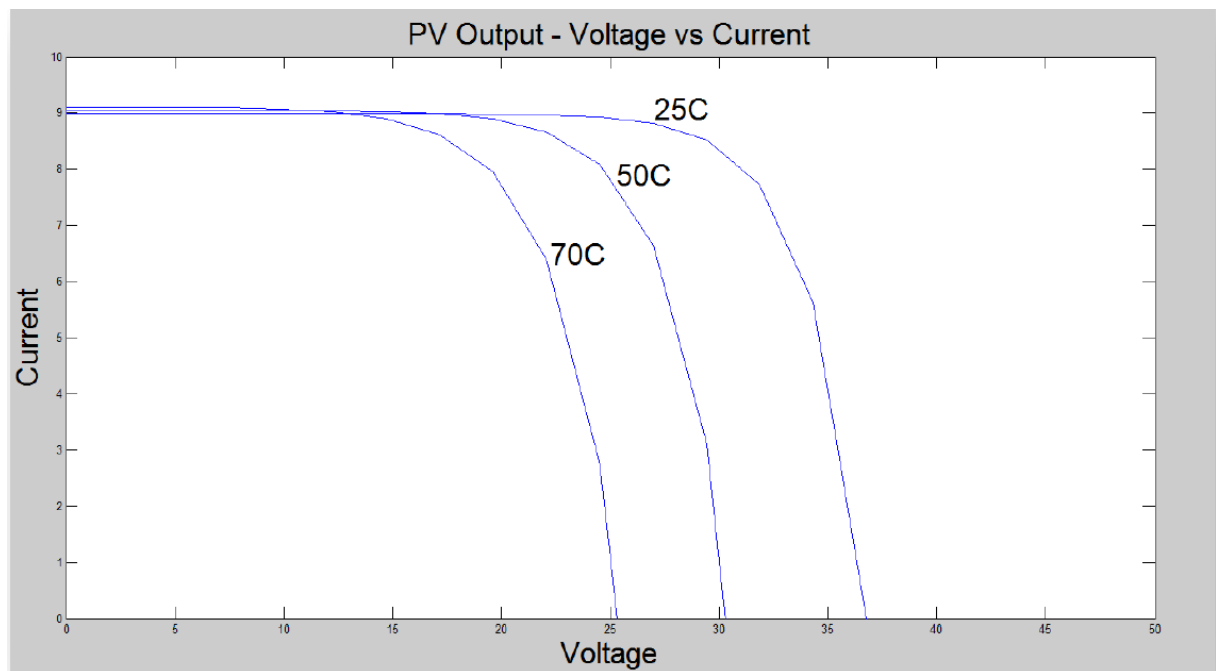


Figure 4-6: Voltage versus current trend for the designed PV model with varying temperature

In Figure 4-6, the following trends are observed:

- At a temperature of 25°C, the voltage versus current relationship starts at a higher point, indicating a stronger current flow.
- At higher temperatures (50°C and 70°C), the voltage and current values decrease, suggesting reduced efficiency due to increased heat.

Evaluation

Overall, results from the designed PV model with variable irradiance and temperature points align with expected trends. Although some inaccuracies may arise due to the chosen parameter values, the results are consistent with known behaviours of PV systems

(Pandiarajan & Muthu, 2011). The impact of the series resistance (R_s) is crucial, as higher values lead to reduced accuracy in outputs.

These findings confirm the satisfactory performance of the designed PV model, providing a reliable basis for integrating the model with the DC/AC PWM converter and other components of the HPS.

4.3 Modelling the Wind System

In this section, the modelling and assumptions for the complete wind system are described. The wind system model for this thesis incorporates a DFIG, implemented using MATLAB Simulink. This model allows for variable speed operation and efficient energy generation, as outlined below.

- Assumptions:

1. **Output Power:** The wind system's output power is assumed to be significant enough to meet the load demand and ensure optimal performance.
2. **Load Demand:** The wind system's output is expected to meet the load requirements.
3. **Synchronous Speed:** The DFIG is assumed to operate at a value slightly higher than synchronous speed, allowing for variable speed control.

4.3.1 Wind System Design

The wind system model chosen for this thesis is depicted in Figure 4-7, showing the DFIG design selected for simulation purposes. This specific implementation allows the wind turbine system to be controlled efficiently.

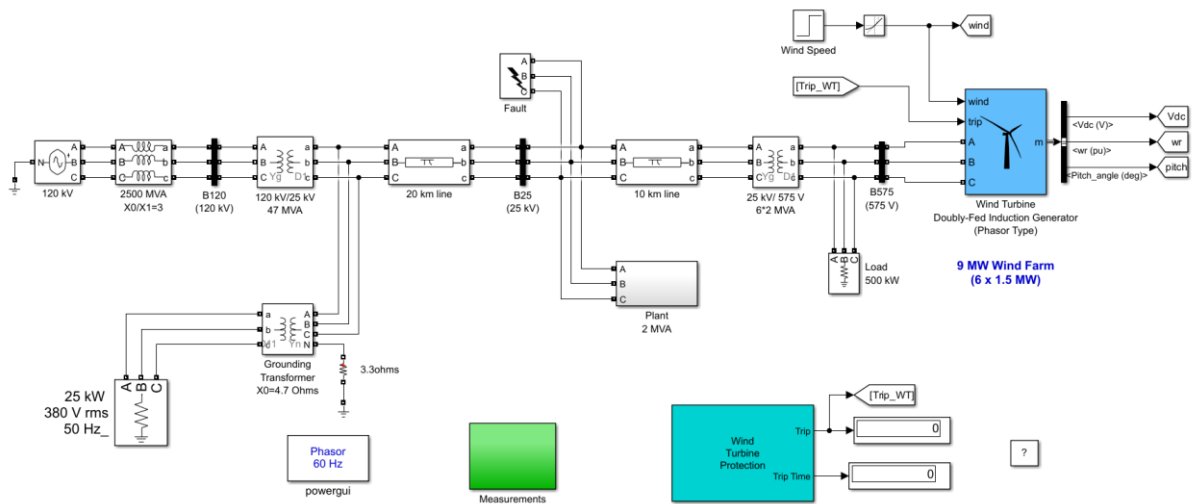


Figure 4-7 The three-phase voltage source connected to the doubly-fed induction generator wind turbine.

The DFIG wind turbine connects to a 500kW load and a 25kV/575V transformer. Additionally, the system includes a 120kV/25kV transformer, which is linked to a 120kV grid through mutual inductance. This connection is established via a 30km transmission line, allowing for effective integration with the larger grid infrastructure.

The wind turbine operates at a frequency of 50Hz and has a capacity of 1.5MW for each turbine, leading to a total capacity of 9MW for the entire wind farm (The MathWorks, Inc., n.d.).

The simulation of the WTDFIG produced results consistent with expected outcomes, indicating that the wind turbine operates as designed. These results are detailed in Chapter 5.

4.3.2 Data Integration and Processing

Due to differences in simulation modes, with the Wind Turbine DFIG model running in phasor mode and the PV and battery models running in discrete mode, data from the wind system is transmitted to the MATLAB workspace.

The internal working system of the wind subsystem captures and processes the wind energy data received from the workspace. This setup ensures that data from the wind energy system is accurately integrated and synchronized with the data from the PV and battery systems within the HPS. By doing so, it facilitates a seamless flow of information across the various components, enabling a more comprehensive and accurate analysis of the overall system performance. Figure 4-8 shows a MATLAB Simulink diagram where data from the workspace is used to generate visuals. This configuration allows data imported from the workspace to be

visualized in real-time on the scope, enabling the monitoring and analysis of the wind subsystem's performance within the HPS.

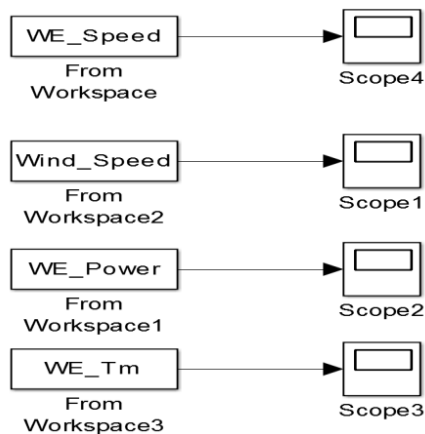


Figure 4-8:The wind equivalent block internal system captures and processes the wind energy data received from the workspace.

4.4 Wind System testing methodology

To validate the wind system performance and ensure its adequacy within the Hybrid Power System (HPS), the Wind Turbine DFIG model, as shown in Figure 4-7, was simulated in phasor mode for a duration of 50 seconds. This duration was chosen to observe the system's response to varying wind conditions and determine its stability and reliability.

4.4.1 Test Setup and Results

The wind system was subjected to a step input with a starting wind speed at 8m/s and increased by 1m/s every second, reaching 14m/s over a duration of 10 seconds. This step input allowed for the examination of the Wind Turbine DFIG's behaviour under changing wind conditions, providing insights into its dynamic response.

The figures in 4-9 and 4-10 displays the simulation results, demonstrating the expected performance for the Wind Turbine DFIG in terms of DC link voltage (Vdc), wind speed, rotor speed, pitch angle, and other grid-related measurements.

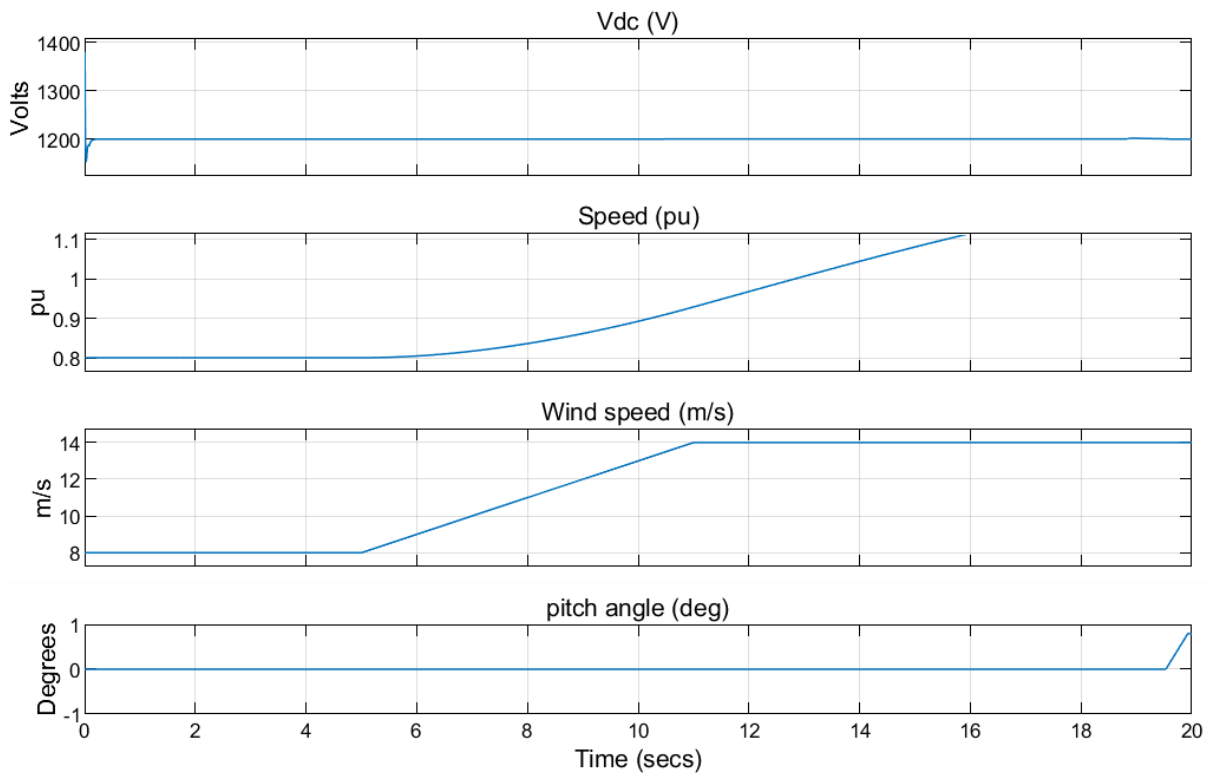


Figure 4-9 Simulated outputs of the DFIG wind turbine, showing DC link voltage (Vdc), rotor speed, wind speed, and pitch angle in response to a step input, where wind speed increases from 8 m/s to 14 m/s over 10 seconds.

In Figure 4-9a, the results show that the DC link voltage (Vdc) remains stable throughout the simulation. This stability indicates that the Wind Turbine DFIG's control system effectively manages the variable wind speeds without causing significant voltage fluctuations. Additionally, in figure 4-9b the speed of the rotor increases as the speed of the wind rises, which demonstrates the Wind Turbine DFIG's ability to operate effectively at variable speeds. In figure 4-9d the pitch angle also adjusts in response to the changing wind speed, highlighting pitch effectiveness of the control system in regulating the turbine's performance. Lastly, in figure 4-9c the wind speed increase is consistent with the step input applied during the simulation, reflecting the accurate modelling of wind speed variations.

The simulation results confirm that the Wind Turbine DFIG maintains stability and performs as expected under varying wind conditions. Additionally, the grid data acquisition results provide further insights into the interaction between the Wind Turbine DFIG and the grid, as displayed in Figure 4-12.

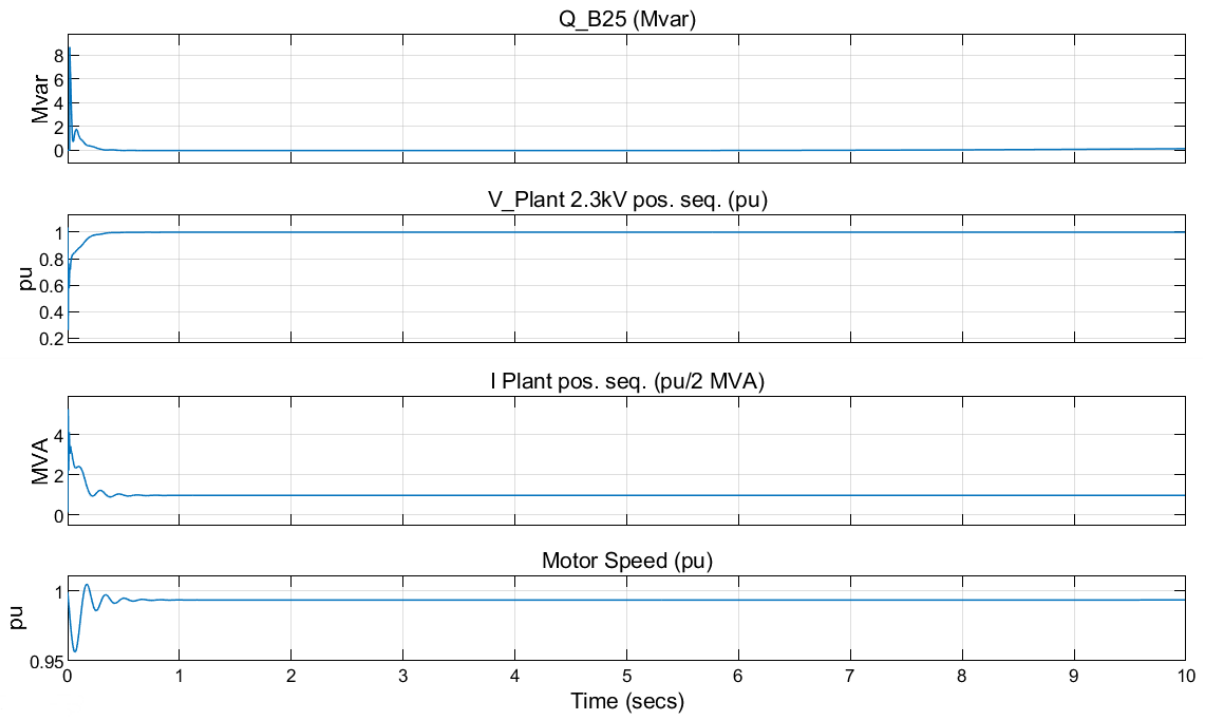


Figure 4-10 Grid data acquisition results, showing reactive power, positive sequence voltage and current of the plant, and motor speed of the DFIG wind turbine, highlighting its interaction with the grid.

In Figure 4-10a, the reactive power output remains within the expected ranges, which indicates that the Wind Turbine DFIG's control system effectively manages the grid reactive power exchange. Additionally, in figure 4-10b and figure 4-10c, the plant's voltage and current maintain a stable positive sequence, suggesting that the Wind Turbine DFIG operates without introducing significant disturbances to the grid. Furthermore, the motor speed mirrors the rotor speed observed in Figure 4-10d, confirming the turbine's responsiveness to varying wind conditions.

These results justify the wind system performance and confirm its stability when subjected to varying wind speeds. The data acquired during the simulation provides a comprehensive understanding of the wind system's behaviour and its interaction with the grid, ensuring that the Wind Turbine DFIG can meet the HPS's load requirements while maintaining stability and reliability.

4.5 Battery Storage Unit Modelling

The following assumptions are made regarding the operation of the battery storage unit within the Hybrid Power System (HPS):

1. The battery has the capacity to meet load demand during discharge.
2. The battery charges up to its maximum capacity and can reliably power the load when needed.
3. The battery operates consistently under steady-state conditions.

4.5.1 Battery Model Design

The battery storage model applied in this study is a modified version of the Lead-Acid model from MATLAB Simulink, adapted to represent a Lithium-Ion battery (The MathWorks, Inc., n.d.). The original MATLAB Simulink model was adjusted to match the specific requirements of this study. The results from the simulation of the modified battery model confirmed satisfactory performance, as detailed in Chapter 5. Figure 4-11 shows the MATLAB Simulink lithium-ion battery model.

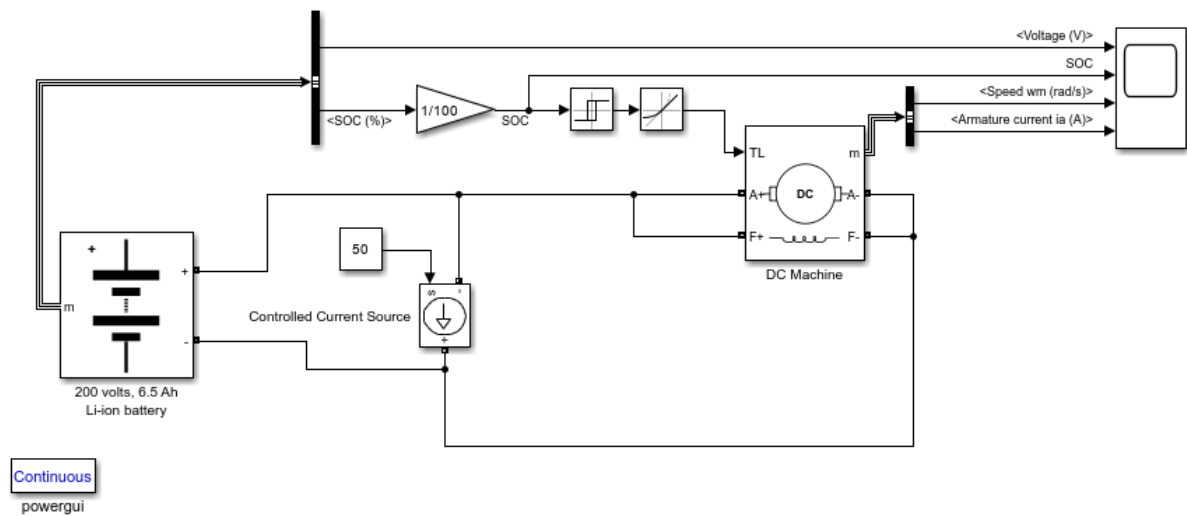


Figure 4-11 Model of the Lithium-Ion battery used in Simulink

To maintain the State of Charge (SOC) above 0.2, a -200 Nm mechanical torque is applied to the machine, causing it to act like a generator and produce 100 amps. This arrangement enables the load to be supplied with 50A while the remaining 50A are used for recharging the battery. Once the SOC gets to 0.8, indicating sufficient charge, mechanical torque is eliminated, allowing free operation of the machine. This cycle repeats until the simulation is completed.

storage unit is vital to the overall HPS design, providing flexibility and backup power to ensure consistent energy supply.

4.6 Battery Model Testing Methodology

This segment provides the obtained results by simulating the integrated AC/DC/AC PWM converter and Lithium-Ion battery model within the Hybrid Power System (HPS). The simulation aims to assess the battery model's response and performance based on State of Charge (SOC) and armature current when subjected to varying load conditions.

To conduct the simulation, the battery model was connected to the AC/DC/AC PWM converter with a load, representing the HPS's typical operation. The simulation was run for a duration of 10 seconds, and the outputs from the battery model were recorded to assess its behaviour during this period.

Figure 4-14 below shows the initial setup for the simulation, illustrating the connection between the battery model, AC/DC/AC PWM converter, and load:

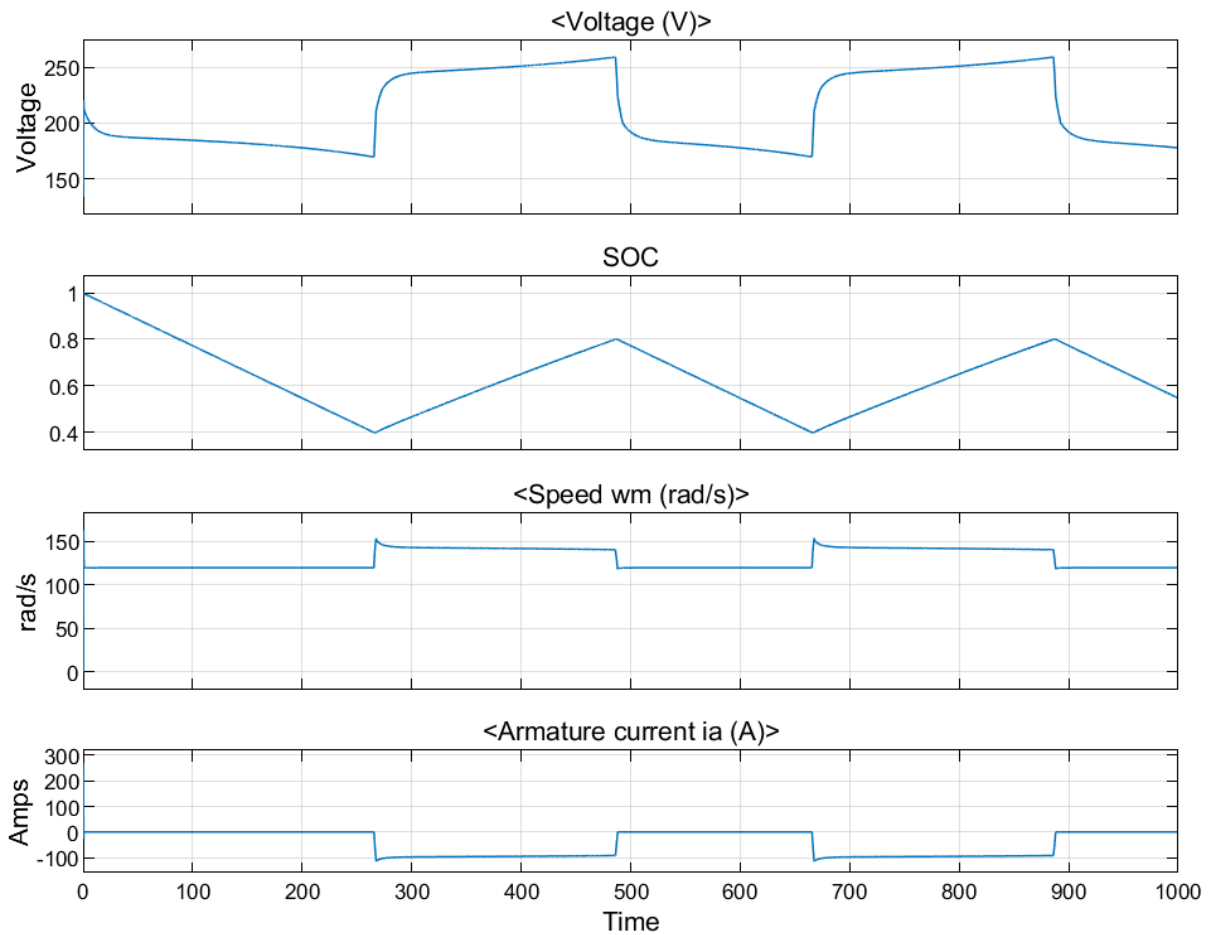


Figure 4-14 Battery model output when connected to AC/DC/AC PWM converter with load

To ensure the simulation results aligned with expected outcomes, the battery model's specifications were adjusted to produce the result shown in Figure 4-14. The adjustment involved fine-tuning the battery model's specifications, like the capacity, state of charge (SOC) limits, and discharge rates, to ensure that the simulation accurately reflected the expected performance of a Lithium-Ion battery within the HPS. These modifications were essential to align the simulation with the specific requirements and operational dynamics of the HPS design.

4.6.1 Test Results

The figures below display the simulation outcomes, focusing on the SOC levels and armature current outputs for the 10-second simulation.

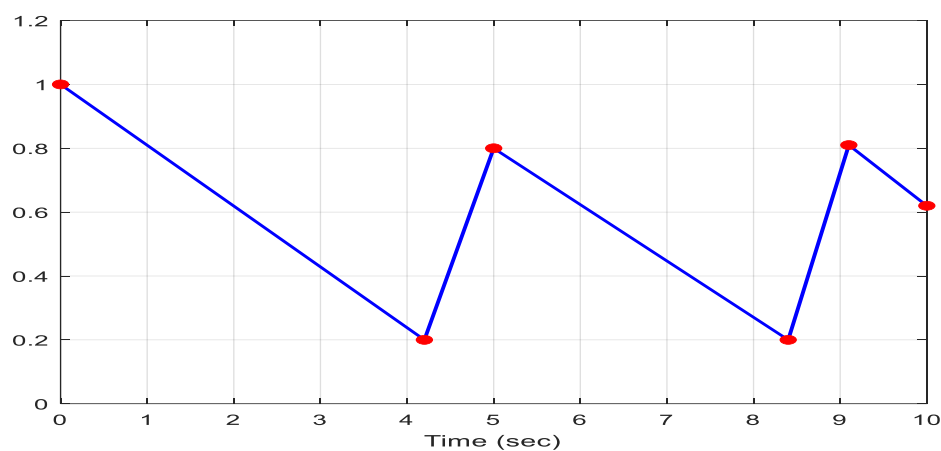


Figure 4-15 Modified SOC levels for a 10-second simulation in the equivalent battery model integrated into the HPS.

Figure 4-15 shows the SOC levels during the simulation. The results indicate that the SOC remained above the minimum threshold, confirming the battery's ability to maintain an adequate charge level during the simulation. This observation aligns with the expected Lithium-Ion battery model's behaviour.

The following figure demonstrates the armature current output from the battery during the 10-second simulation: (Note: The y-axis represents the armature current).

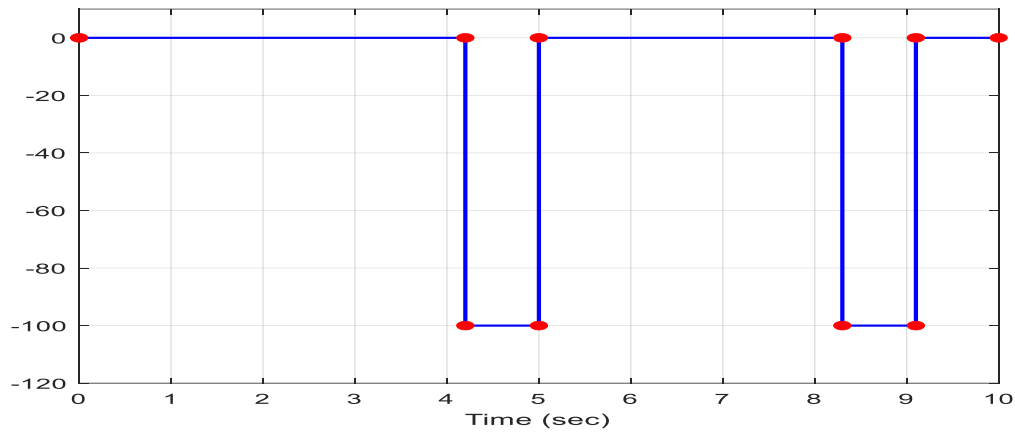


Figure 4-16 Modified armature current output for the 10-second simulation in the equivalent battery model integrated into the HPS

In Figure 4-16 the armature current output is depicted along the y-axis, showing the current fluctuations during the simulation. The results indicate that the armature current remained within the expected range, suggesting stable operation of the battery model during the 10-second simulation.

Overall, these results validate the battery model's performance and its integration into the HPS. The observed trends for SOC levels and armature current outputs confirm that the battery model can supply the load while maintaining a stable charge level, meeting the design requirements of the HPS.

4.7 Modelling the Event-Based Controller for the Hybrid Power System (HPS)

The controller for the HPS is vital in managing the sources of energy to ensure stable and efficient operation. The design and simulation of the controller in MATLAB Simulink are based on specific assumptions regarding its functionality and interactions with the PV, wind, and battery storage units.

Assumptions for the Event-Based Controller Model:

1. At any given moment, only one energy source will supply the load, allowing the controller to assign a single source based on its availability and system conditions.
2. The controller has the authority to determine when the battery should be charged, ensuring efficient utilization of renewable energy and preventing overcharging.
3. The controller operates continuously under steady-state conditions, maintaining consistent control over the energy sources and battery storage.

The event-based controller's design approach leverages MATLAB Simulink's library components to implement the desired functionality. The algorithm guiding the controller's

operation, as detailed in Chapter 3, outlines the flow of control decisions to manage the HPS effectively. This design ensures that the controller can make decisions in real-time based on the system's state and resource availability.

Figure 4-17 below depicts the MATLAB Simulink schematic for the designed controller, showing its various components and the connections to the PV, wind, and battery storage systems:

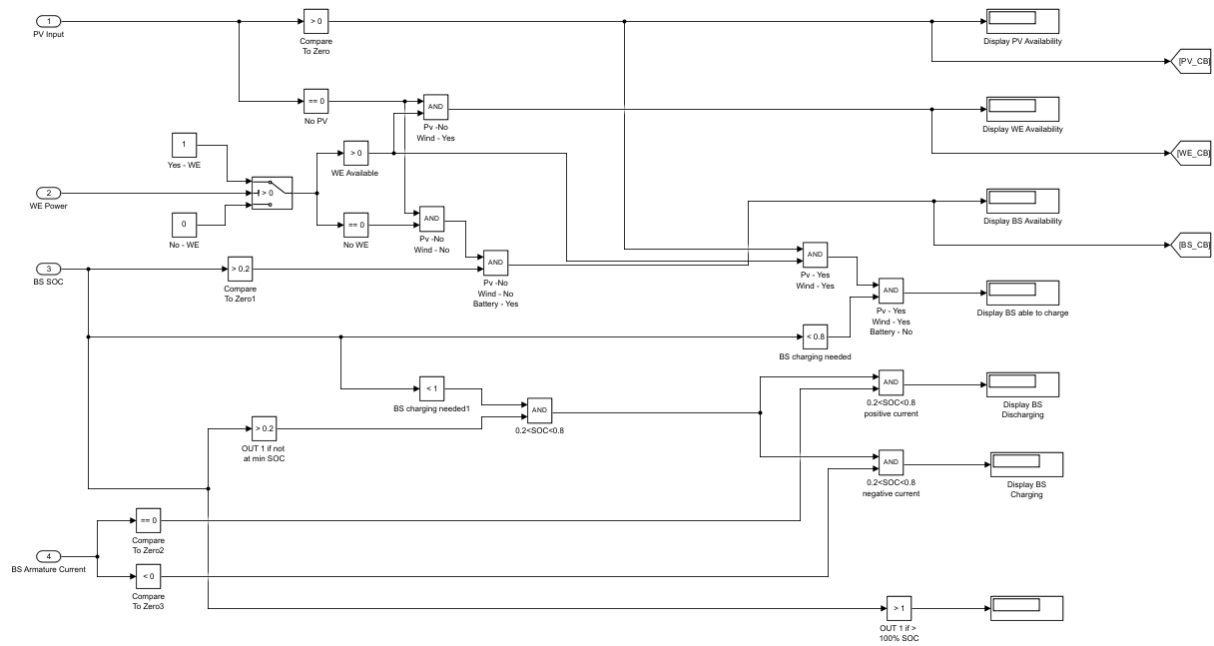


Figure 4-17 Simulink schematic of the event-based controller

The controller continuously monitors the status of the HPS, receiving inputs from the PV, wind, and battery storage systems. Based on these inputs, it determines which energy source is available and can supply the load. The controller then sends signals to the appropriate circuit breakers to open or close as needed, ensuring a seamless transition between energy sources.

An important aspect of the controller's functionality is the monitoring of the battery storage unit's SOC. The controller is designed to prevent overcharging by triggering an alert if the SOC exceeds a predefined threshold. Additionally, the controller displays the battery's charging and discharging processes, providing battery status insights and its role within the HPS.

The controller's operation is guided by a simplified algorithm implemented in MATLAB Simulink, ensuring robustness and reliability in its decision-making process. This design approach facilitates seamless integration with the rest of the HPS components and allows for easy modifications and scalability to meet future requirements.

Overall, the controller's design and simulation in MATLAB Simulink demonstrate its effectiveness in managing the Hybrid Power System, providing a stable and reliable solution for energy resource allocation and battery storage monitoring.

4.8 Modelling the Entire Hybrid Power System (HPS)

To successfully integrate the Photovoltaic (PV), wind, and battery storage units into a complete Hybrid Power System (HPS), specific design adjustments were made to combine these components and ensure a reliable supply of power to the load.

Assumptions for the HPS:

1. The energy generated from renewable resources is abundant to meet the power requirements of the load.
2. The integrated battery in the HPS can supply the load when it discharges.
3. The output from the HPS is adequate for the load demand to be met.
4. The HPS operates consistently under steady-state conditions.

The design of the HPS in MATLAB Simulink involves combining equivalent systems and ensuring seamless data integration from each subsystem. The following assumptions and design considerations were made to create the HPS model:

1. **Battery Storage Unit Simulation:** The battery storage unit was simulated as signal generators to generate the necessary outputs for the controller's operation. The integration of the Lead-Acid battery design with the AC/DC/AC PWM converter required a longer battery simulation time compared to the PV and wind simulation times, which presented challenges during the integration of all three systems in MATLAB Simulink.
2. **Wind System Simulation:** The DFIG was simulated separately using Simulink, while results were stored in the MATLAB workspace. This data was later retrieved and incorporated into the hybrid power system MATLAB file
3. **PV System Integration:** The PV system was integrated into the same MATLAB file as the controller, as it did not face compatibility issues.

Figure 4-18 below illustrates the integrated HPS Simulink design.

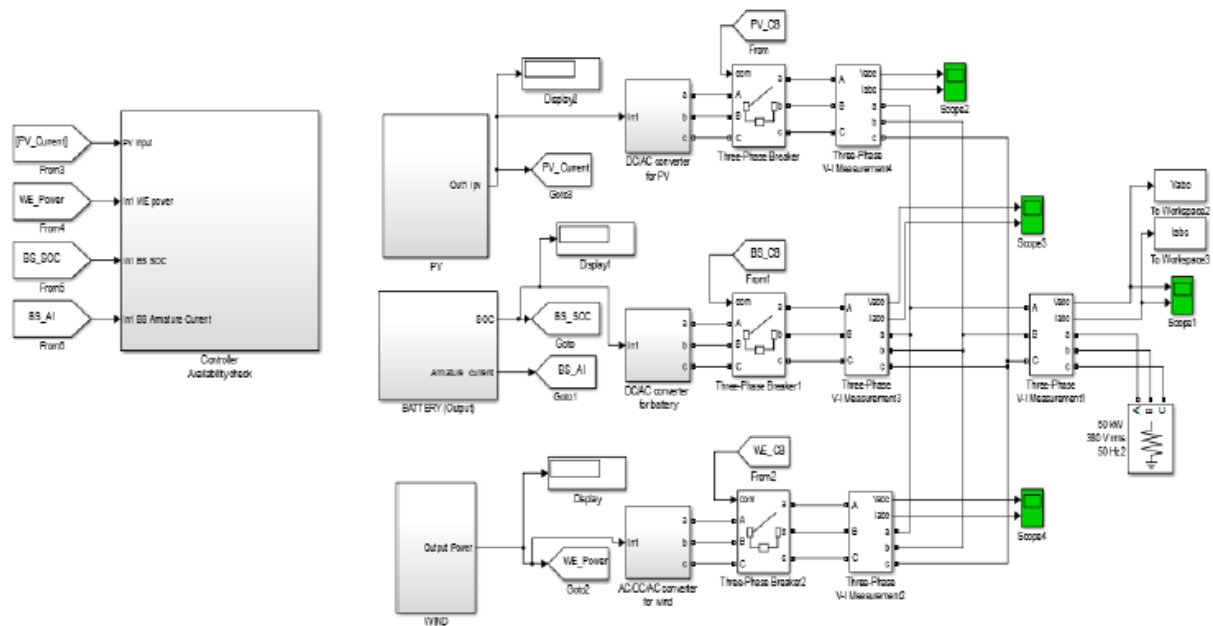


Figure 4-18: Hybrid Power System (HPS) Simulink design showing the PV system, wind system, battery storage, controller, and load interconnected.

In Figure 4-18, the V-I measurement blocks are interconnected to form the AC bus, establishing the HPS connection and the load. With voltage regulators integrated within the AC/DC/AC PWM converter subsystem blocks, the network is designed to allow the PV module and wind generator to harness solar and wind energy, respectively, when these resources are available. When these systems can generate energy, they signal the respective circuit breakers to close, supplying energy to the load.

Conversely, when solar and wind resources are unavailable, and the systems cannot generate energy, the controller receives signals indicating the inability to supply energy to the load. The controller then sends a signal to the circuit breaker to remain open, indicating that no energy is being supplied.

Monitoring the battery's SOC level, the controller assesses the battery's capacity to supply the load. If the SOC is 80%, it indicates that the battery can discharge and supply the load. If the SOC is 20%, it indicates the battery is depleted and cannot supply the load. The controller continuously evaluates each system's status, searching for available sources to supply the load, and sends appropriate signals to circuit breakers to manage the energy flow.

CHAPTER FIVE: DISCUSSION OF RESULTS

5.1 Introduction

Chapter 5 builds upon the analyses depicted in Chapter 4, focusing on the findings from the simulation and evaluation of the HPS model, which integrates PV, wind, and battery storage components. The primary focus is on evaluating the performance of the HPS under various scenarios, which include different availability conditions of each energy resource. Detailed results from the MATLAB Simulink simulations are provided to illustrate the efficiency of the energy management controller developed. The results are analysed to determine the system's efficiency, reliability, and capability to meet load demands. This chapter aims to validate the design and implementation of the HPS and the event-based controller, highlighting key performance metrics and identifying any areas for further improvement.

5.2 PV Model Results in the HPS

The following figures confirm the accuracy of the PV model operation within the Hybrid Power System (HPS). Figures 5-1 and 5-2 illustrate the signals produced by the simulation of the PV model while connected to the AC/DC/AC converter. In this configuration, the AC/DC section represents an equivalent PV system, allowing for seamless integration under varying irradiance (G) and constant temperature (T):

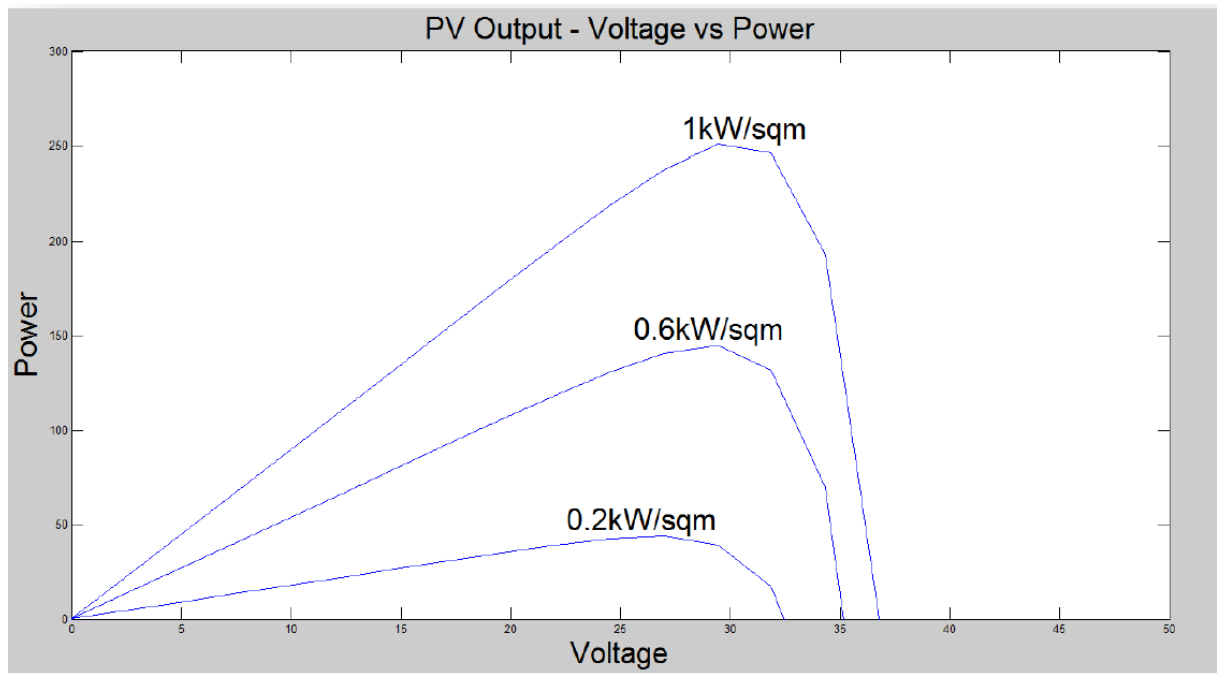


Figure 5-1: Voltage vs. Power for PV model integrated with DC/AC converter

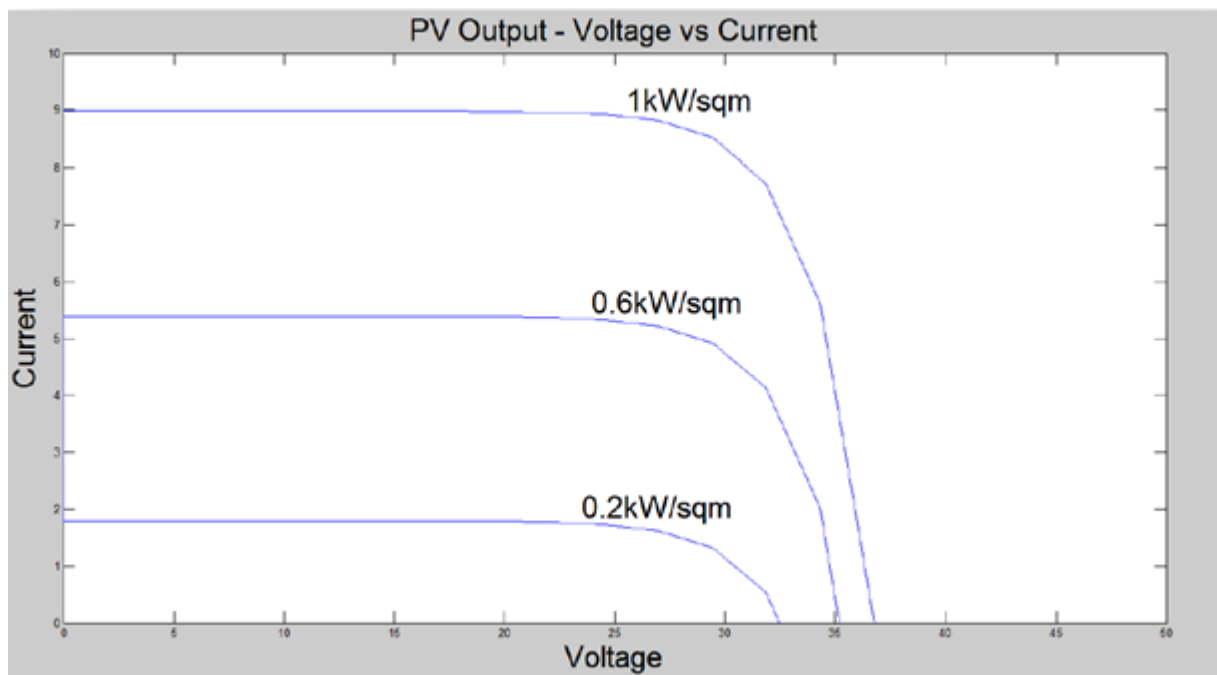


Figure 5-2: Voltage vs. Current for PV model integrated with DC/AC converter

Figures 5-3 and 5-4 demonstrate the signals produced by the same simulation of the PV model, again connected to the AC/DC/AC converter. This time, the AC/DC section represents an equivalent PV system under constant irradiance (G) and varying temperature (T):

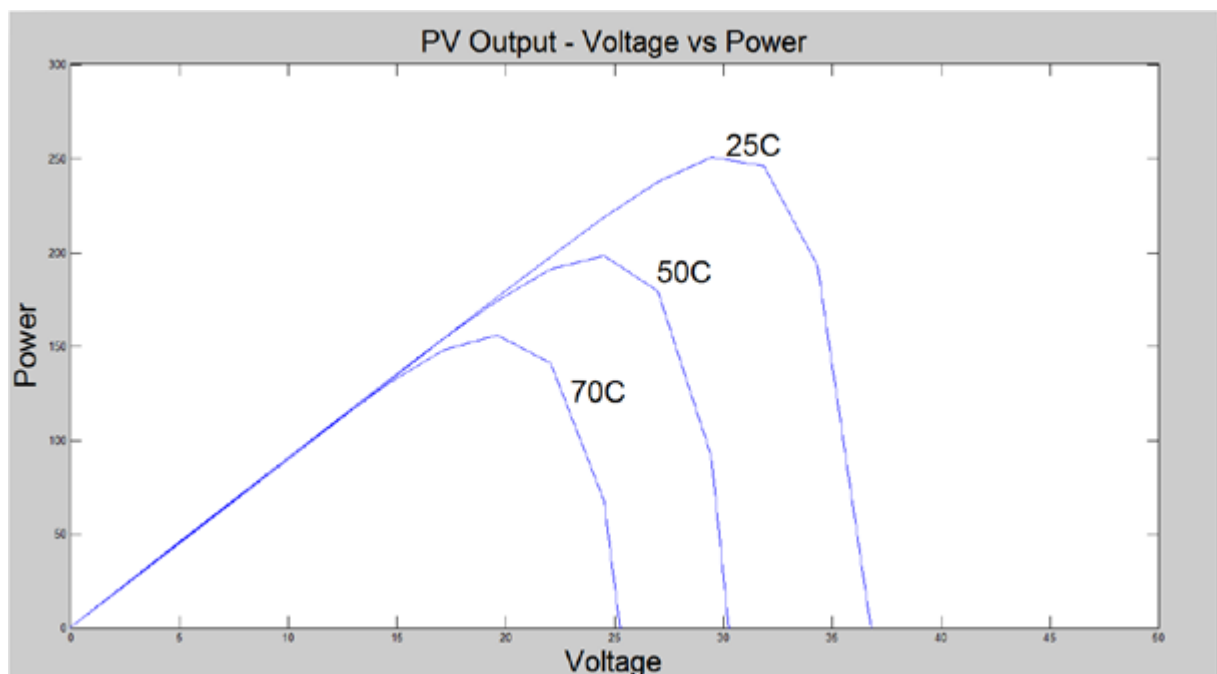


Figure 5-3: Voltage vs. Power output for PV model integrated with DC/AC converter

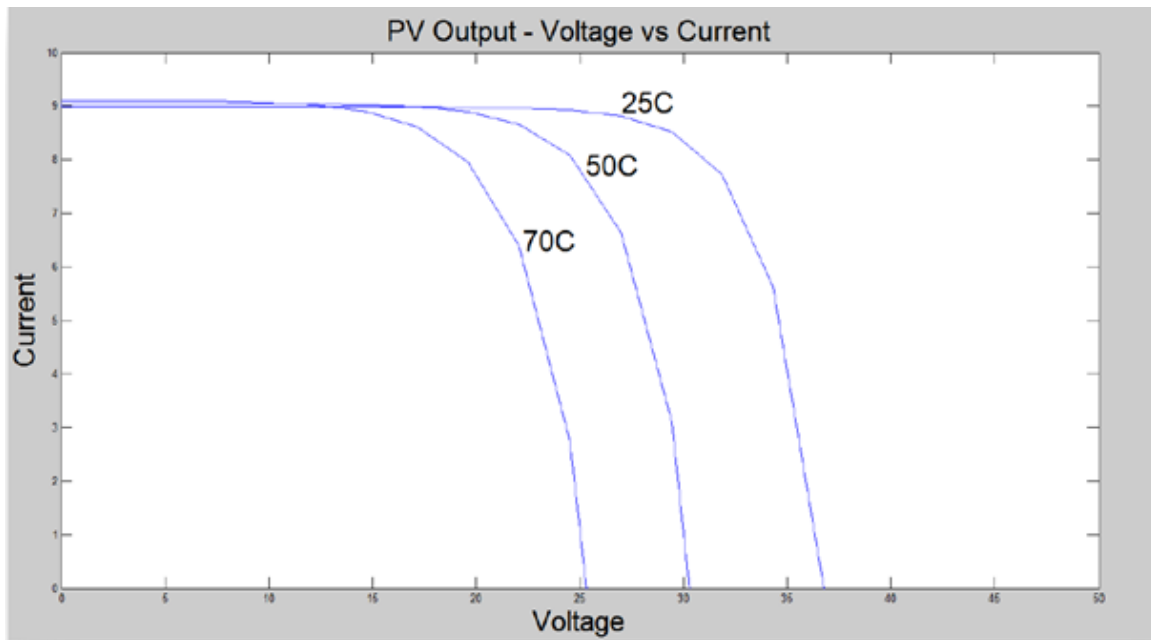


Figure 5-4: Voltage vs. Current output for PV model integrated with DC/AC converter

The fill factor (FF) is a crucial constraint in assessing the performance of a photovoltaic (PV) cell. It is expressed as the ratio of the maximum power point (MPP) power ($V_{MPP} * I_{MPP}$) to the open-circuit voltage (V_{OC}) product and the short-circuit current (I_{SC}). The higher the fill factor, the more efficient the PV cell, as it represents the squareness of the I-V curve. In this study, the fill factor technique was used to assist in identifying and displaying the MPP for the PV model in varying irradiance conditions. The results obtained using this technique are displayed in figures 5-5 and 5-6 receptively below:

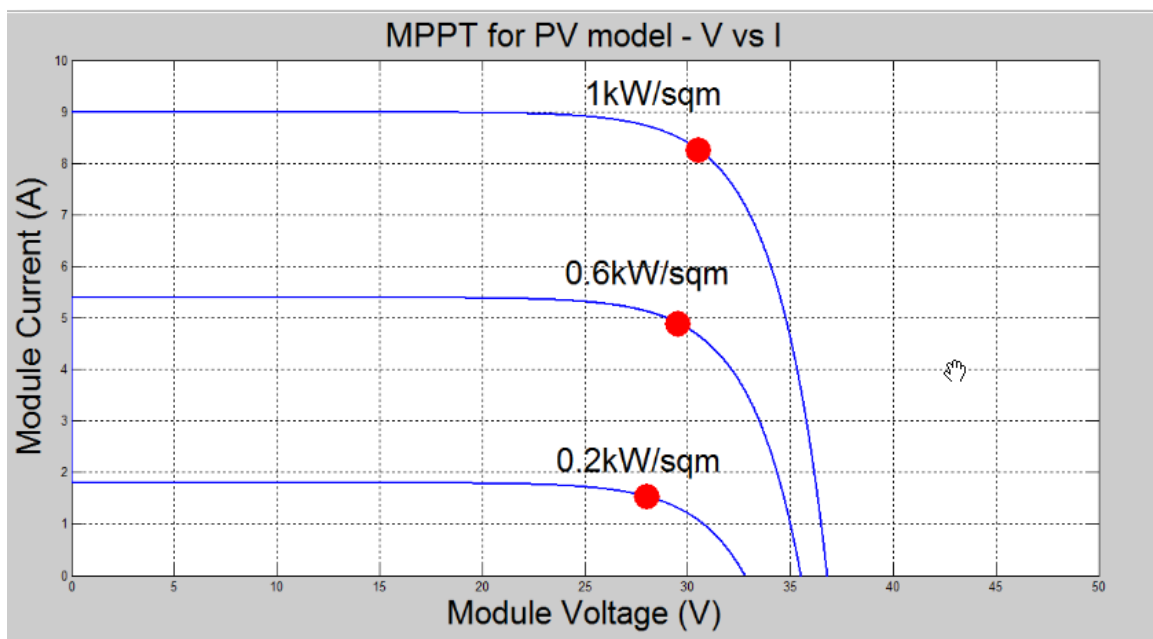


Figure 5-5: Ideal tracking of MPPT points for Voltage vs. Current output for the PV model resulting in optimal performance with maximum output

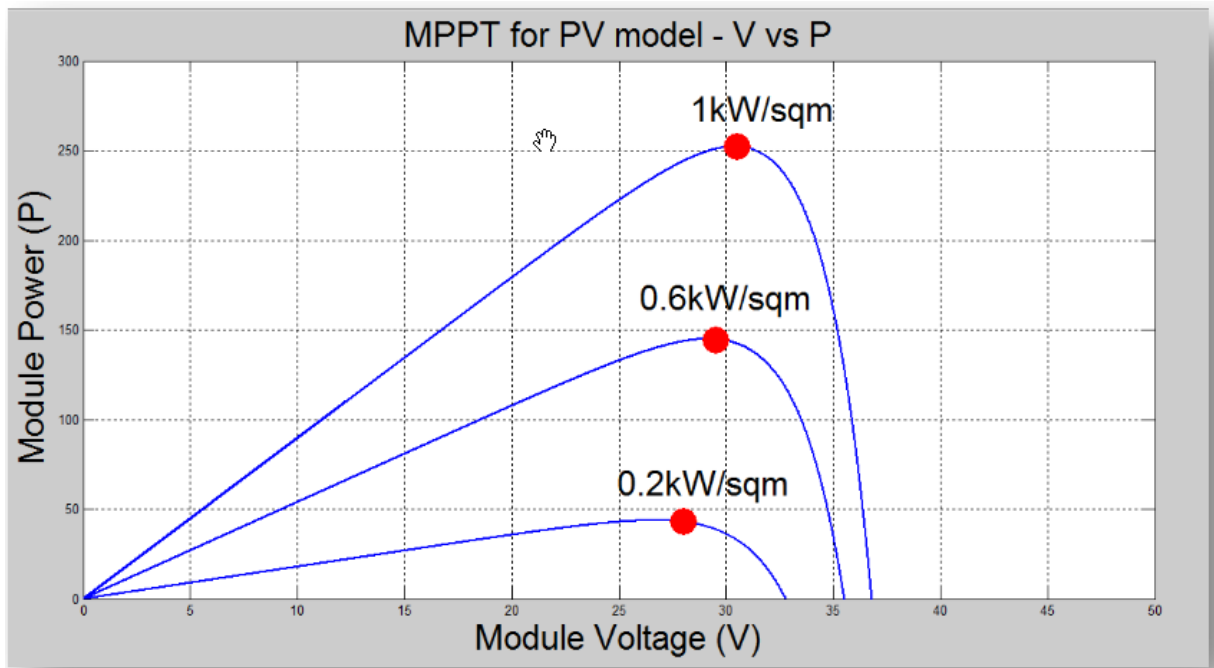


Figure 5-6: Ideal tracking of MPPT points for the Voltage vs. Power output of the PV model resulting in optimal performance and maximum power output

When the PV model was unavailable to supply the load, the following result in figure 5-7 was observed at the AC/DC/AC PWM converter with the PV model equivalent system:

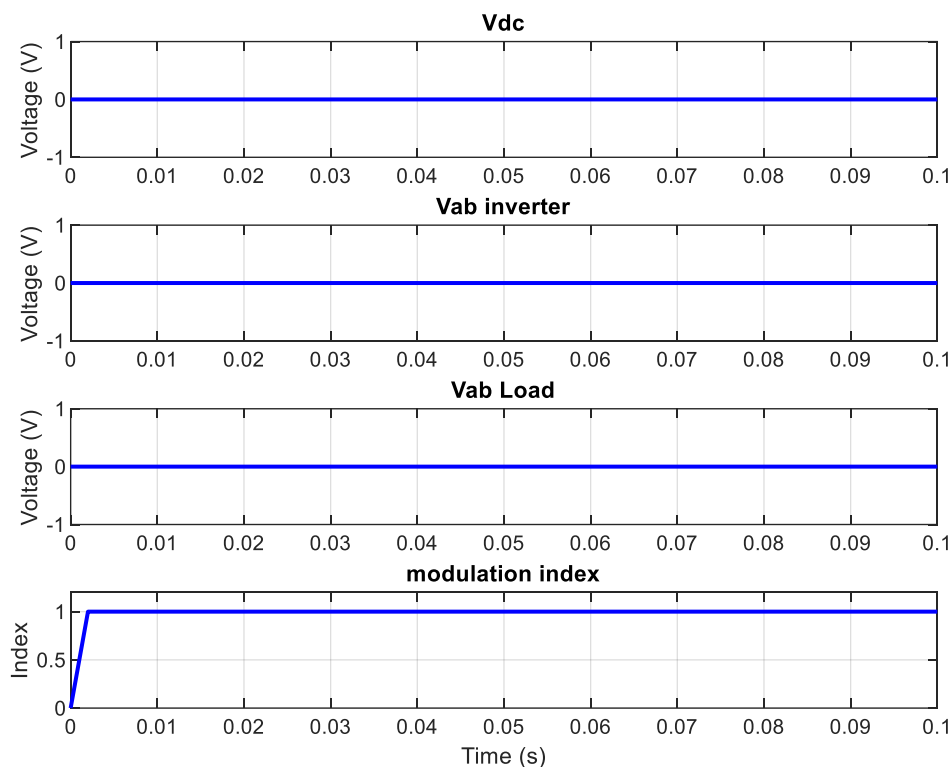


Figure 5-7: Display on the AC/DC/AC PWM converter with the PV model equivalent when the PV model is not available for supply

5.3 Results of the Battery Storage Unit in the HPS

The equivalent model was simulated using the inputs displayed in Figures 4-15 and 4-16, producing the following results.

During the first 5 seconds of this simulation test, the battery was discharging, and the result for the PWM converter is displayed in Figure 5-8:

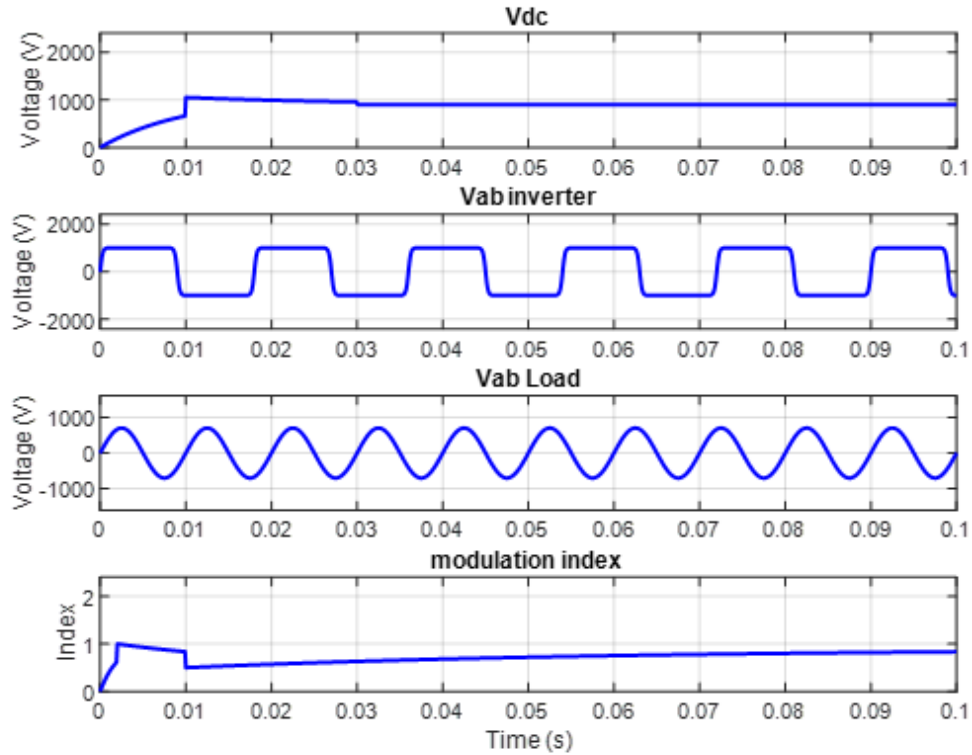


Figure 5-8: The PWM converter's operation during discharging of the Lithium-Ion battery model equivalent.

At 4.27 seconds, the SOC hit the 0.2 limit, and the battery transitioned into the charging phase. The PWM converter result during this phase is displayed in Figure 5-9:

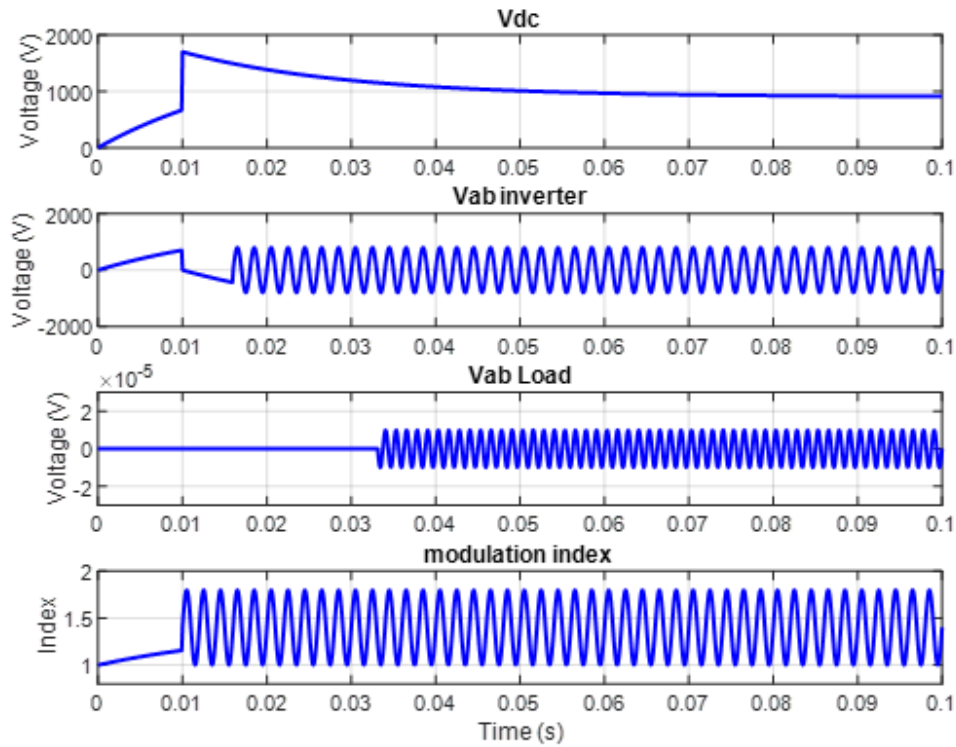


Figure 5-9: The PWM converter's operation during the charging of the Lithium-Ion battery model equivalent.

5.4 Results of Controller Monitoring the Availability of Each Source Supply

This segment offers the effectiveness of using the event-based controller in managing the HPS by monitoring the availability of each energy source—photovoltaic (PV), wind, and battery storage—and ensuring optimal energy distribution based on real-time conditions.

The primary function of the controller is to dynamically allocate available energy sources to satisfy the demanded load efficiently. Throughout the simulation, the controller successfully monitored the status of each energy source, evaluated their availability, and made decisions to prioritize the most effective use of the available resources. The displays indicate a "1" for the eight scenarios when the controller detects the source is available and selects it to supply the load. The following scenarios highlight how the controller managed the energy within the system:

CASE 1: Zero supply (scenario 000)

In this scenario, no source is available to satisfy the demanded load. The zeros in indicate that all three-phase circuit breakers remain open, and there is no supply to the load.

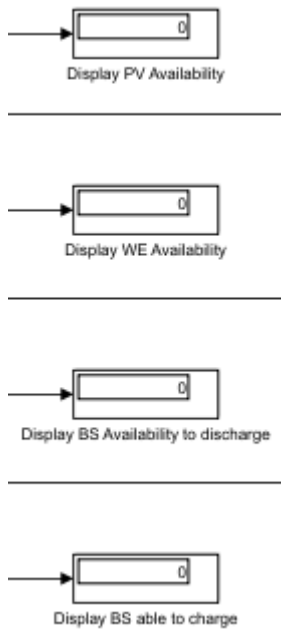


Figure 5-10: Output of controller for CASE 1 illustrating that no source is available to supply the load.

CASE 2: No sun, no wind, only battery storage (scenario 001)

The display below shows that the battery is available for discharge, while the PV and wind energy sources cannot satisfy the demanded load. This is consistent with CASE 2 expectations, forcing the battery to discharge. The display result "1" is sent to the three-phase circuit breaker accountable for connecting the battery storage unit to the load, enabling the circuit breaker to close and discharge the battery into the load. If the circuit breakers for the wind or PV systems were closed, the display result would be sent to the respective breakers to open them.

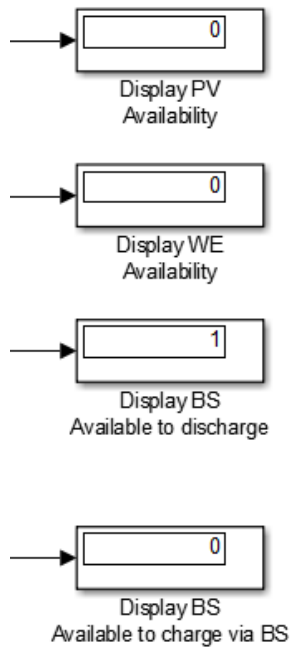


Figure 5-11: The output of the controller for CASE 2 illustrating the battery is discharged to supply the load.

CASE 3: No sun, no battery storage, only wind energy (scenario 010)

The display of "1" indicates that the controller has identified the wind energy scheme as available to supply the load, which matches CASE 3 expectations. This result is sent to the three-phase circuit breaker responsible for connecting the wind energy scheme to the load, enabling it to close and supply the load. If the circuit breakers for the PV system or battery storage were closed, the display result would be sent to the respective breakers to open them.

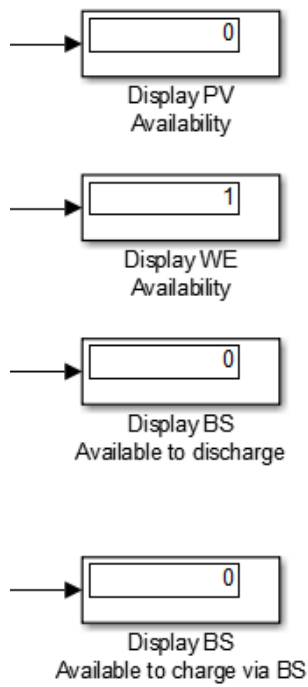


Figure 5-12: The output of the controller for CASE 3 illustrating that the wind energy system supplies the load.

CASE 4: No sun, only wind energy and battery storage available (scenario 011)

In this scenario, even though the battery storage unit is available for discharge, the wind energy scheme is selected for load supply to preserve the stored battery energy. The displays indicate the controller's decision that the wind energy scheme will solely supply the load. This result is sent to the three-phase circuit breaker connecting the wind energy scheme to the load, enabling it to close and supply the load. If the circuit breaker for the PV system was closed, the display result would be sent to open the respective breaker.

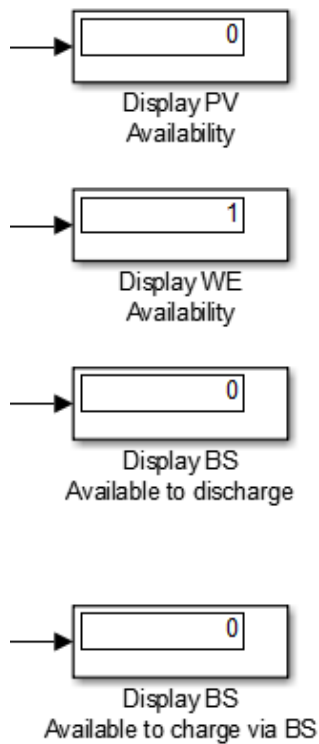


Figure 5-13: The output of the controller for CASE 4 illustrating that the wind energy system supplies the load.

CASE 5: No wind, no battery, PV available (scenario 100)

In this scenario, the PV system supplies the load as previously stated. The display indicates that the controller has determined that the load can be supplied by the PV system. This result is sent to the circuit breaker connecting the load to the PV system, enabling it to close and supply the load. If the circuit breakers for the wind energy or battery storage schemes were closed, the display result would be sent to open the respective breakers.

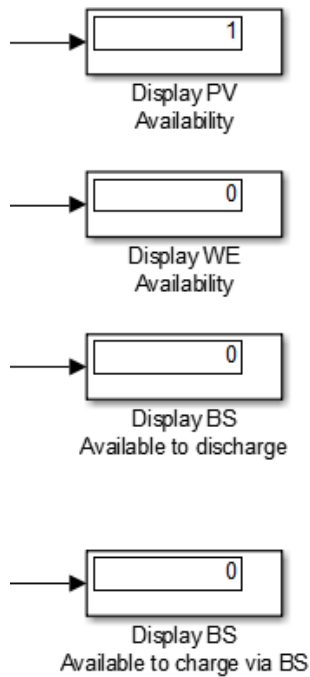


Figure 5-14: The output of the controller for CASE 5 illustrating that the PV system supplies the load.

CASE 6: No wind, only battery storage and PV available (scenario 101)

In this scenario, the controller decides that although the battery storage unit can supply the load, the PV system will be used instead to prevent wasting available solar energy. The display below shows the controller's decision, which is sent to the three-phase circuit breaker responsible for connecting the load to the PV system. The load demand will be met by the PV system. If the circuit breakers for the wind energy or battery storage schemes are closed, the result on the display will be sent to open the respective circuit breakers.

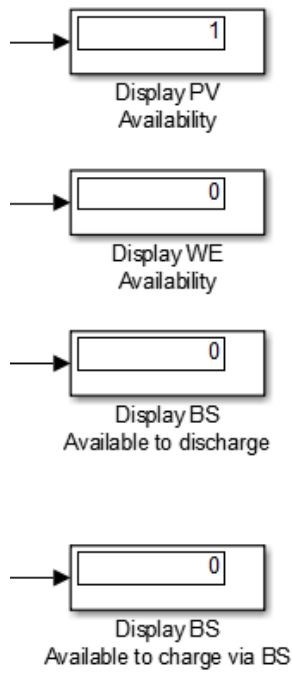


Figure 5-15: The output of the controller for CASE 6 illustrating that the PV system supplies the load.

CASE 7: No battery storage, only PV and wind available (scenario 110)

In this case, the PV system and wind energy scheme can supply the load, but the battery storage is depleted. The controller allocates the PV system to supply the load whilst the depleted battery is charged by the wind energy scheme. The display indicates that the load will be supplied by the PV system, while the wind energy scheme charges the battery, as discussed in a prior section of this thesis.

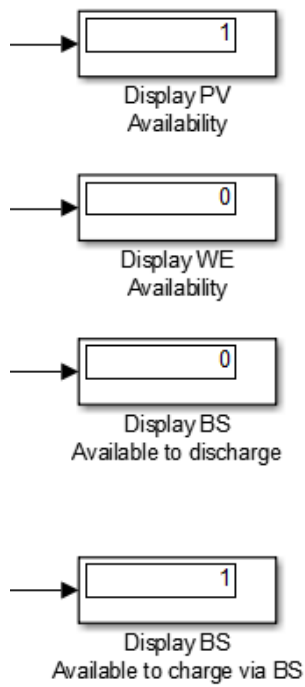


Figure 5-16: The output of the controller for CASE 7 illustrating that the battery will charge via the wind energy system while the PV system supplies the load.

CASE 8: All three resources are available (scenario 111)

In this scenario, all three resources are available to supply the load. The display shows the controller has chosen the PV system to supply the load. This scenario may result in wasted wind energy, as the available wind energy is not utilized.

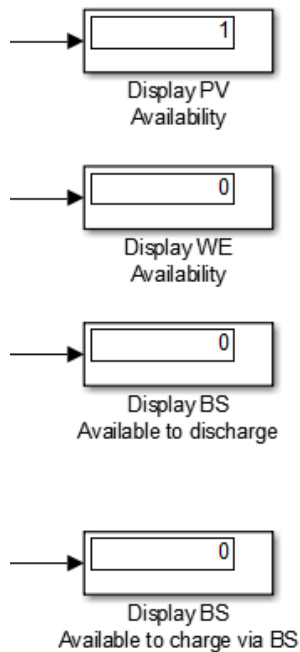


Figure 5-17: The output of the controller for CASE 8 illustrating that the PV system will supply the load.

5.4.1 ERROR: Over-Charged Battery

If the battery overcharges, indicating the need for maintenance or replacement, the controller will display the following alert. In practical implementations, this alert would trigger a maintenance notification.

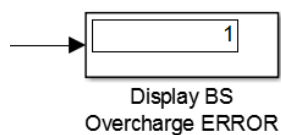


Figure 5-18: The output of the controller display when the battery exceeds the maximum limit of SOC

5.5 Battery Status Results

- Discharging

In CASE 2, the scenario where only the battery storage unit is available for load supply, the controller confirms the battery is available and has been chosen to supply the load. The

controller continuously monitors the battery status and displays the following result while discharging the battery.

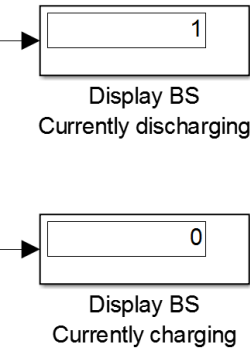


Figure 5-19: Battery status output from the controller for CASE 2, showing the battery supplying the load

- Charging

In CASE 7, the battery is identified as depleted, and while the load is supplied by the PV system, the wind system can charge the battery. To facilitate this, circuit breakers will be utilized to connect the battery and wind system, enabling the energy generated by the wind system to charge the battery. During this process, the controller displays the following status.

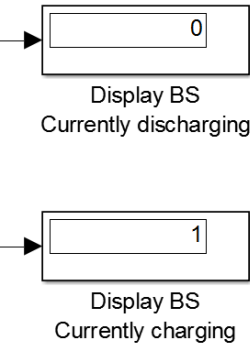


Figure 5-20: The battery status output from the controller for CASE 7, showing the load being supplied by PV while wind energy charges the battery

5.6 Load Results

When the load had a source of supply—covering CASES 2 through 8—the following result was observed.

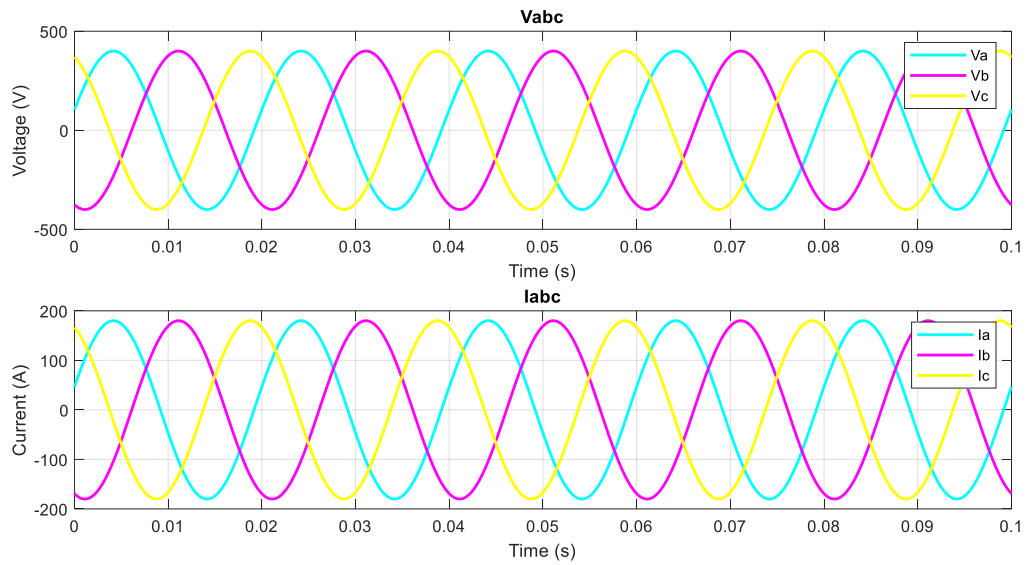


Figure 5-21: The load result when supplied by one of the HPS sources

When the load was without a source of supply—specifically in CASE 1—the following result was observed.

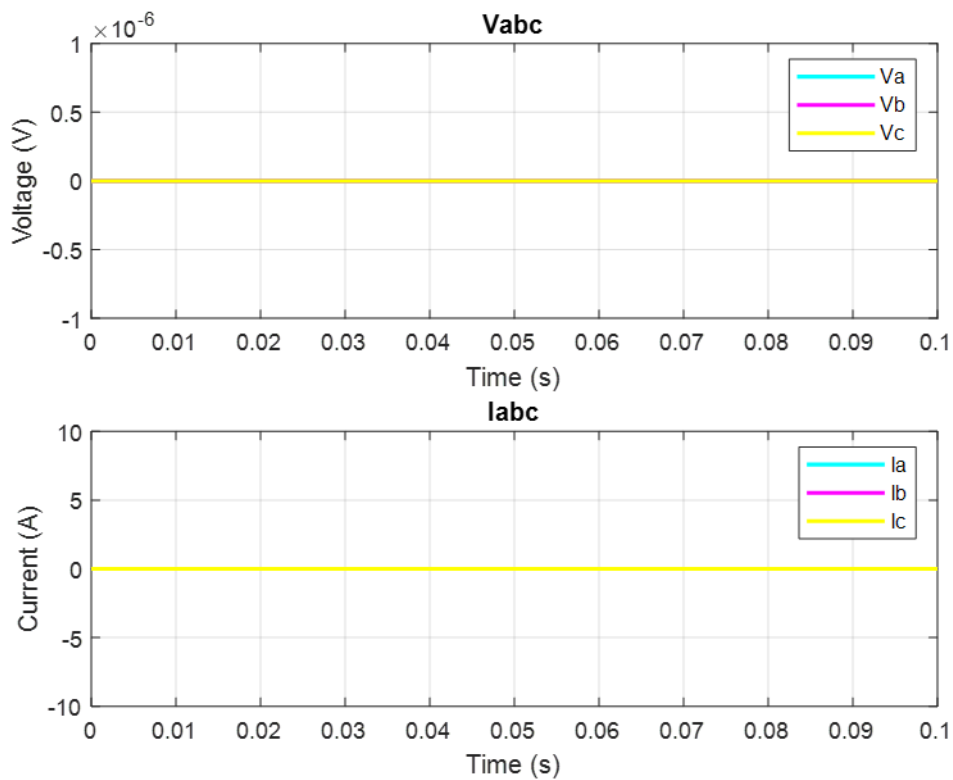


Figure 5-22: The load result when no source is available to supply the load

The full set of results is provided in Appendix D.

5.7 AC/DC/AC PWM Converter Results When the Load Demand is Met

The following results were obtained from the PWM converter connected to the source which was selected to supply the load:

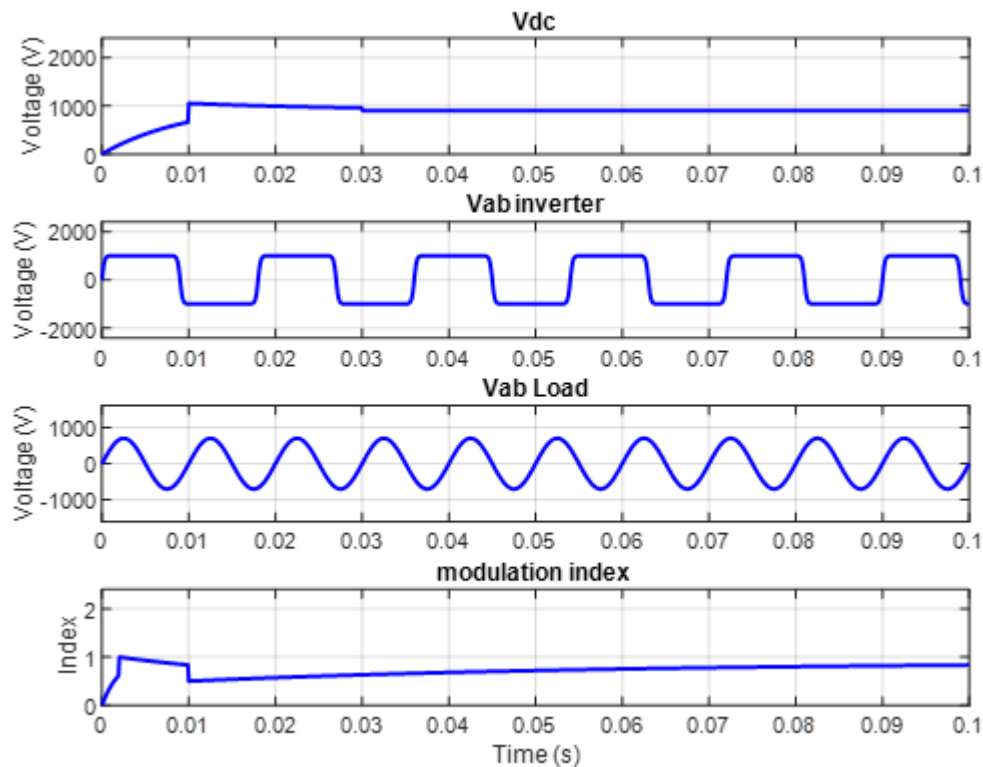


Figure 5-23: AC/DC/AC PWM converter result connected to energy source the controller has selected to supply the load

5.8 AC/DC/AC PWM Converter Results for the Source Available but Not Selected to Supply the Load

When multiple sources were available for load supply, the controller detected this and selected only one source. The source(s) not selected exhibited the following result on the AC/DC/AC PWM converter:

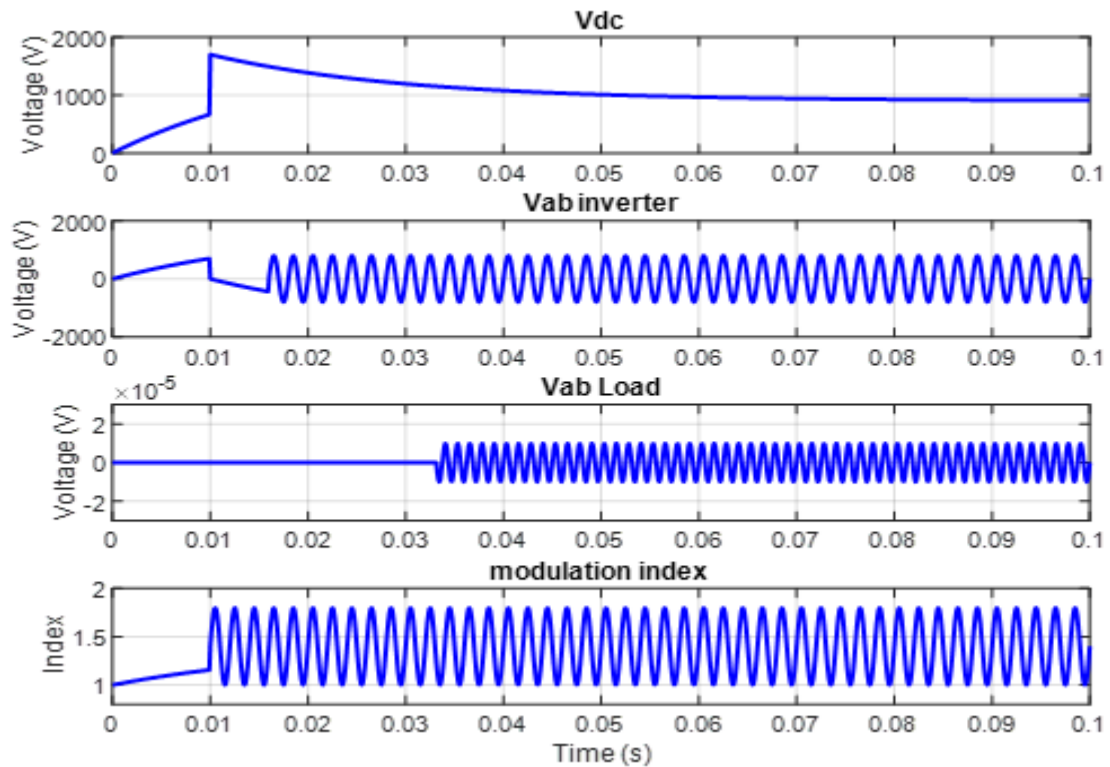


Figure 5-24: The result on the AC/DC/AC PWM converter connected to the available source that was not selected to supply the load

Note that these AC/DC/AC PWM converter results specifically reflect the behaviour of the HPS designed for this thesis and are not the standard expected results for such an HPS.

5.9 Discussion on the Results of the PV Performance in the HPS

The results obtained in Chapter 5 indicate that the PV model operates adequately within the HPS, producing desirable output. In Chapter 3, satisfactory results were observed for the PV model simulated without the DC/AC converter and load. The results in Chapter 5, however, are smoother and more precise due to the number of samples taken during the simulations of each model. In Chapter 3, the PV Model on its own file was simulated in continuous mode with an auto sample time, whereas the complete HPS model file was simulated in discrete mode with a much smaller sample time of $2e-5$ seconds. This indicates that the more samples taken, the smoother the signal output.

The results demonstrate that with larger irradiance input, the model produces a larger current output and hence greater power output. For varying temperatures and constant irradiance, the results show that the MPP is larger at lower operating temperatures. Thus, the PV model

operates most effectively at ambient temperatures and maximum irradiance, resulting in efficient use of the PV model's capabilities.

The MPP tracked is larger for higher input irradiance and smaller for lower input irradiance, implying that the PV system would output less power on cloudy days. These results align with research on PV models, confirming that the performance of the PV model is satisfactory and within expected norms.

The DFIG operates as desired within the HPS. The figures show that the outputs settle quickly and the DFIG wind turbine performs effectively. The DFIG was simulated separately, and the data was captured in the MATLAB workspace, allowing the HPS to gather this data during simulations. The interaction between the HPS and the DFIG equivalent model did not hinder the controller's performance.

5.10 Discussion of the Battery Status Results

The results from the controller confirm its effectiveness in analysing the inputs for each case. The results shown in Fig 5-11 and Fig 5-12 clearly show distinct charging and discharging procedures, matching the design of the HPS. The results are not fixed and may vary with different HPS battery models. For a 3600s simulation scaled down to 10s, the discharge time was approximately 4.27s and the charge time was 0.74s. This is desirable, as the charge time should be shorter than the discharge time for optimal battery performance in an HPS.

5.11 Discussion on the Controller Results

The controller performed as required, with results in Chapter 5, figures 5-24 – 5-28, indicating that it correctly delegated the roles of each source for the eight cases set up for the HPS. The availability of the sources was accurately determined, and the load was supplied whenever possible. The controller correctly identified when the wind system needed to supply the battery for charging (case 7) and detected an overcharge situation, indicating a need for maintenance or replacement. Overall, the controller's performance was satisfactory.

5.12 Simulation Analysis

- **Simulation Times:** The simulation times varied for different models. The PV model and DC/AC converter simulated quickly independently (within seconds). When integrated, the system required several minutes to complete the simulation.

- **Battery Model Compilation:** The battery model compiled quickly. When integrated with the AC/DC/AC converter and load, the compilation time was extended to approximately 40 minutes due to the smaller sample time ($2e-5s$) required for accurate PWM stage sampling.

5.13 Drawbacks Associated with the Models Simulated

5.13.1 Drawbacks of HPS Design

- **Inefficient Resource Utilization:** In CASE 1 (scenario 000), the load is left without a source of supply, rendering the network setup inefficient.
- **Energy Wastage:** In CASE 8 (scenario 111), the system wastes energy. A solution is needed to reduce the likelihood of encountering scenario 000.

5.13.2 Drawbacks of Using MATLAB Simulink for Simulation

1. **Simulation Speed:** Simulations in MATLAB Simulink took longer than required. The entire HPS file took a few hours to simulate each case with the required sample time of $2e-5s$.
2. **Memory Requirements:** Simulations required too much memory, and in some cases (e.g., battery model simulation), MATLAB crashed a few times due to insufficient memory.
3. **Incompatibility of Simulation Types:** The wind system runs in phasor simulation type while the battery storage unit and PV system run in discrete simulation type. This incompatibility created constraints in integrating the systems into the HPS, requiring alternative solutions to test the HPS operation with the controller.

CHAPTER SIX: CONCLUSION AND RECOMMENDATIONS

This thesis aimed to tackle the critical challenge of efficiently integrating and managing sources of renewable energy—specifically PV panels, wind turbines, and battery storage—within an HPS. The primary goal was to develop an energy management strategy and a controller capable of safeguarding a reliable and dependable electricity supply, despite the intrinsic alterability and intermittency of solar and wind energy.

The research began by outlining the significance of switching to renewable energy sources to mitigate environmental impacts and improve energy security. Given the growing global demand for sustainable energy solutions, this study's contribution lies in demonstrating how a hybrid system, effectively managed by an event-based controller, can optimize the use of available renewable resources.

Key findings from the simulations include:

- **Integration of PV and Wind Systems:** The PV system, coupled with an efficient MPPT algorithm, was successfully integrated into the HPS and proved capable of reliably supplying power when solar resources were available. The DFIG wind system complemented the PV system by providing power during periods of insufficient sunlight, ensuring the continuity of energy supply.
- **Critical Role of Battery Storage:** The battery storage unit played a pivotal role in the HPS, providing a dependable backup source of power when neither solar nor wind energy was available. This redundancy was crucial in maintaining system reliability, particularly during periods of low renewable energy generation.
- **Effective Controller Operation:** The event-based controller designed for this study effectively managed the energy flows within the HPS, ensuring that the load was consistently supplied with power from the most appropriate source. The controller's ability to prioritize energy sources based on availability and demand was essential for maximizing system efficiency.

6.1 HPS Adequate Performance Under All Test Cases

The HPS model, following necessary adjustments to resolve simulation and integration issues, performed adequately across most test scenarios. The event-based controller successfully managed the energy distribution among the PV, wind, and battery components, ensuring reliable power supply to the load under varying conditions. However, the system faced limitations in CASE 1, where it failed to supply the load, highlighting potential challenges for real-world applications. This indicates that while the system is functional, further refinements are needed to ensure it can meet all customer demands under different scenarios.

6.2 Challenges and Issues Encountered During Integration

Several challenges were encountered during the integration and simulation of the HPS:

1. **Simulation Speed:** The MATLAB Simulink simulations took longer than anticipated, with each HPS simulation requiring between 2 to 4 hours to complete using a sample time of $T_s = 2e-5s$. This slow processing speed hindered the efficiency of testing and model adjustments.
2. **Memory Requirements:** The high memory demand of the simulations, particularly when modeling the battery system, led to frequent crashes. This significantly complicated the integration of the HPS components and necessitated alternative approaches to ensure the system could be tested effectively.
3. **Simulation Type Incompatibilities:** The wind system was modeled using a phasor simulation type, while the battery and PV systems were modeled in discrete mode. This mismatch created integration constraints, requiring careful coordination to ensure that the different components could interact within the HPS. The incompatibility between simulation types also posed challenges in achieving a seamless and coherent simulation environment.

6.3 Recommendations for Future Research and System Improvements

In the light of the results and challenges encountered during the study, the following recommendations are proposed to improve the design, implementation, and performance of energy management systems in hybrid PV-wind-battery setups:

1. **Advanced Energy Management Algorithms:** Future research should explore the development of more sophisticated and adaptive energy management algorithms. Integrating artificial intelligence (AI) and machine learning (ML) techniques may facilitate dynamic prediction of resource availability and more efficient energy distribution, thereby improving the overall performance and responsiveness of the HPS.
2. **Scalability and Flexibility:** It is crucial to design energy management systems (EMS) that are scalable and flexible, allowing for future expansion and incorporation of additional sources of renewable energy. This will enable the HPS to adapt to changing energy demands and resource availability, ensuring long-term sustainability and reliability.
3. **Enhanced Controller Design:** Investigating strategies using advanced control, such as fuzzy logic controllers or neural networks, could improve the decision-making processes within the EMS. These sophisticated controllers are better equipped to handle the uncertainties and non-linearities coupled with renewable energy systems, leading to more energy management efficiency.
4. **Robust Battery Management Systems:** The development of robust BMS is critical for enhancing the charging and discharging cycles of battery storage units. Incorporating

state-of-charge (SOC) and state-of-health (SOH) estimation methods can extend battery life and improve overall system performance, ensuring reliable energy storage and supply.

5. **Grid Integration and Smart Grid Technologies:** Exploring HPS integration with smart grid technologies could augment the efficiency and reliability of entire power systems. Smart grids permit energy flows in two directions, monitoring in real-time, and intelligent energy distribution, which makes them a valuable addition to hybrid energy systems.
6. **Optimization of Hybrid Systems:** Further studies should focus on optimizing hybrid systems, including determining the ideal sizing and placement of PV panels, wind turbines, and battery storage units. This optimization can be achieved through advanced simulation techniques and real-world testing, leading to more efficient and cost-effective hybrid energy systems.

REFERENCES

1. Abdullah, M. A., Yatim, A. H. M., Tan, C. W. & Saidur, R., 2012. A review of maximum power point tracking algorithms for wind energy systems. *Renewable and Sustainable Energy Reviews*, Volume 16, pp. 3220-3227.
2. Abo-Khalil, A. G., 2012. Synchronization of DFIG output voltage to utility grid in wind power system. *Renewable Energy*, Volume 44, pp. 193-198.
3. Achaihou, N., M.Haddadi & A.Malek, 2012. Modeling of lead acid batteries in PV systems. *Energy Procedia*, Volume 18, pp. 538-544.
4. Alibaba.com, 2022. *Solar Monocrystalline panels 100w 200w 250watt 300w 350watt 400w price in solar cells solar Panel for power system*. [Online] Available at: https://www.alibaba.com/product-detail/Solar-Monocrystalline-panels100w-200w-250watt-300w_1600050916778.html?spm=a2700.galleryofferlist.normal_offer.d_title.3eed514fakYKGF [Accessed 02 April 2024].
5. Alibaba.com, 2022. *YRO Monocrystalline Solar Panel for solar system cheap price 75W-230W Mono PV Panel MBB*. [Online] Available at: https://www.alibaba.com/product-detail/Monocrystalline-Solar-Panel-YRO-Monocrystalline-Solar_1600348268260.html?spm=a2700.galleryofferlist.normal_offer.d_title.122f6652rgQSgE&s=p [Accessed 02 April 2024].
6. Anon., 2018. MPC Energy Management System For A Grid-Connected Renewable Energy/Battery Hybrid Power Plant. *2018 7th International Conference on Renewable Energy Research and Applications (ICRERA)*.
7. Ayamolowo, O. J., P.T.Manditereza & K.Kusakana, 2022. South Africa power reforms: The Path to a dominant renewable energy-sourced grid. *Energy Reports*, 8(1), pp. 1208-1215.
8. Baba, A. O., Liu, G. & Chen, X., 2020. Classification and Evaluation Review of Maximum Power Point Tracking Methods. *Sustainable Futures*, Volume 2, p. 100020.
9. Babazadeh, H., Gao, W. & Duncan, K., 2012. *A New Control Scheme in a Battery Energy Storage System for Wind Turbine Generators*. Online, s.n.
10. Babouri, R., Aouzellag, D. & Ghedamsi, K., 2013. Integration of Doubly Fed Induction Generator Entirely Interfaced With Network in a Wind Energy Conversion System. *Energy Procedia*, Volume 36, pp. 169-178.

11. Battery University, 2017. *What's the Best Battery?*. [Online] Available at: <https://batteryuniversity.com/article/whats-the-best-battery> [Accessed 07 April 2024].
12. Battery University, 2021. *BU-501: Basics about Discharging*. [Online] Available at: <https://batteryuniversity.com/article/bu-501-basics-about-discharging> [Accessed 06 April 2024].
13. C. Albea, F. G. a. C. C.-d.-W., 2011. Adaptive control design for boost inverter. *Control Engineering Practice*, Volume 19, pp. 32-44.
14. Camacho, E. & R. D. & L. D. & P. D. & A. T., 2010. Model predictive control techniques for hybrid systems. *Annual Reviews in Control*, Volume 34, pp. 21-31.
15. carbonbrief.org, 2020. *Mapped: The world's coal power plants*, s.l.: carbonbrief.org.
16. Carbone, R. & Tomaselli, A., 2011. *Recent Advances on AC PV-modules for Grid-Connected Photovoltaic*. Online, s.n.
17. Carbone, R. & Tomaselli, A., 2011. *Recent Advances on AC PV-modules for Grid-Connected Photovoltaic*. Online, s.n.
18. Centre Environmental Rights, 2021. *Deadly Air: Eskom is now world's most polluting power company*. [Online] Available at: <https://cer.org.za/news/deadly-air-eskom-is-now-worlds-most-polluting-power-company> [Accessed 14 May 2024].
19. Chowdhury, S., Chowdhury, S. & Crossley, P., 2009. *Microgrids and Active Distribution Networks*. London: United Kingdom: The Institution of Engineering and Technology,.
20. Coppez, G., Chowdhury, S. & Chowdhury, S. P., 2010. *The importance of energy storage in Renewable Power Generation: A review*. Online, s.n.
21. Coppez, G., Chowdhury, S. & Chowdhury, S. P., 2011. *Battery storage and testing protocols for CHP systems*. Online, s.n.
22. CYUBAHIRO, O. K., 2020. *BUILDING INTEGRATED SOLAR PV-WIND AND BATTERY HYBRID SYSTEM*, Cape Town: s.n.
23. Dang, C.-L., Zhang, L. & Zhou, M.-X., 2011. Optimal Power Control Model of Direct Driven PMSG. *Energy Procedia*, Volume 12, pp. 844-848.
24. data.worldbank.org, 2019. *Access to electricity (% of population) - South Africa*. [Online] Available at: <https://data.worldbank.org/indicator/EG.ELC.ACCS.ZS?locations=ZA> [Accessed 26 March 2024].
25. Dubey, S., Jadhav, N. Y. & Zakirova, B., 2013. Socio-Economic and Environmental Impacts of Silicon Based Photovoltaic (PV) Technologies. *Energy Procedia*, Volume 33, pp. 322-334.

26. Eltawil, M. A. & Zaho, Z., 2013. MPPT techniques for photovoltaic applications. *Renewable and Sustainable Energy Reviews*, Volume 25, pp. 793-813.
27. Encalada, Á. et al., 2022. Conceptual Design of a Vibration Test System Based on a Wave Generator Channel for Lab-Scale Offshore Wind Turbine Jacket Foundations. *Journal of Marine Science and Engineering* 10, 10(9), p. 1247.
28. Eynde, N. W. V., Chowdhury, S. & Chowdhury, S. P., 2010. *Modeling and Simulation of a Stand-Alone Photovoltaic Plant with MPPT Feature and Dedicated Battery Storage*. s.l., s.n.
29. Fendri, D. & Chaabene, M., 2012. Dynamic model to follow the state of charge of a lead-acid battery connected to photovoltaic panel. *Energy conversion and management*, Volume 64, pp. 587-593.
30. G. Coppez, S. C. a. S. P. C., 2012. The importance of energy storage in Renewable Power Generation: A review. *45th International Universities Power Engineering Conference UPEC2010*, pp. 1-5.
31. Gagnon, R. et al., 2002. Modeling and Real-Time Simulation of a Doubly-Fed Induction Generator Driven by a Wind Turbine. *Engineering, Environmental Science*.
32. Hatta, T., 2012. *Applications of sodium-sulfur batteries*. Online, s.n.
33. Hong, C.-M., Chen, C.-H. & Tu, C.-S., 2013. Maximum power point tracking-based control algorithm for PMSG wind generation system without mechanical sensors. *Energy Conversion and Management*, Volume 69, pp. 58-67.
34. Huang, B. J., Hsu, P. C., Wu, M. S. & Ho, P. Y., 2010. System dynamic model and charging control of lead-acid battery for stand-alone solar PV system. *Solar Energy*, Volume 84, pp. 822-830.
35. International Energy Agency, 2021. *Renewables 2021: Analysis and forecasts to 2026*, Paris, France: s.n.
36. Ishaque, K., Salam, Z. & Taheri, H., 2011. Simple, fast and accurate two-diode model for photovoltaic modules. *Solar Energy Materials & Solar Cells*, Volume 95, pp. 586-594.
37. Islam, M. R., Mekhilef, S. & Saidur, R., 2013. Progress and recent trends of wind energy technology. *Renewable and Sustainable Energy Reviews*, Volume 21, pp. 456-468.
38. Kayaalp, R. İ., Cuma, M. U. & Tümay, M., 2023. A new rule-based self-reconfigurable energy management control of grid and batteries connected hybrid regenerative solar power system for critical loads. *Simulation Modelling Practice and Theory*, 125(102749).
39. Labuschagne, H., 2022. *Eskom guzzling enough diesel to fill 200,000 cars per day*. [Online]
Available at: <https://mybroadband.co.za/news/energy/436770-eskom-guzzling-enough-diesel-to-fill-200000-cars-per-day.html>
[Accessed 24 March 2024].

40. Lange, M., 2013. *Solar Energy Technology*. [Online] Available at: <https://www.sciencedirect.com/topics/earth-and-planetary-sciences/solar-energy-technology> [Accessed 12 August 2024].
41. M.A.Hyams, 2012. Wind energy in the built environment. *Metropolitan Sustainability*, pp. 457-499.
42. Ma, J. et al., 2013. DEM: Direct Estimation Method for Photovoltaic Maximum Power Point Tracking. *Procedia Computer Science*, Volume 17, pp. 537-544.
43. Manwell, J. F., Rogers, A. L. & McGowan, J. G., 2009. *Wind Energy Explained*. West Sussex: John Wiley & Sons Ltd.,.
44. Marsh, J., 2023. *Monocrystalline vs. Polycrystalline solar panels*. [Online] Available at: <https://www.energysage.com/solar/monocrystalline-vs-polycrystalline-solar/> [Accessed 23 July 2024].
45. Modu, B. et al., 2024. Optimal Design of a Grid-Independent Solar-Fuel Cell-Biomass Energy System Using an Enhanced Salp Swarm Algorithm Considering Rule-Based Energy Management Strategy. *IEEE Access*, Volume 12, pp. 23914-23929.
46. Mtshali, T., Coppez, G., Chowdhury, S. & Chowdhury, S., 2011. *Simulation and Modelling of PV-Wind-Battery Hybrid Power System*. Online, s.n., pp. 1-7.
47. Nair, N.-K. C. & Garimella, N., 2010. Battery energy storage systems: Assessment for small-scale renewable energy integration. *Energy and Buildings*, 42(11), pp. 2124-2130.
48. Narayana, M. et al., 2012. Generic maximum power point tracking controller for small-scale wind turbines. *Renewable Energy*, Volume 44, pp. 72-79.
49. Odoi-Yorke, F., Abaase, S., Zebilila, M. & Atepor, L., 2022. Feasibility analysis of solar PV/biogas hybrid energy system for rural electrification in Ghana. *Cogent Engineering*, 9(1).
50. Olabode, O. et al., 2021. Hybrid power systems for off-grid locations: A comprehensive review of design technologies, applications and future trends. *Scientific African*, p. e00884.
51. Ouerghi, F. H. et al., 2024. Investigating the potential of geothermal energy as a sustainable replacement for fossil fuels in commercial buildings. *Alexandria Engineering Journal*, Volume 97, pp. 215-229.
52. P. Udhayakumar, C. S. a. M. L., 2013. Stand - Alone Wind Energy Supply System Using Permanent Magnet Synchronous Generator. *International Journal of Innovative Technology and Exploring Engineering*, 2(3), pp. 2278-3075.
53. Pandiarajan, N. & Muthu, R., 2011. Mathematical Modeling of Photovoltaic Module with Simulink. *2011 1st International Conference on Electrical Energy Systems*, pp. 258-263.

54. Paska, J., Biczek, P. & Klos, M., 2009. Hybrid power systems – An effective way of utilising primary energy sources. *Renewable Energy*, 34(11), pp. 2414-2421.
55. Proton Solar, 2022. 250W 24V MONO SOLAR PANELS. [Online] Available at: https://protonsolardistributors.co.za/product/250w-24v-solar-panels-mono/?utm_source=Google%20Shopping&utm_campaign=All%20Products&utm_medium=cpc&utm_term=443&qclid=Cj0KCQjw6J-SBhCrARIsAH0yMZj_DbL27Ww52wuau2XOgYp0xXO4Auu6c-Qd23ByeQ8bUSkVcRspolcaAIHSEALw_w [Accessed 02 April 2024].
56. Qian, H., Zhang, J., Lai, J.-S. & Yu, W., 2011. A High Efficiency Grid-Tie Battery Energy Storage System. *IEEE Transactions on Power Electronics*, 23(3), pp. 886-896.
57. R.Saidur, N.A.Rahim, M.R.Islam & K.H.Solangi, 2011. Environmental impact of wind energy. *Renewable and Sustainable Energy Reviews*, 15(5), pp. 5423-2430.
58. Ritchie, H., Rosado, P. & Roser, M., 2024. *Greenhouse gas emissions*. [Online] Available at: <https://ourworldindata.org/greenhouse-gas-emissions> [Accessed 14 May 2024].
59. Rodrigues, E., Melicio, R., Mendes, V. & Catalão, J., 2011. *Simulation of a Solar Cell considering Single-Diode Equivalent Circuit Model*. Lisbon, s.n.
60. Roy, P. K. & H. J. & Z. T. & S. Y., 2022. Recent Advances of Wind-Solar Hybrid Renewable Energy Systems for Power Generation: A Review. *IEEE Open Journal of the Industrial Electronics Society*, 3(1), p. 1.
61. S.Mathew & G.S.Philip, 2012. Wind Turbines: Evolution, Basic Principles, and Classifications. *Comprehensive Renewable Energy*, Volume 2, pp. 93-111.
62. Sanchez, A., Molina, M. & Lede, A., 2012. Dynamic model of wind energy conversion systems with PMSG-based variable-speed wind turbines for power system studies. *International Journal of Hydrogen Energy*, 37(13), pp. 10064-10069.
63. Sawle, Y., Gupta, S. C., Kumar Bohre, A. & Meng, W., 2016. PV-wind hybrid system: A review with case study. *Cogent Engineering*, 3(1).
64. SNADI, 2022. Poly PV system 250w solar panel with cable. [Online] Available at: https://www.alibaba.com/product-detail/Poly-PV-system-250w-solar-panel_62069928337.html [Accessed 31 March 2024].
65. Solar, S., 2022. Poly PV system 250w solar panel with cable. [Online] Available at: https://www.alibaba.com/product-detail/Poly-PV-system-250w-solar-panel_62069928337.html [Accessed 31 March 2024].

66. Statista Research Department, 2024. *Global electricity mix 2022, by energy source*. [Online]
Available at: <https://www.statista.com/statistics/269811/world-electricity-production-by-energy-source/>
[Accessed 14 May 2024].
67. Tafon Solar, 2022. *24V 250 Watt Monocrystalline Solar Panel Price*. [Online]
Available at: <https://www.tanfon.com/products/solar-inverter-&system-materials/250-watt-solar-panel-price.html>
[Accessed 02 April 2024].
68. Team, M. E. V., 2008. *A Guide to Understanding Battery Specifications*. [Online]
Available at: https://web.mit.edu/evt/summary_battery_specifications.pdf
[Accessed 07 April 2024].
69. The MathWorks, Inc., n.d. *Battery*. [Online]
Available at: <https://www.mathworks.com/help/sps/powersys/ref/battery.html>
[Accessed 12 July 2024].
70. The MathWorks, Inc., n.d. *Wind Turbine Doubly-Fed Induction Generator (Phasor Type)*. [Online]
Available at: <https://www.mathworks.com/help/sps/powersys/ref/windturbinedoublyfedinductiongeneratorphasortype.html>
[Accessed 12 July 2024].
71. tradingeconomics.com, 2019. *South Africa - Access To Electricity (% Of Population)*. [Online]
Available at: [https://tradingeconomics.com/south-africa/access-to-electricity-percent-of-population-wb-data.html#:~:text=Access%20to%20electricity%20\(%25%20of%20population\)%20in%20South%20Africa%20was,compiled%20from%20officially%20recognized%20sources.](https://tradingeconomics.com/south-africa/access-to-electricity-percent-of-population-wb-data.html#:~:text=Access%20to%20electricity%20(%25%20of%20population)%20in%20South%20Africa%20was,compiled%20from%20officially%20recognized%20sources.)
[Accessed 26 March 2024].
72. Ullah, F. et al., 2024. A comprehensive review of wind power integration and energy storage technologies for modern grid frequency regulation. *Heliyon*, May.10(9).
73. Urtasun, A. et al., 2013. Modeling of small wind turbines based on PMSG with diode bridge for sensorless maximum power tracking. *Renewable Energy*, Volume 55, pp. 138-149.
74. Wang, J. & Azam, W., 2024. Natural resource scarcity, fossil fuel energy consumption, and total greenhouse gas emissions in top emitting countries. *Geoscience Frontiers*, 15(2), p. 101757.

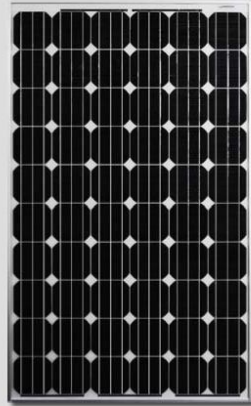
75. Wang, Y., Sun, Z. & Chen, Z., 2019. Development of energy management system based on a rule-based power distribution strategy for hybrid power sources. *Energy*, 175(0360-5442), pp. 1055-1066.
76. Wasim, M. et al., 2024. An efficient energy management scheme using rule-based swarm intelligence approach to support pulsed load via solar-powered battery-ultracapacitor hybrid energy system. *Sci Rep* 14, Volume 3962.
77. Will Coley, P. S. G., 2020. *Market assessment for modern energy*, Glasgow: University of Strathclyde.
78. Yang, Y., Wei, Q., Liu, S. & Zhao, L., 2022. Distribution Strategy Optimization of Standalone Hybrid WT/PV System Based on Different Solar and Wind Resources for Rural Applications. *Energies*, Issue 15.
79. Zebra, E. I. C., Windt, H. J. v. d., Nhumaio, G. & Faaij, A. P., 2021. A review of hybrid renewable energy systems in mini-grids for off-grid electrification in developing countries. *Renewable and Sustainable Energy Reviews*, July, Volume 144, p. 111036.
80. Zhang, J., 2024. Energy access challenge and the role of fossil fuels in meeting electricity demand: Promoting renewable energy capacity for sustainable development. *Geoscience Frontiers*, September, 15(5), p. 101873.

APPENDIX A: PV Model Specifications



CS6P

235/240/245/250/255M



Key Features

- High module efficiency up to 15.85%
- Positive power tolerance: 0 ~ +5W
- Robust frame to up to 5400 Pa load
- Anti-reflective with self-cleaning surface
- Outstanding performance at low irradiance
- High energy yield at Low NOCT
- **Backed By Our New 10/25 Linear Power Warranty Plus our added 25 year insurance coverage**



- 10 year product warranty on materials and workmanship
- 25 year linear power output warranty

CS6P is a robust solar module with 60 solar cells. These modules can be used for on-grid solar applications. Our meticulous design and production techniques ensure a high-yield, long-term performance for every module produced. Our rigorous quality control and in-house testing facilities guarantee Canadian Solar's modules meet the highest quality standards possible.

Best Quality

- 235 quality control points in module production
- EL screening to eliminate product defects
- Current binning to improve system performance
- Accredited Salt mist/Ammonia resistant

Best Warranty Insurance

- 25 years worldwide coverage
- 100% warranty term coverage
- Providing third party bankruptcy rights
- Non-cancellable
- Immediate coverage
- Insured by 3 world top insurance companies

Comprehensive Certificates

- IEC 61215, IEC 61730, IEC 61701 ED2, UL 1703, KEMCO, CEC Listed, CE, JET and MCS
- ISO 9001: 2008: Quality Management System
- ISO/TS 16949:2009: The automotive quality management system
- ISO 14001:2004: Standards for Environmental management system
- QC 080000 HSPM: The Certification for Hazardous Substances Regulations
- OHSAS 18001:2007 International standards for occupational health and safety
- Reach Compliance



www.canadiansolar.com

CS6P-235/240/245/250/255M

Electrical Data

STC	CS6P-235M	CS6P-240M	CS6P-245M	CS6P-250M	CS6P-255M
Nominal Maximum Power (Pmax)	235W	240W	245W	250W	255W
Optimum Operating Voltage (Vmp)	30.1V	30.2V	30.3V	30.4V	30.5V
Optimum Operating Current (Imp)	7.82A	7.95A	8.09A	8.22A	8.35A
Open Circuit Voltage (Voc)	37.2V	37.3V	37.4V	37.5V	37.7V
Short Circuit Current (Isc)	8.34A	8.46A	8.61A	8.74A	8.74A
Module Efficiency	14.61%	14.92%	15.23%	15.54%	15.85%
Operating Temperature	-40°C~+85°C				
Maximum System Voltage	1000V (IEC) /600V (UL)				
Maximum Series Fuse Rating	15A				
Application Classification	Class A				
Power Tolerance	0 ~ +5W				

Under Standard Test Conditions (STC) of Irradiance of 1000W/m², spectrum AM 1.5 and cell temperature of 25°C

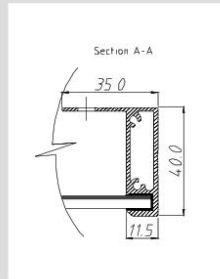
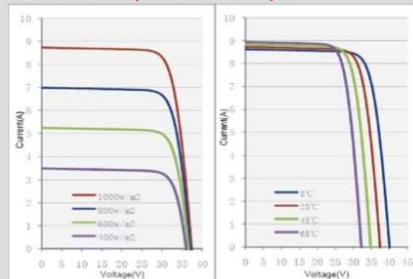
NOCT	CS6P-235M	CS6P-240M	CS6P-245M	CS6P-250M	CS6P-255M
Nominal Maximum Power (Pmax)	170W	173W	177W	180W	184W
Optimum Operating Voltage (Vmp)	27.5V	27.5V	27.6V	27.7V	27.8V
Optimum Operating Current (Imp)	6.18A	6.29A	6.40A	6.51A	6.62A
Open Circuit Voltage (Voc)	34.1V	34.2V	34.3V	34.4V	34.6V
Short Circuit Current (Isc)	6.75A	6.85A	6.97A	7.08A	7.18A

Under Normal Operating Cell Temperature, Irradiance of 800 W/m², spectrum AM 1.5, ambient temperature 20°C, wind speed 1 m/s

Mechanical Data

Cell Type	Mono-crystalline 156 x 156mm, 2 or 3 Busbars
Cell Arrangement	60 (6 x 10)
Dimensions	1638 x 982 x 40mm (64.5 x 38.7 x 1.57in)
Weight	19kg (41.9 lbs)
Front Cover	3.2mm Tempered glass
Frame Material	Anodized aluminium alloy
J-BOX	IP65, 3 diodes
Cable	4mm ² (IEC)/12AWG(UL), 1000mm
Connectors	MC4 or MC4 Comparable
Standard Packaging (Modules per Pallet)	24pcs
Module Pieces per container (40 ft. Container)	672pcs (40'HQ)

I-V Curves (CS6P-250M)



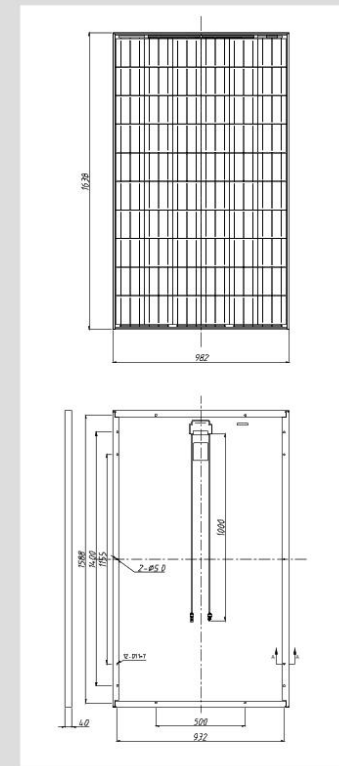
Temperature Characteristics

Temperature Coefficient	Pmax	-0.45%/°C
	Voc	-0.35 %/°C
	Isc	0.060 %/°C
Normal Operating Cell Temperature		45±2°C

Performance at Low Irradiance

Industry leading performance at low irradiation environment, +95.5% module efficiency from an irradiance of 1000w/m² to 200w/m² (AM 1.5, 25 °C)

Engineering Drawings



*Specifications included in this datasheet are subject to change without prior notice.

About Canadian Solar

Canadian Solar Inc. is one of the world's largest solar companies. As a leading vertically-integrated manufacturer of ingots, wafers, cells, solar modules and solar systems, Canadian Solar delivers solar power products of uncompromising quality to worldwide customers. Canadian Solar's world class team of professionals works closely with our customers to provide them with solutions for all their solar needs.

For product and purchase inquiries contact:

ecoDIRECT
CLEAN ENERGY SOLUTIONS
www.ecodirect.com

Canadian Solar was founded in Canada in 2001 and was successfully listed on NASDAQ Exchange (symbol: CSIQ) in November 2006. Canadian Solar has module manufacturing capacity of 2.05GW and cell manufacturing capacity of 1.3GW.

Headquarters | 545 Speedvale Avenue West
Guelph | Ontario N1K 1E6 | Canada
Tel: +1 519 837 1881
Fax: +1 519 837 2550
Inquire.ca@canadiansolar.com
www.canadiansolar.com

EN-Rev 3.50 Copyright 2012 Canadian Solar Inc.

APPENDIX B: Code

- **MPPT Code**

```
%code for MPPT method for PV model using Incremental Conductance
lk = zeros(1, lpv_out.signals.values); %array of zeros
lpv = zeros(1, lpv_out.signals.values);
lwork = lpv_out.signals.values; %collecting data from workspace
lk = lwork; %storing the collected data from workspace into the empty array
lpv = lwork;

Vk = zeros(1, Vpv_out.signals.values); %array of zeros
Vpv = zeros(1, Vpv_out.signals.values);
Vwork = Vpv_out.signals.values; %collecting data from workspace
Vk = Vwork; %filling array with data gathered from the workspace
Vpv = Vwork;

Pk = zeros(1, Ppv_out.signals.values); %array of zeros
Ppv = zeros(1, Ppv_out.signals.values);
Pwork = Ppv_out.signals.values; %collecting data from the workspace
Pk = Pwork; %filling the empty array with data collected from the workspace
Ppv = Pwork;

Impp = zeros(1, lpv_out.signals.values); %store maximum
Vmpp = zeros(1, lpv_out.signals.values); %store maximum
Pmpp = zeros(1, Ppv_out.signals.values); %store maximum

% Incremental Conductance method
for x = 2:size(lk, 2)
    dl = lk(x) - lk(x-1); % change in current
    dV = Vk(x) - Vk(x-1); % change in voltage

    if dV == 0
        if dl == 0
            % MPP reached
            Vmpp(x) = Vk(x);
            Impp(x) = lk(x);
            Pmpp(x) = Pk(x);
        else
            % Edge case: Voltage is constant, but current changes
            if dl > 0
                Vk(x) = Vk(x-1) - abs(Vk(x) - Vk(x-1)); % Decrease voltage
            else
                Vk(x) = Vk(x-1) + abs(Vk(x) - Vk(x-1)); % Increase voltage
            end
        end
    else
        % Perform the incremental conductance check
        if (dl/dV) == (-lk(x)/Vk(x))
            % MPP reached
            Vmpp(x) = Vk(x);
            Impp(x) = lk(x);
            Pmpp(x) = Pk(x);
        elseif (dl/dV) > (-lk(x)/Vk(x))
            % Left of MPP, increase voltage
            Vk(x) = Vk(x-1) + abs(Vk(x) - Vk(x-1));
        else
            % Right of MPP, decrease voltage
            Vk(x) = Vk(x-1) - abs(Vk(x) - Vk(x-1));
        end
    end
end
```

```

    % Update power
    Pk(x-1) = Pk(x);
end

% Plotting results
figure
for G=0.2:0.4:1;
    plot(Vpv, Ipv, 'b', 'LineWidth', 2)
    hold on
    plot(30.5,8.26,'r.','MarkerSize',40);
    hold on
    plot(29.5,4.89,'r.','MarkerSize',40);
    hold on
    plot(28,1.53,'r.','MarkerSize',40);
    hold on
    plot(Vmpp,Impp, 'r.', 'MarkerSize', 25)
    hold on
end
title('MPPT for PV model - V vs I', 'FontSize' , 25)
xlabel('Module Voltage (V)', 'FontSize' , 25)
ylabel('Module Current (A)', 'FontSize' , 25)
grid
axis([0 50 0 10])

figure
for G=0.2:0.4:1;
    plot(Vpv, Ppv, 'b', 'LineWidth', 2)
    hold on
    plot(Vmpp, Pmpp, 'r')
    hold on
end
title('MPPT for PV model - V vs P', 'FontSize' , 25)
xlabel('Module Voltage (V)', 'FontSize' , 25)
ylabel('Module Power (P)', 'FontSize' , 25)
grid
axis([0 50 0 300])

```

- **PV Output Signals Plot Code**

```

% PV model visualization

% Extract data from the PV model simulation
voltage = Vpv.signals.values; % Voltage data
current = Ipv.signals.values; % Current data
power = Ppv.signals.values; % Power data

% Plot Voltage vs Current (V-I curve)
figure(1) % Open a new figure window
plot(voltage, current, 'r', 'LineWidth', 1.5) % Plot V-I curve with a red line
xlabel('Voltage (V)', 'FontSize', 20) % Label x-axis
ylabel('Current (A)', 'FontSize', 20) % Label y-axis
title('PV Output: Voltage vs Current', 'FontSize', 20) % Add title
axis([0 55 0 12]) % Set axis limits
grid on % Turn on the grid for better readability

% Add annotations for different irradiance levels
gtext('0.2 kW/m^2', 'FontSize', 15)
gtext('0.6 kW/m^2', 'FontSize', 15)
gtext('1.0 kW/m^2', 'FontSize', 15)

% Plot Voltage vs Power (V-P curve)

```



```

figure(2) % Open another figure window
plot(voltage, power, 'b', 'LineWidth', 1.5) % Plot V-P curve with a blue line
xlabel('Voltage (V)', 'FontSize', 20) % Label x-axis
ylabel('Power (W)', 'FontSize', 20) % Label y-axis
title('PV Output: Voltage vs Power', 'FontSize', 20) % Add title
axis([0 55 0 320]) % Set axis limits
grid on % Turn on the grid for better readability

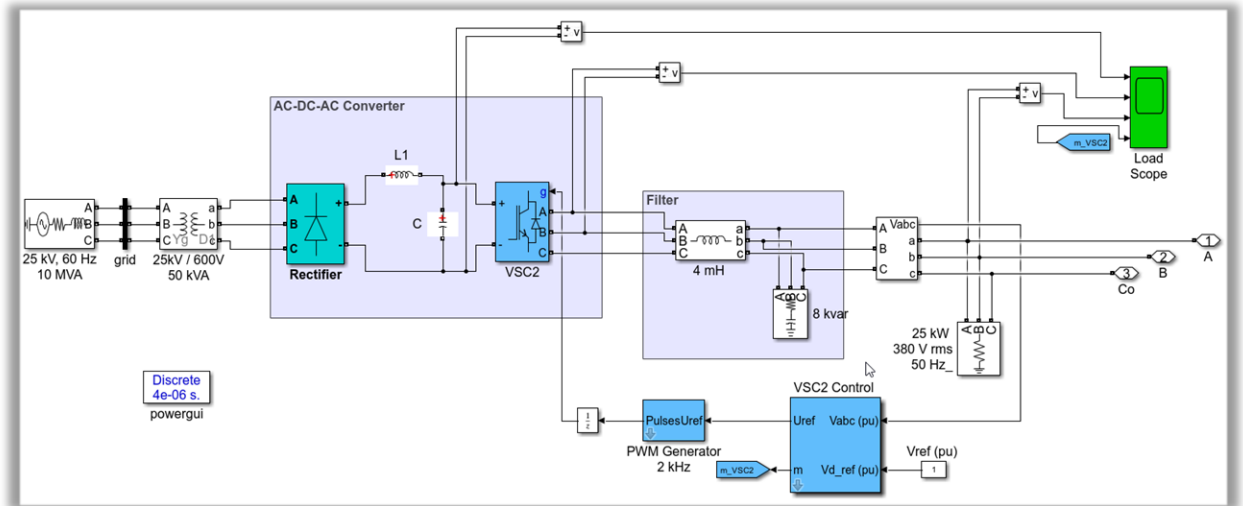
% Add annotations for different irradiance levels
gtext('0.2 kW/m^2', 'FontSize', 15)
gtext('0.6 kW/m^2', 'FontSize', 15)
gtext('1.0 kW/m^2', 'FontSize', 15)

```

APPENDIX C: AC/DC/AC PWM/ Converter

The AC/DC/AC PWM Converter in the HPS system was adapted as needed to seamlessly integrate with the PV, wind, and battery components.

App.1-0

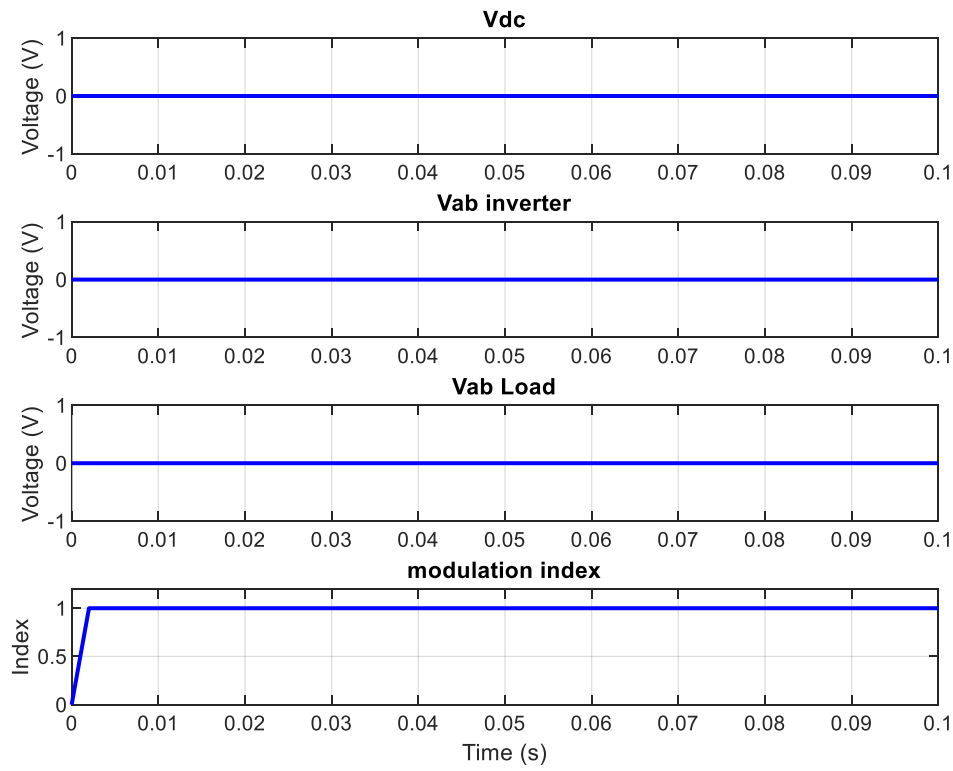


App-1. – AC/SC/AC PWM Converter in the HPS system

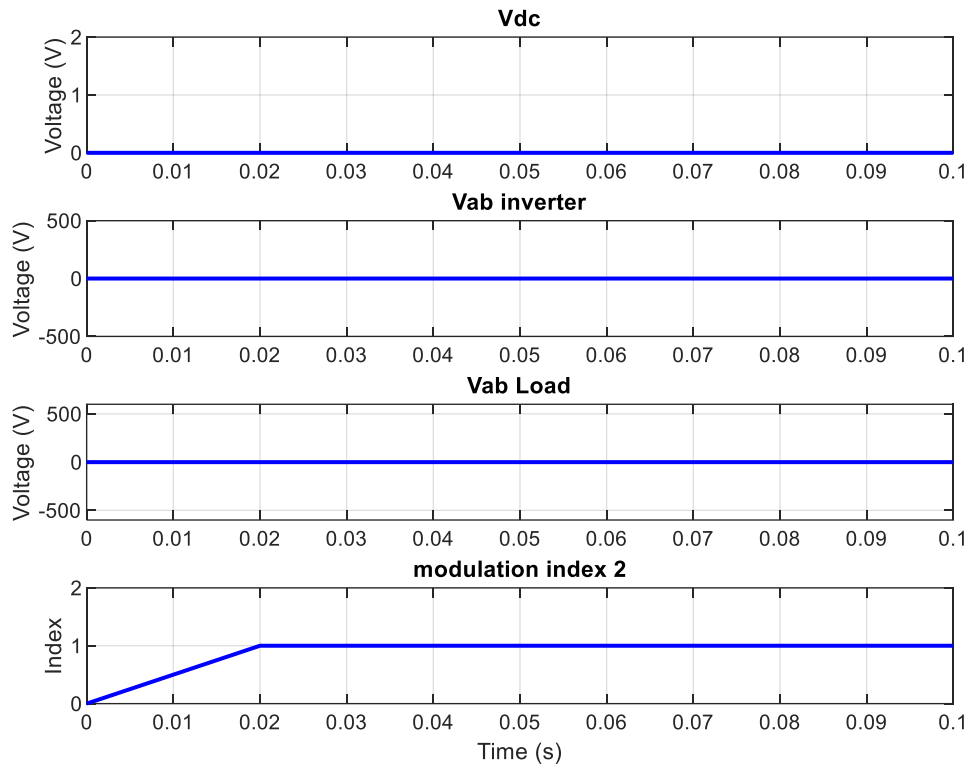
APPENDIX D: HPS Results Under Various Scenarios

Case 1: Complete Resource Unavailability Leading to a "Blackout"

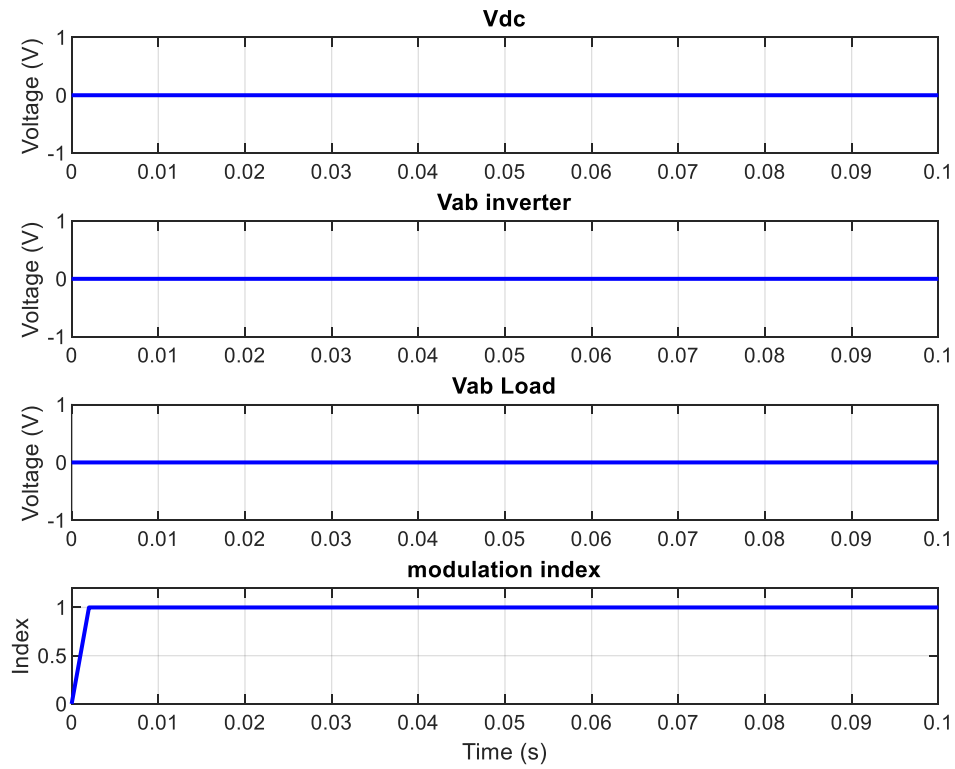
PWM Results During Blackout Condition: The plots show the behaviour of the system when no resources (solar, wind, or battery) are available in a hybrid power system (HPS). V_{dc} , V_{ab} inverter, and V_{ab} load remain at zero, representing the absence of power generation or load activity.



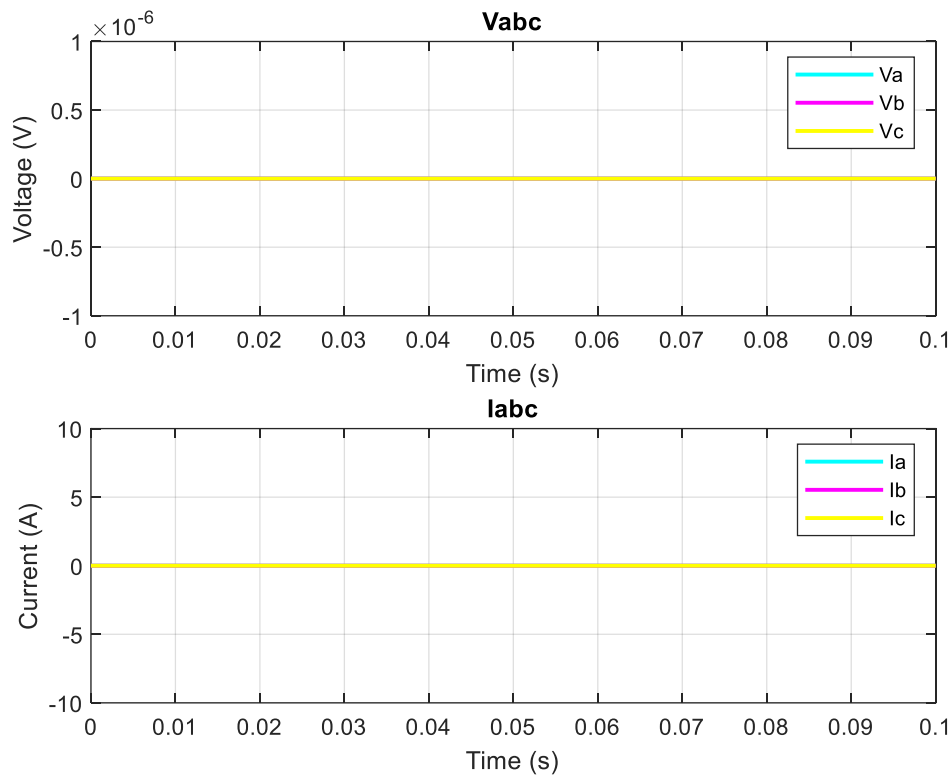
APP-2. PV system equivalent PWM results



APP-3. Wind system equivalent PWM results

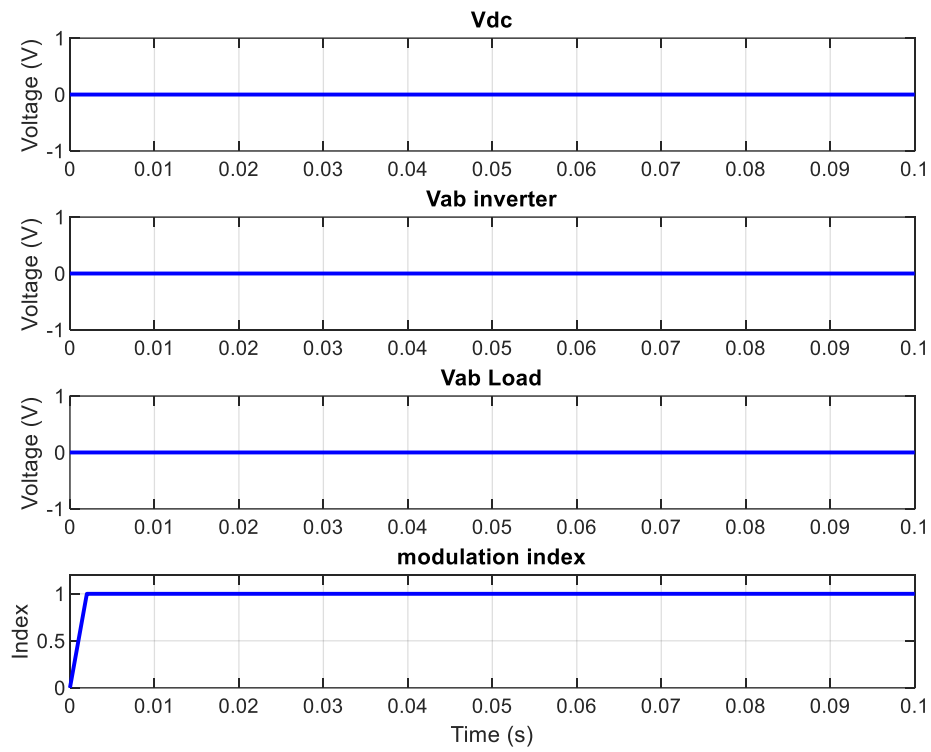


APP-4. Battery storage unit equivalent PWM results

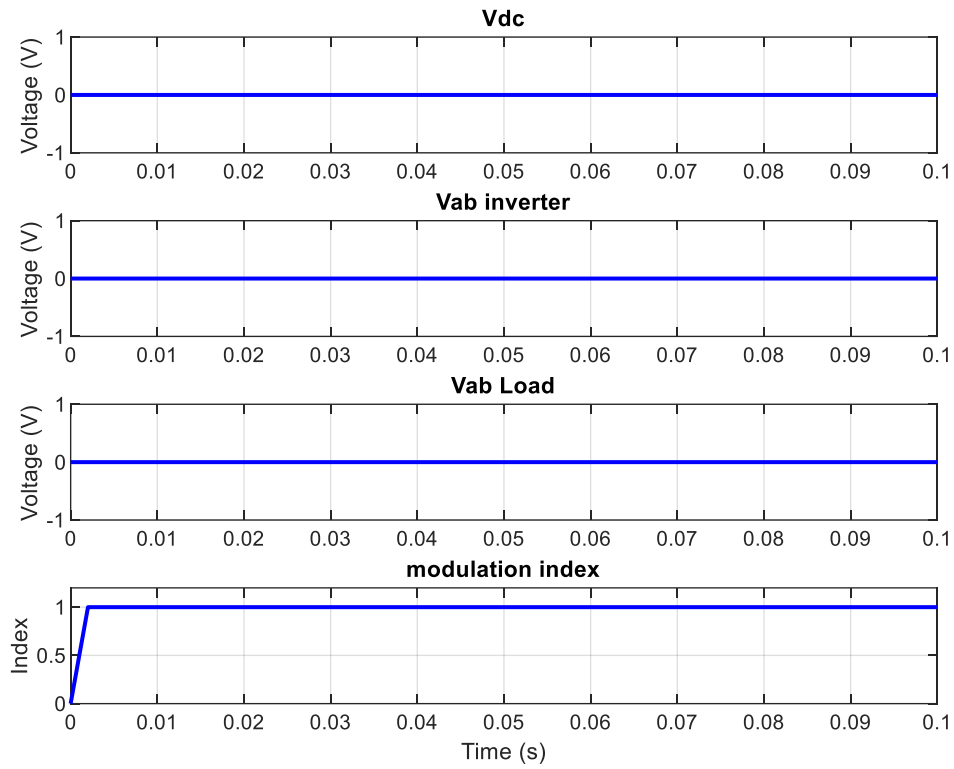


APP-5. Case 1 Load Result

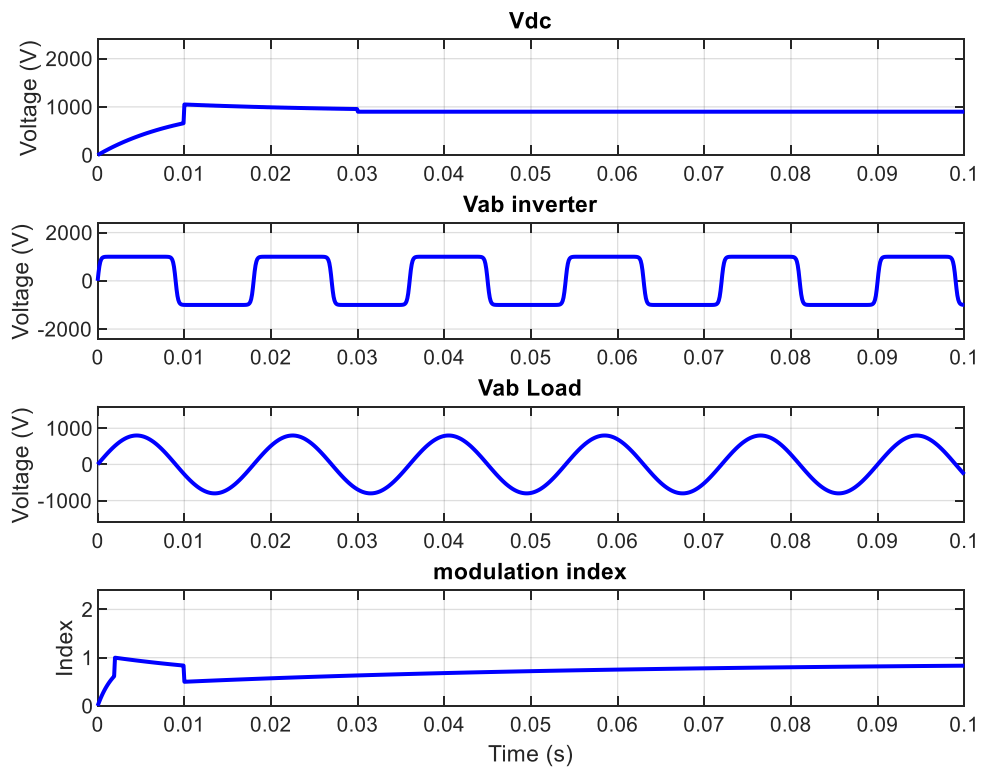
Case 2: Load Supplied with Battery Storage Unit



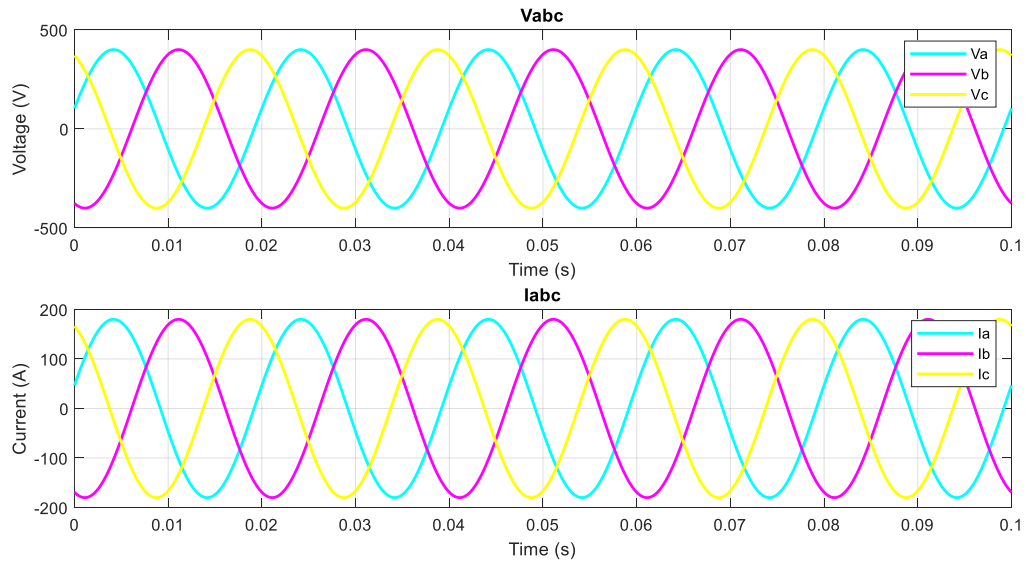
APP-6. PV system equivalent PWM results



APP-7. Wind system equivalent PWM results

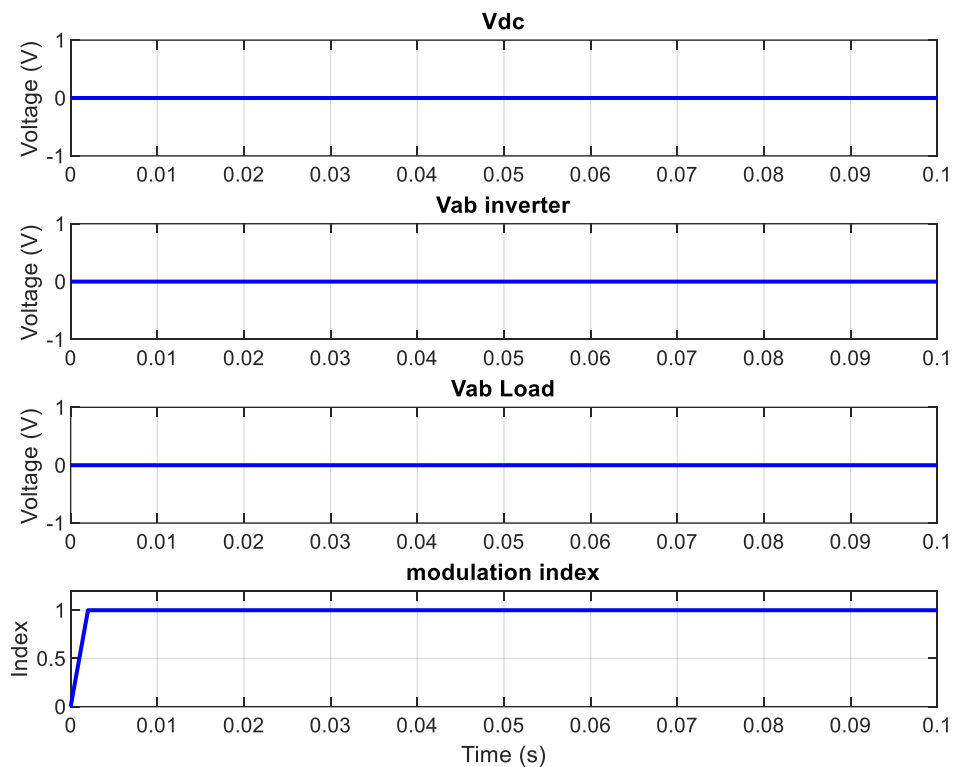


APP-8. Battery storage unit equivalent PWM results

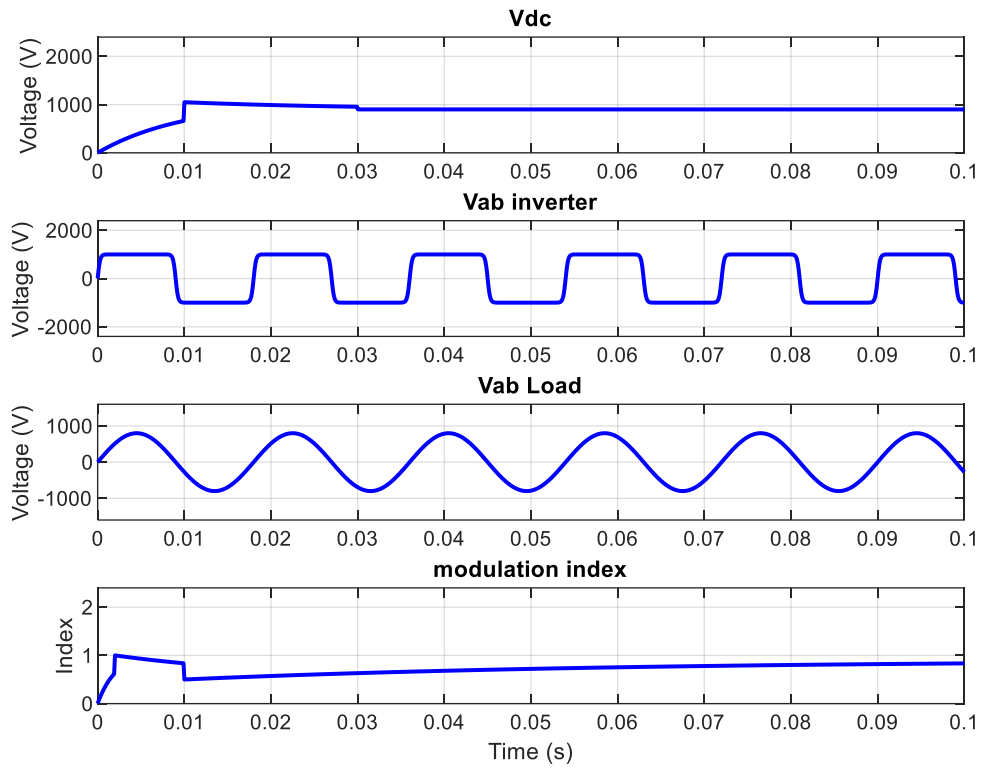


APP-9. Case 2 Load Result of Battery Storage Unit Supply

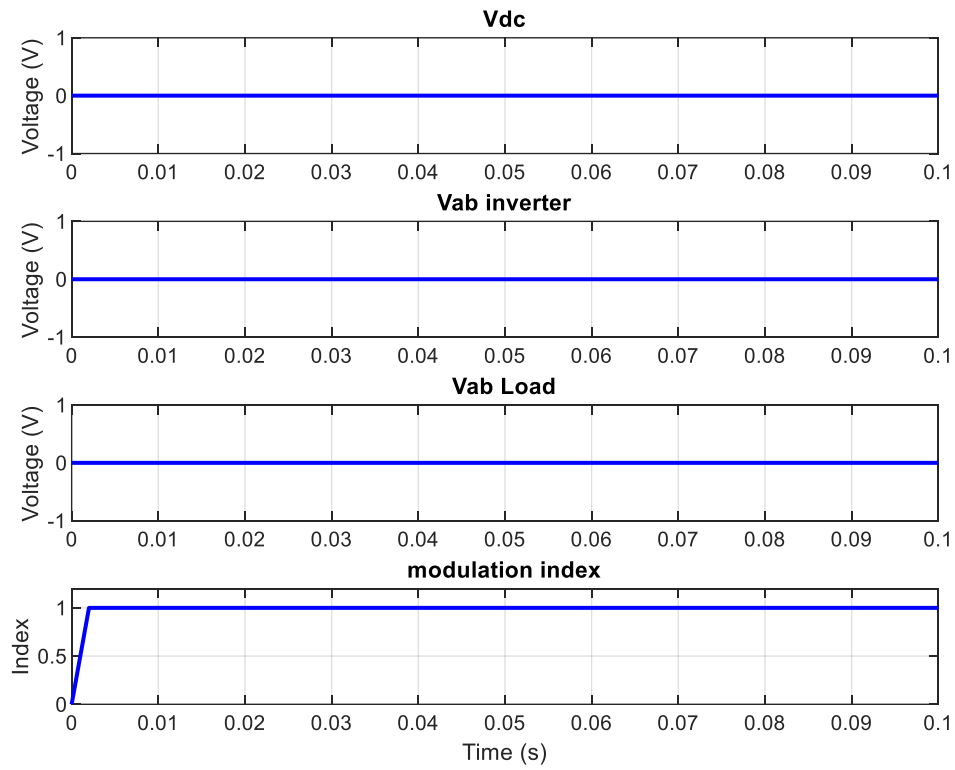
Case 3: The wind energy system is the sole available energy source, and it will supply power to the load.



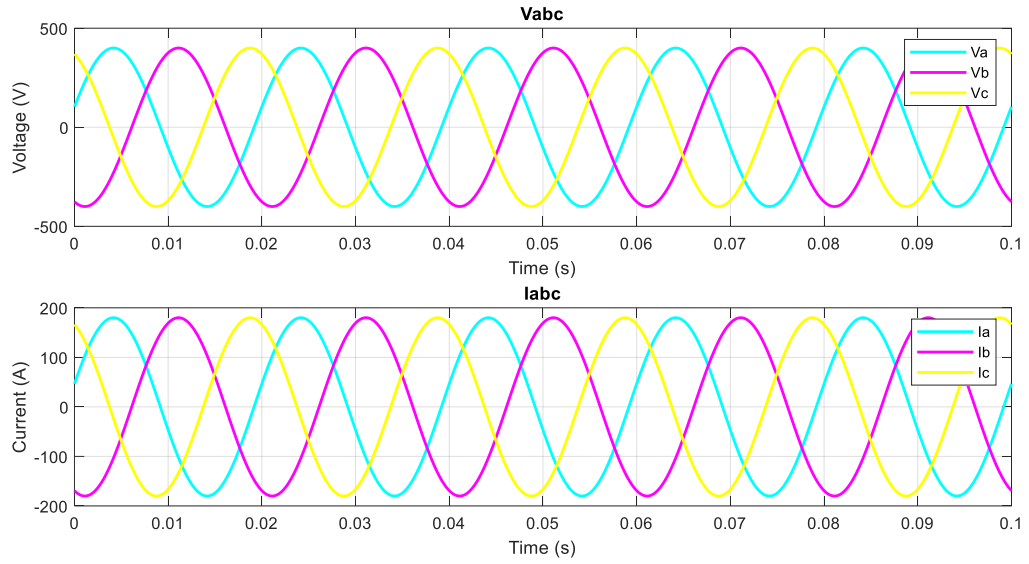
APP-10. PV system equivalent PWM results



APP-11. Wind system equivalent PWM results

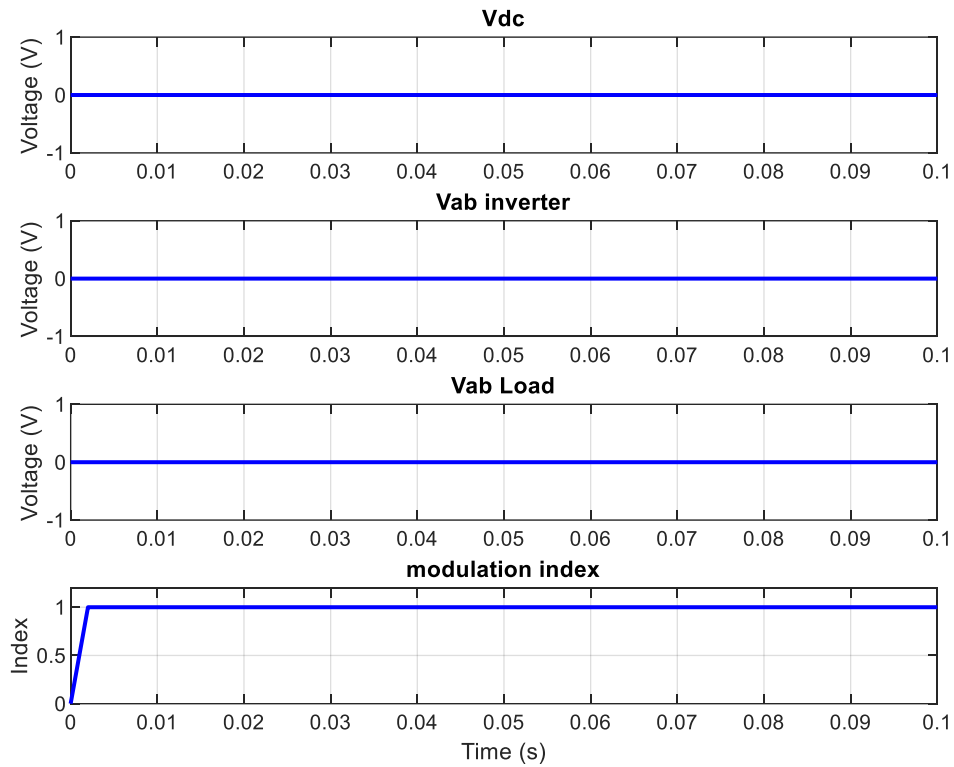


APP-12. Battery storage unit equivalent PWM results

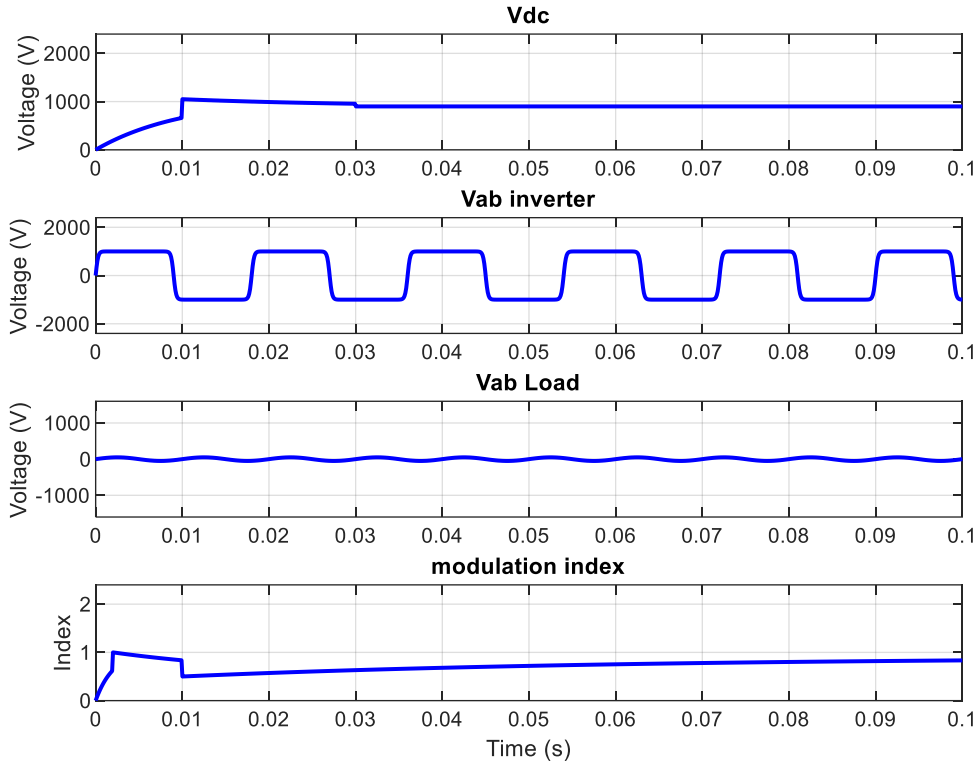


APP-13. Load Results for Case 3 supplied by the DFIG wind energy system.

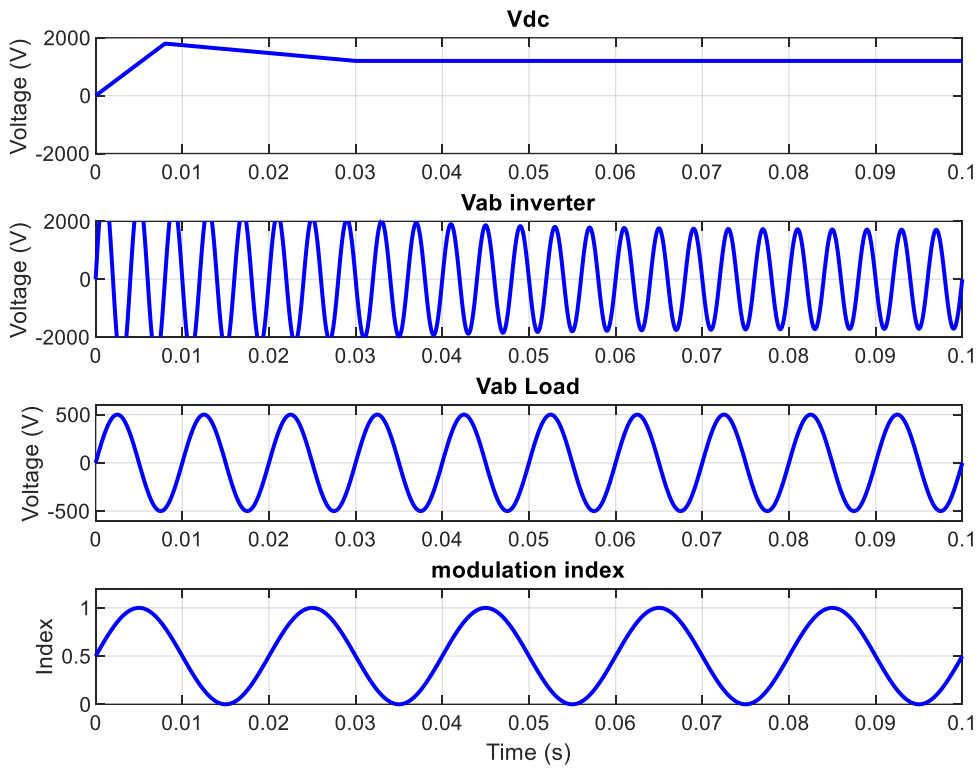
Case 4: Both the battery storage unit and wind energy system are available, but the wind energy system is selected to supply the load.



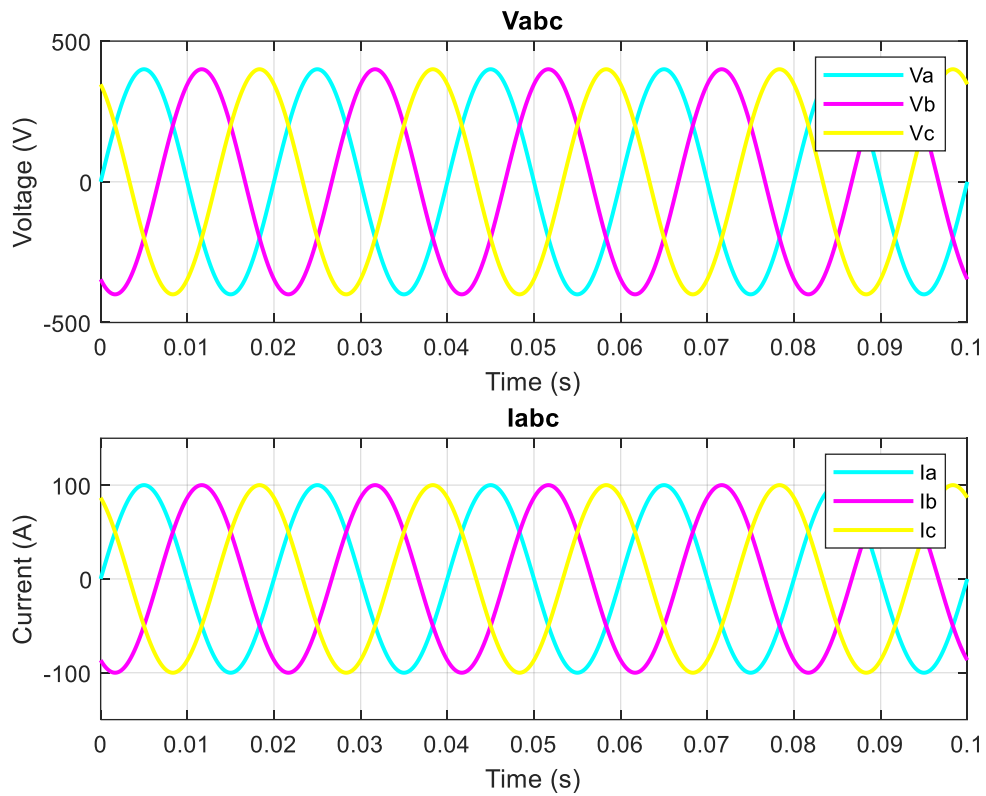
APP-14. PV system equivalent PWM results



APP-15. Wind system equivalent PWM results

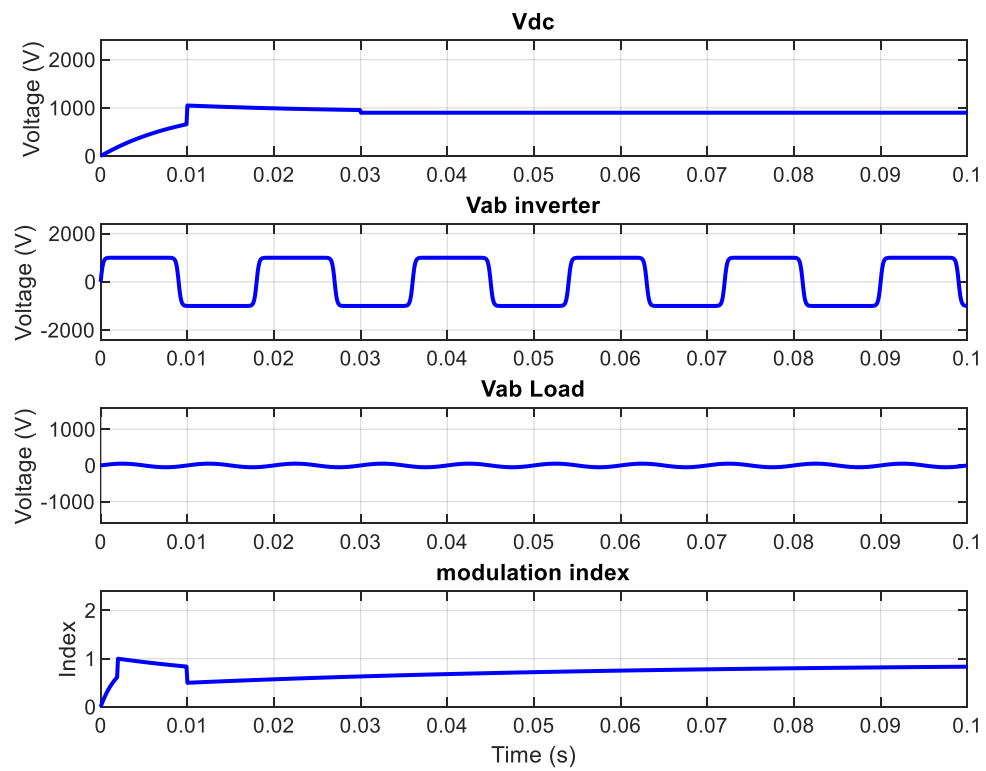


APP-16. Battery storage unit equivalent PWM results

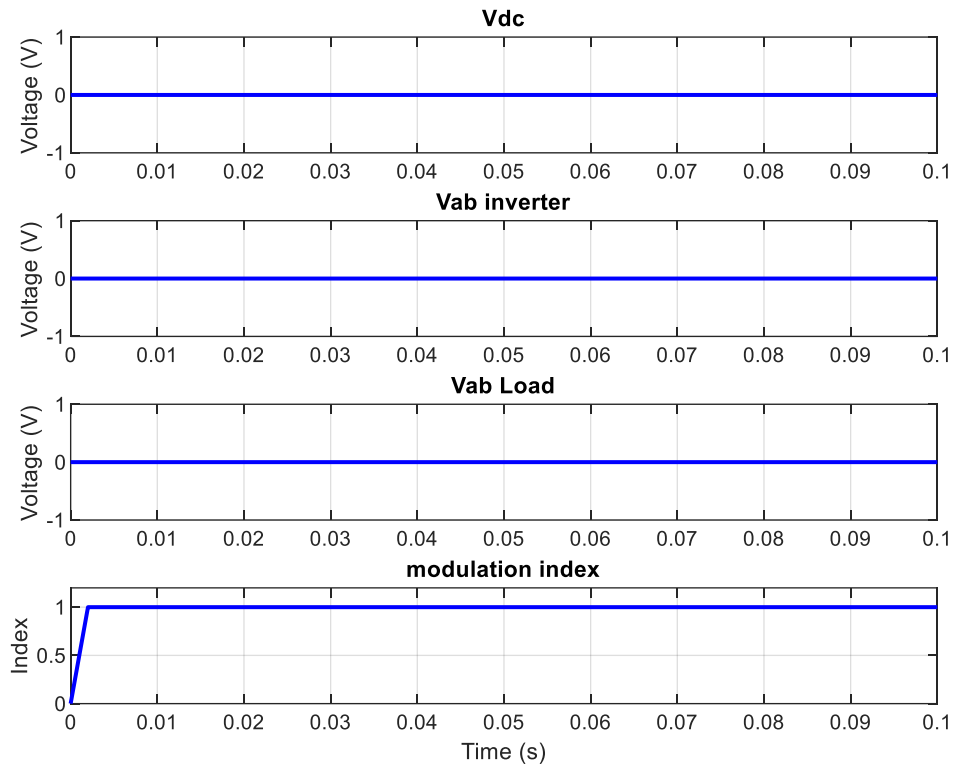


APP-17. Load Result for Case 4, powered by the wind energy system.

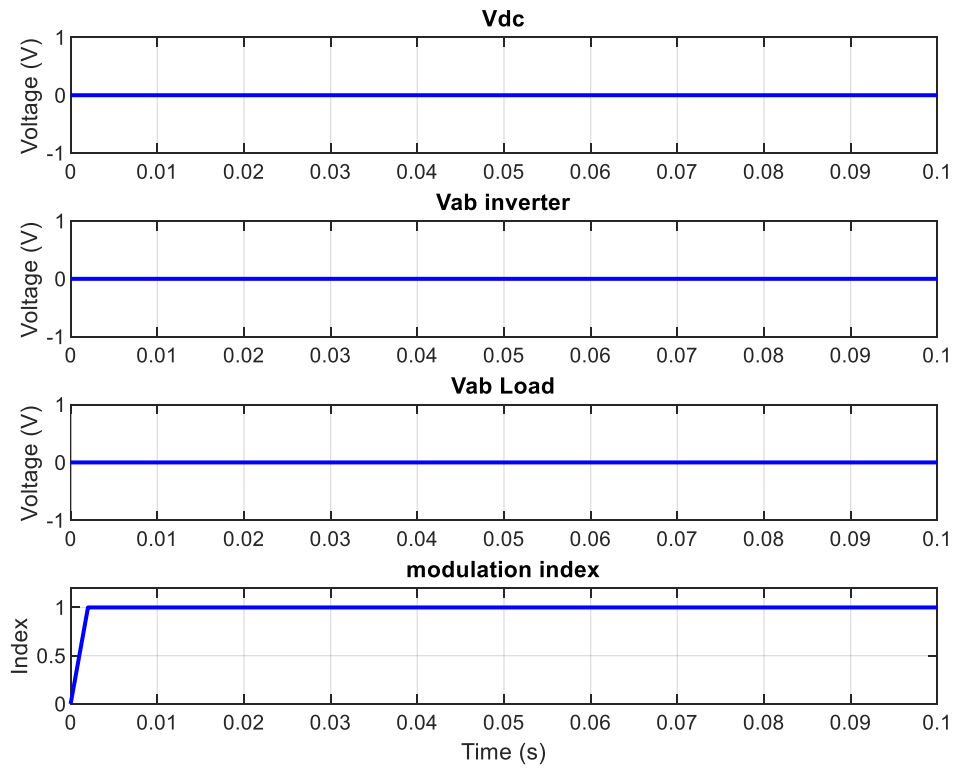
Case 5: The PV system is the sole available energy source and supplies the load.



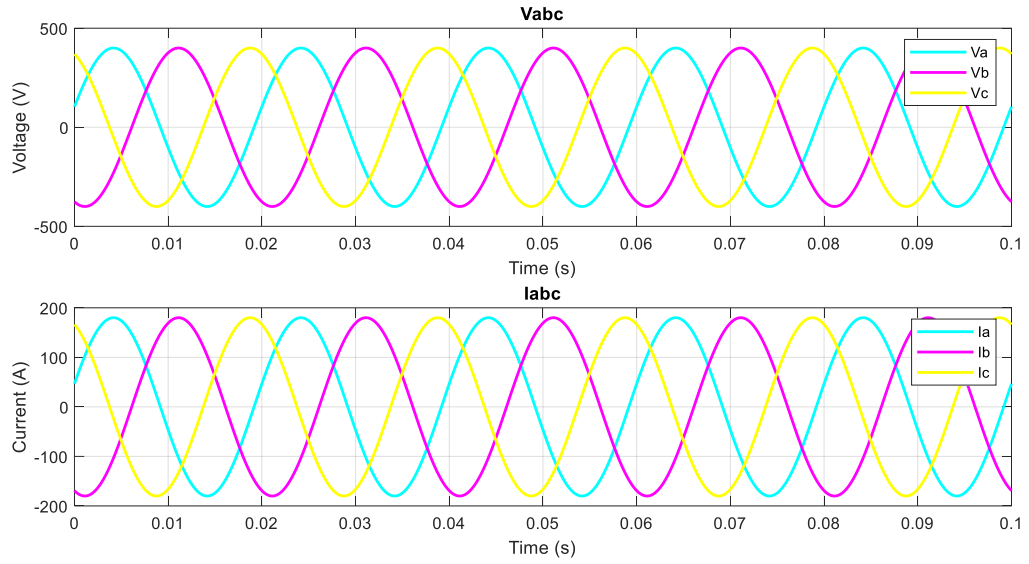
APP-18. PV system equivalent PWM results



APP-19. Wind system equivalent PWM results

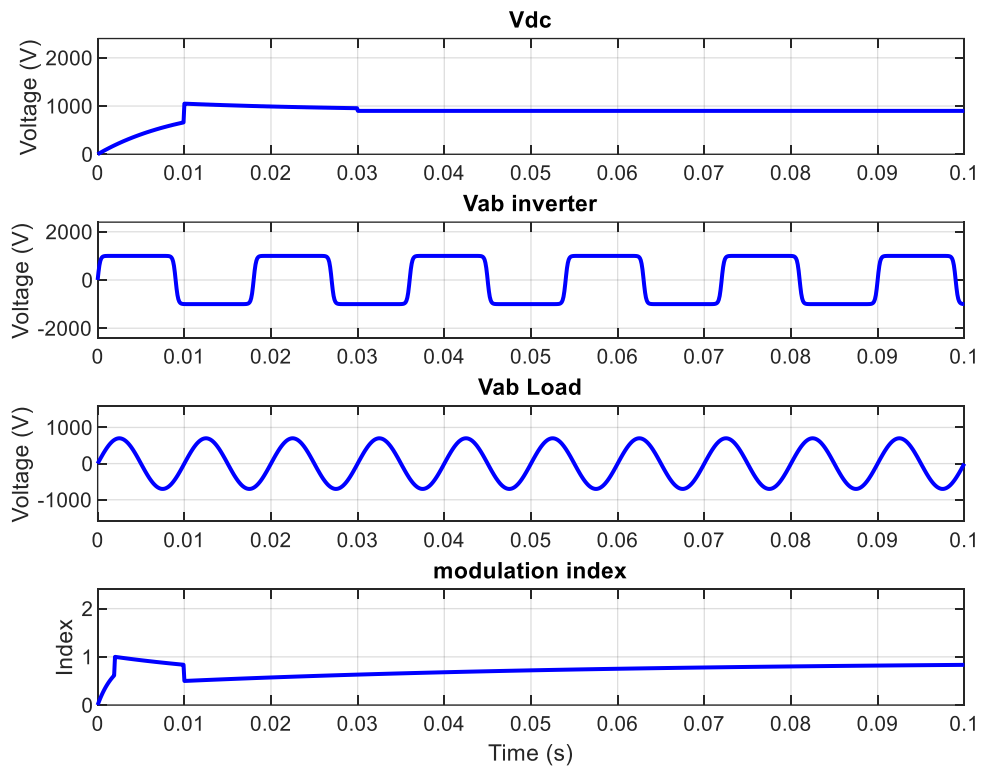


APP-20. Battery storage unit equivalent PWM results

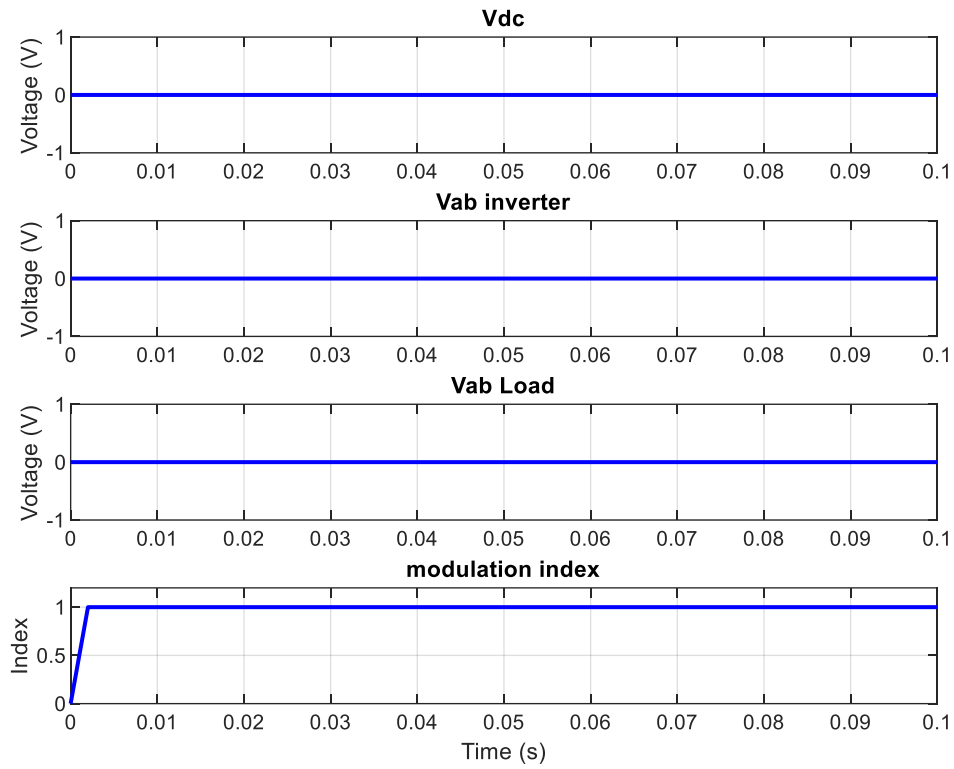


APP-21. Load Result for Case 5, powered by the load.

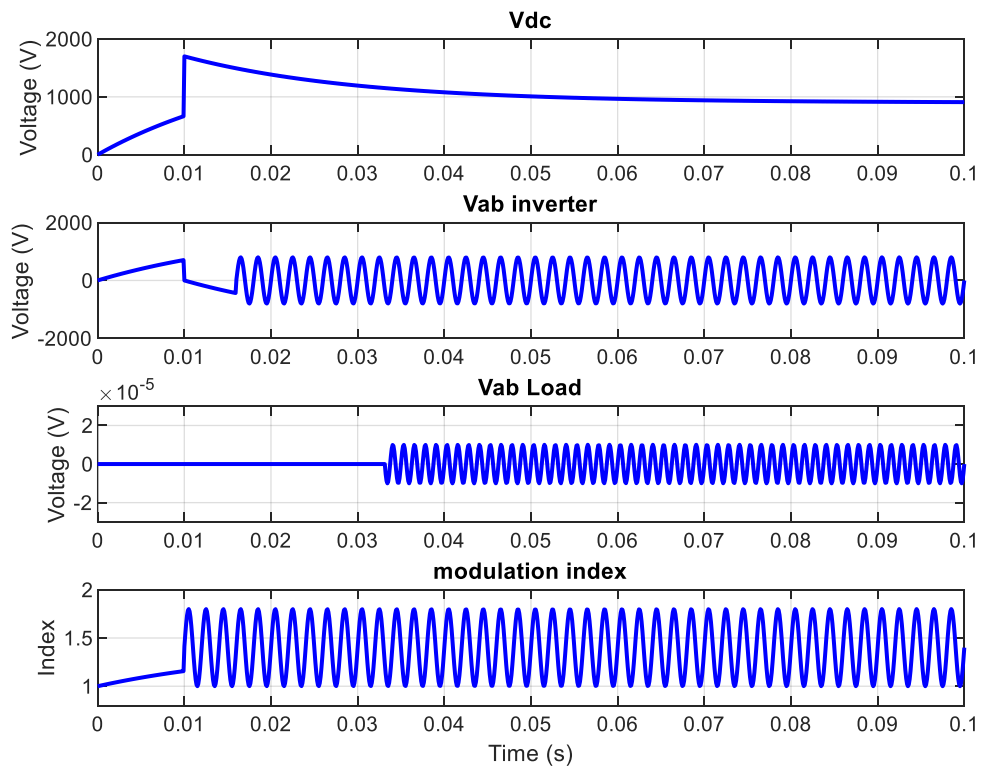
Case 6: Both the PV system and the battery storage unit are available, but the PV system is selected to supply the load.



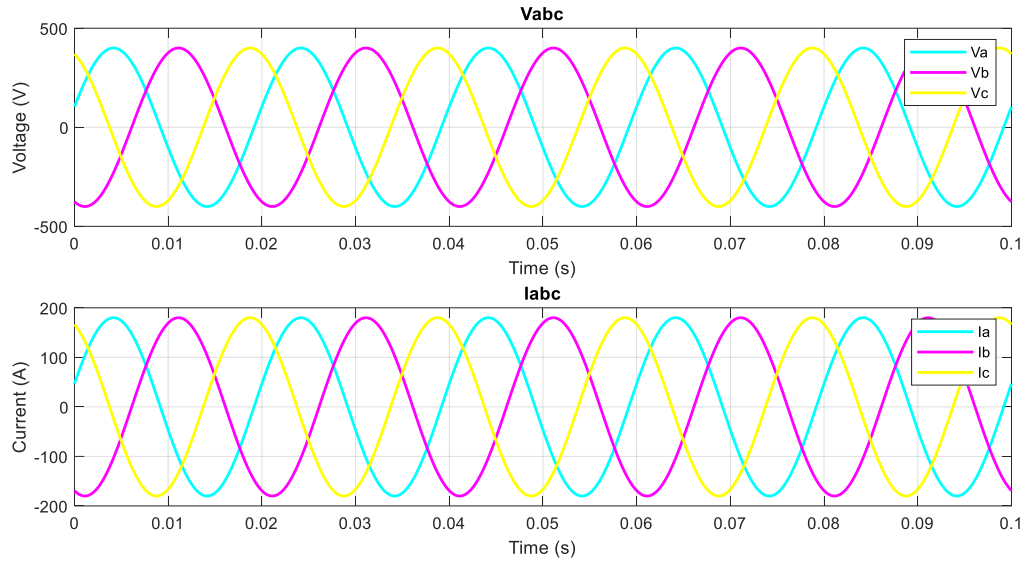
APP-22. PV system equivalent PWM results



APP-23. Wind system equivalent PWM results

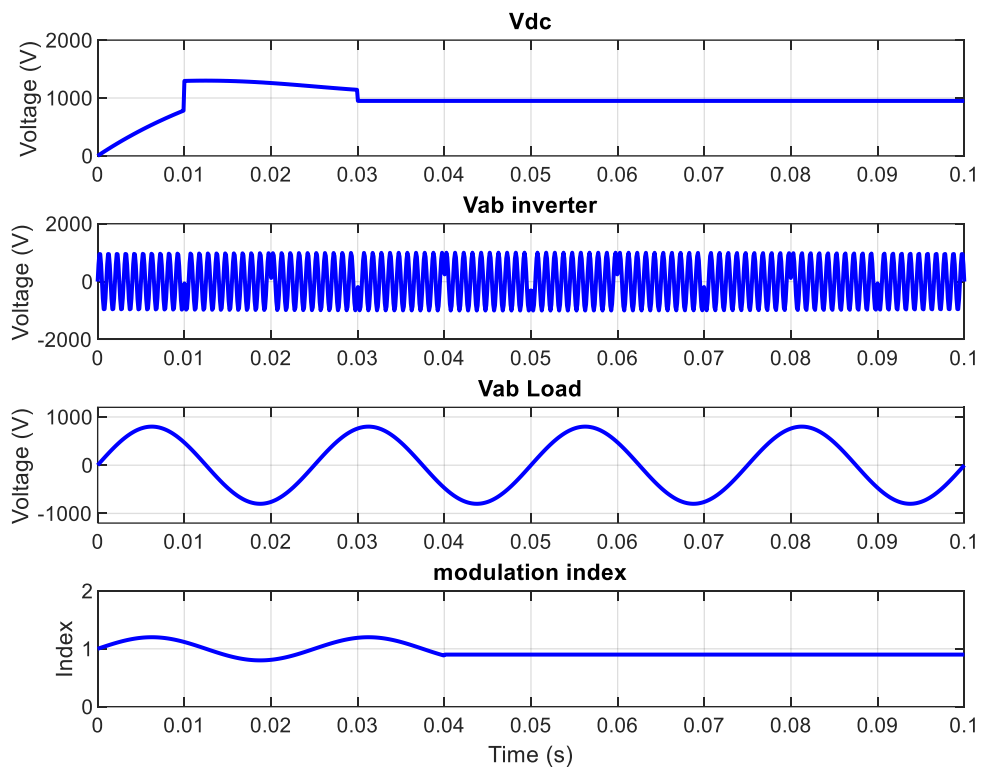


APP-24. Battery storage unit equivalent PWM results

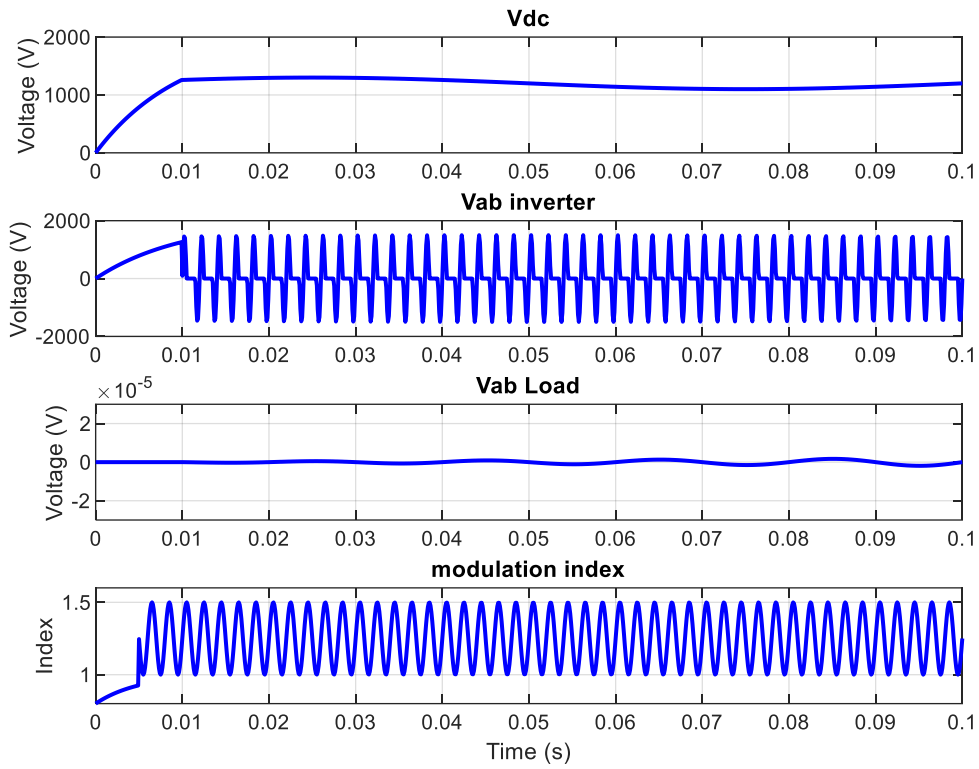


APP-25. Load Result for Case 6, powered by the PV system

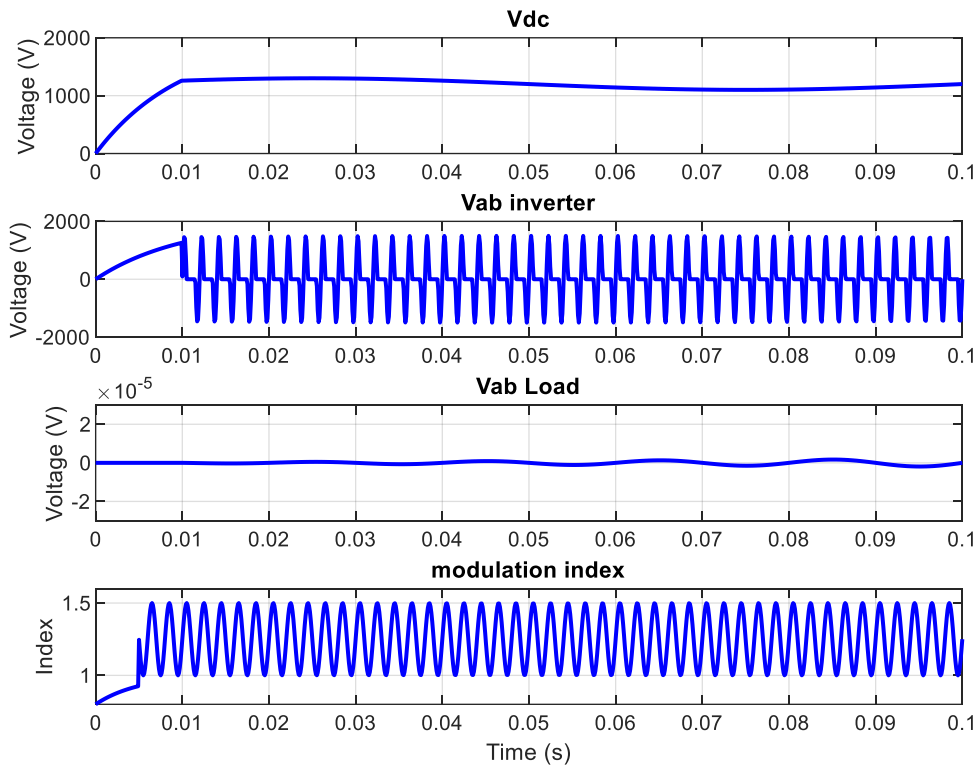
Case 7: Both the PV and wind systems are operational, with the PV system prioritized to supply the load. Meanwhile, the wind energy is utilized to recharge the depleted battery.



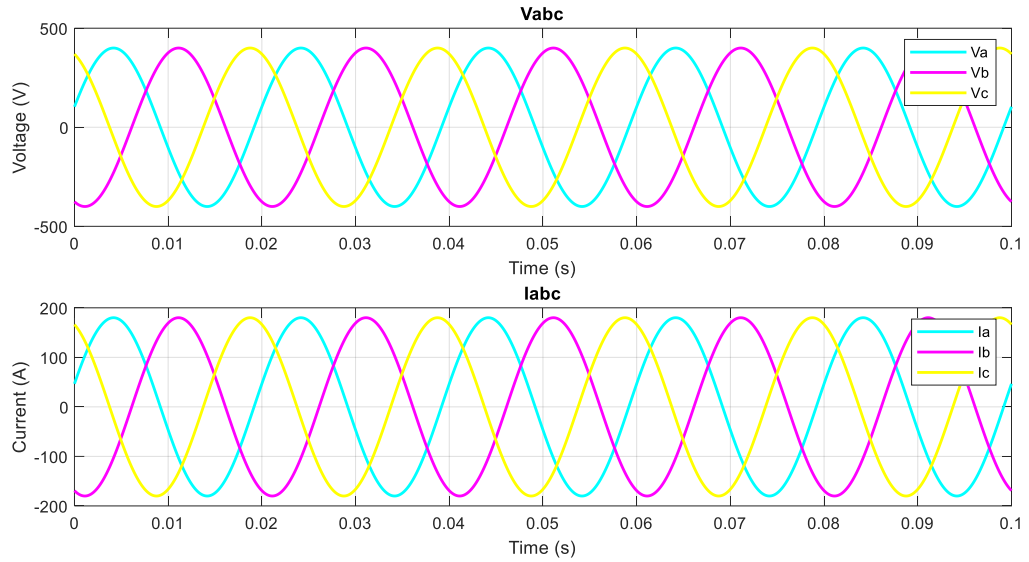
APP-25. PV system equivalent PWM results



APP-26. Wind system equivalent PWM results

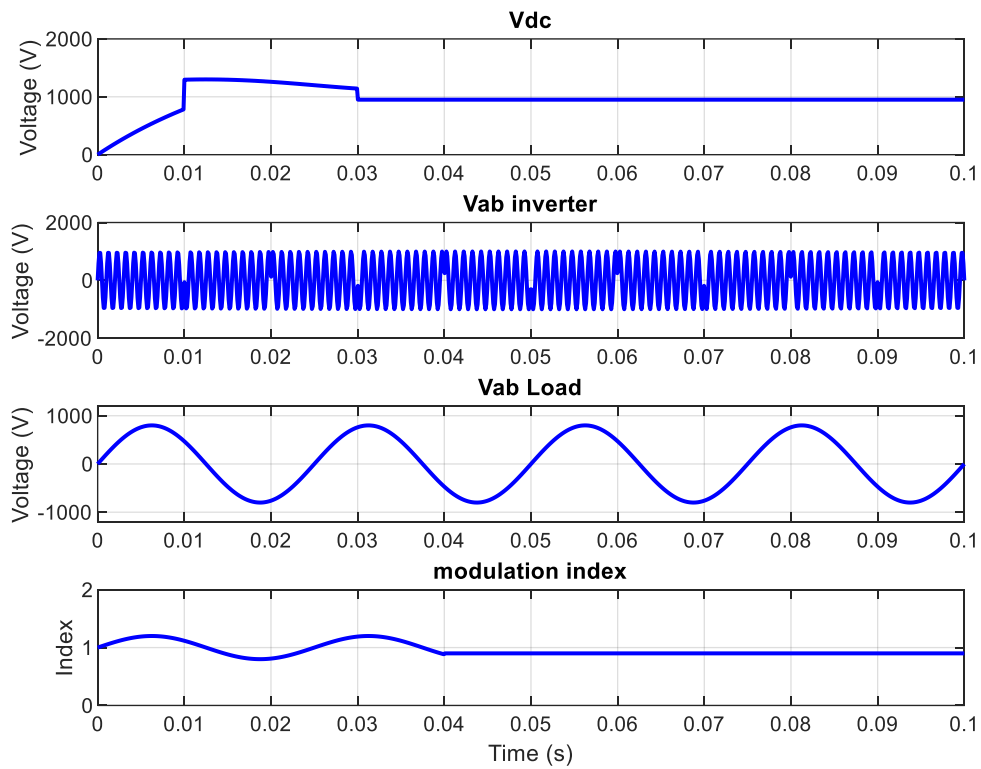


APP-27. Battery storage unit equivalent PWM results

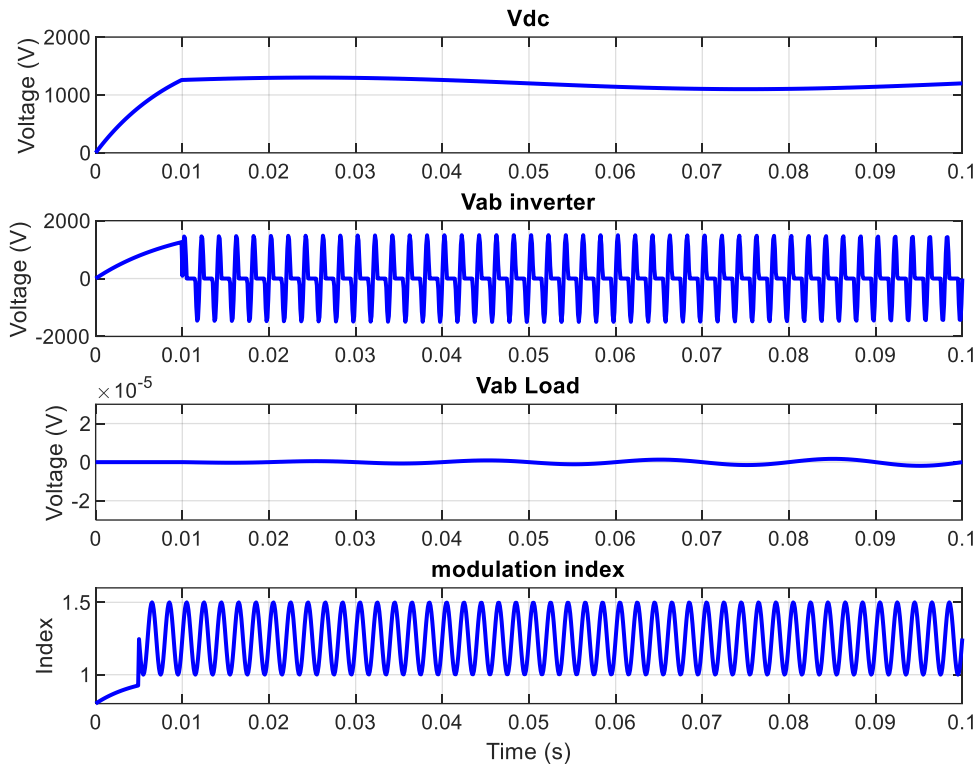


APP-28. Load Result for Case 7, powered by the PV system

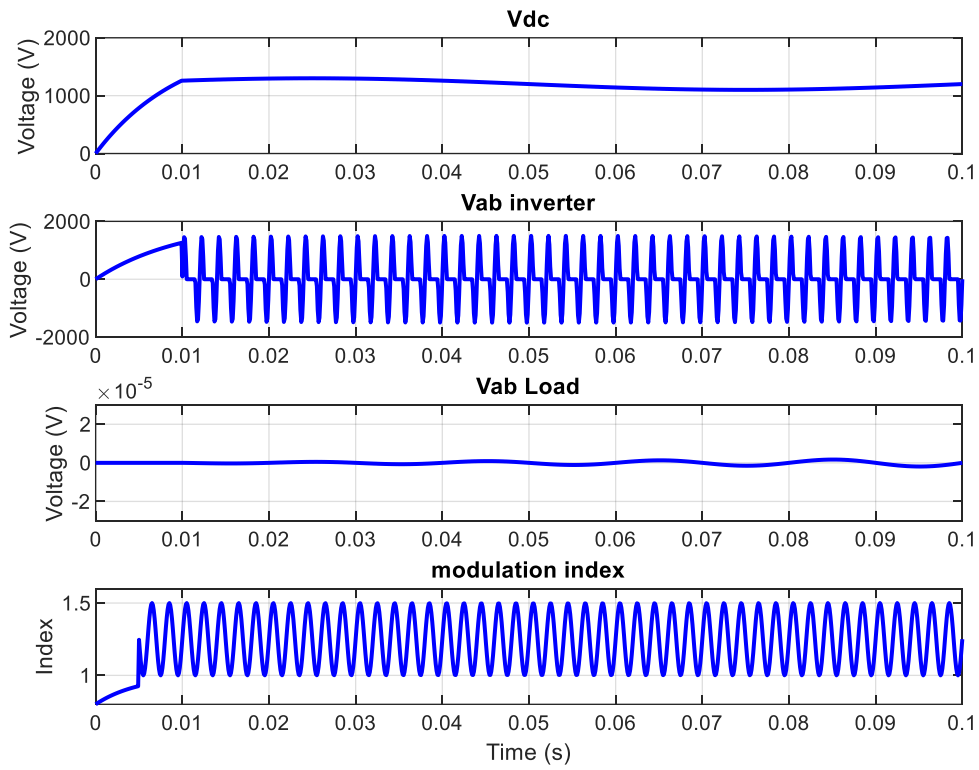
Case 8: All three resources—PV, wind, and battery—are available. However, the PV system is prioritized to supply the load, while the wind energy remains unused.



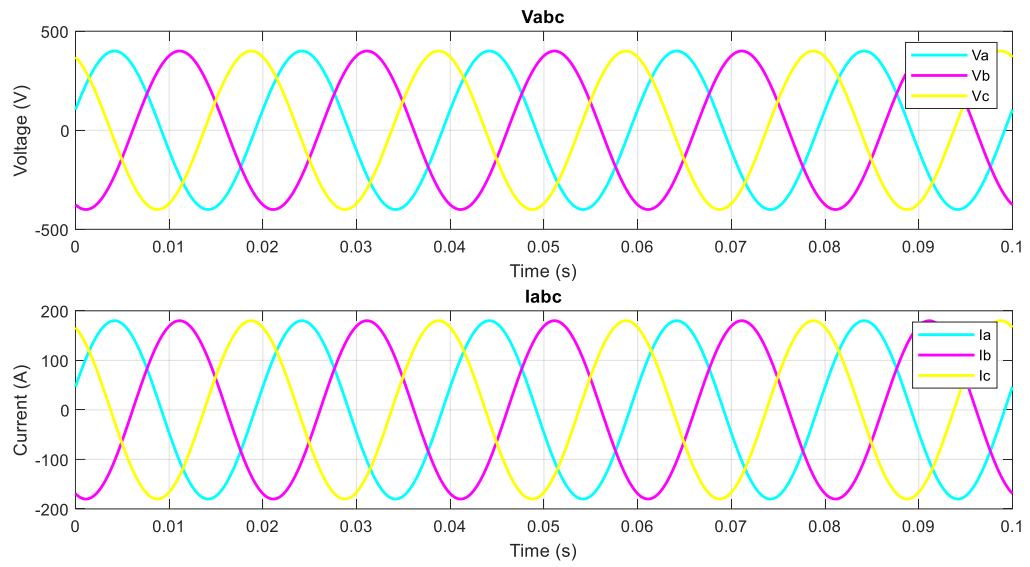
APP-29. PV system equivalent PWM results



APP-30. Wind system equivalent PWM results



APP-31. Battery storage unit equivalent PWM results



APP-32. Load Result for Case 8, powered by the PV system